Master's thesis

NTNU
Norwegian University of Science and Technology
Faculty of Natural Sciences
Department of Physics

Glenn Hoel Kampesveen

Monte Carlo Simulations of Complexation between Annealed/ Quenched Polyelectrolytes and an Annealed/Quenched Nanoparticle

A study of titration behaviour and the influence of polyelectrolyte concentration

Master's thesis in Natural Science with Teacher Education / Lektorutdanning i realfag for trinn 8–13
Supervisor: Rita de Sousa Dias
June 2022

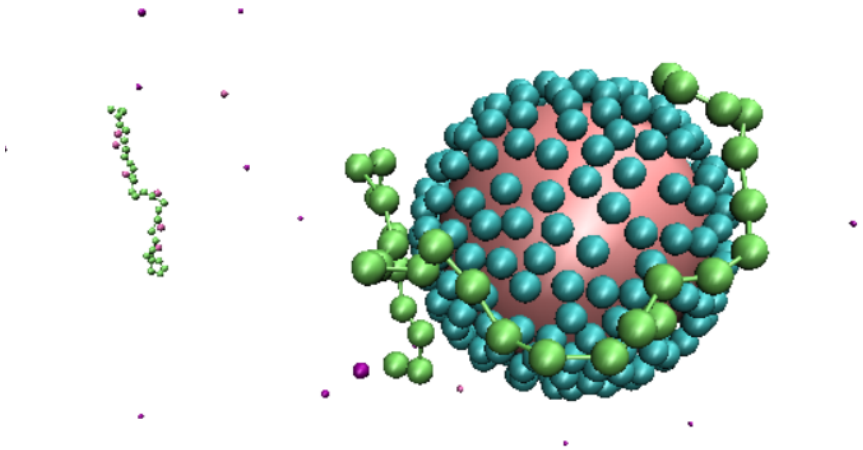

NTNU
Norwegian University of Science and Technology

Glenn Hoel Kampesveen

Monte Carlo Simulations of Complexation between Annealed/ Quenched Polyelectrolytes and an Annealed/Quenched Nanoparticle

A study of titration behaviour and the influence of polyelectrolyte concentration

Master's thesis in Natural Science with Teacher Education /
Lektorutdanning i realfag for trinn 8–13
Supervisor: Rita de Sousa Dias
June 2022

Norwegian University of Science and Technology
Faculty of Natural Sciences
Department of Physics

NTNU
Norwegian University of
Science and Technology

Abstract

In this work we studied how systems with one nanoparticle and 1 – 6 polyelectrolytes are influenced by charge regulations. The influence of pH on complex properties like the number of adsorbed polyelectrolytes, various contact and charge profiles together with conformational properties like the radius of gyration, persistence length and asphericity, were investigated. The systems were calculated using Semi-Grand Canonical Monte Carlo simulations.

The polyelectrolytes are modelled as spheres coupled together with harmonic bonds. The nanoparticle is modelled as a hard sphere with multiple surface charges. Two types of systems have been studied: i) one with quenched/strong polyelectrolytes and a quenched nanoparticle; ii) and one with annealed/weak polyelectrolytes and an annealed nanoparticle.

The presence of charge regulation was found to have a significant impact on the ionization of both macromolecules, the conformational properties of the adsorbed polyelectrolyte and the charge of the resulting complex. It is found that for systems containing 1 polyelectrolyte and 1 nanoparticle, the polyelectrolyte are, and depending on the pH of the solution, some easily bound to the nanoparticle. For systems containing up to 6 polyelectrolytes, some polyelectrolytes remain free while some are bound the nanoparticle. Since the characteristics of the free and bound polyelectrolytes are generally very different, this leads to bimodal distributions in many of the studied properties. In the case of the annealed macromolecules, the charge distribution between polyelectrolytes is also one such property.

Sammendrag

I denne studien har vi sett på hvordan systemer med 1 nanopartikkel og 1–6 polyelektrolytter påvrkes av ladningsendringer. Egenskaper som antall adsorberte polyelektrolytter, kontaktprofiler, ulike representasjoner av ladningstetthet sammen med gyrasjonsradius, persistenslengde og asfærisitet har blitt studert. Systemene har blitt beregnet ved hjelp av Monte Carlo simuleringer.

Polyelektrolyttene er modellert som kuler satt sammen med fjærer (harmonisk potensial). Nanopartikkelen er modellert som en sfære med individuelle overflateladninger. To ulike systemer har blitt studert: i) en sterk (quenched) nanopartikkel sammen med sterke polyelektrolytter; og ii) en svak (annnealed) nanopartikkel med svake polyelektrolytter.

Tilstedeværelsen av ladningsendringene ble funnet til å ha stor påvirkning på ioniseringen til begge makromolekylene, egenskapene til de absorberte polyelektrolyttene og komplekset i sin helhet. Det ble funnet ut at systemer med en polyelektrolytt og en nanopartikkel, avhengig av pH, lett dannet komplekser med hverandre, og når polymerkonsentrasjonen økte, ble det observert både bundede og frie polyelektrolytter ved gitte pH-verdier. Siden egenskapene til frie og bundede polyelektrolytter viste seg å være veldig forskjellige fra hverandre gir det opphav til bimodale sannsynlighetsfordelinger for egenskapene. Et eksempel på en slik fordeling er ladninsfordelingen i de svake makromolekylene.

Preface

This master thesis marks the end of 5 years of studies at Norwegian University of Science and Technology (NTNU) in Trondheim. This is the last assignment of the course FY3950 - Master Thesis in Physics, and is needed to fulfill the Natural Science with Teacher Education program.

During this last semester I have obtained in depth knowledge in biophysics, both through writing this thesis, but also by attending a biophysics conference here in Trondheim. At the conference I got the opportunity to talk and listen to many inspiring scientist about their research. I also made a poster (see Appendix A) based on the work of my thesis and presented it to the attendants, which was a great experience, both for me and my classmates.

I would really like to thank my supervisor Rita de Sousa Dias for outstanding guidance and help throughout this thesis. Without your support, laughter, inspiring work, passion for physics, motivational talks and baking skills, I would not have come this far. Thank you for believing in me.

I would also like to thank the people in the biopolymer group, especially Gjertrud Maurstad, Bjørn Torger Stokke and Astrid Bjørkøy for organizing, questioning and helping me during meetings and random encounters.

Lastly, I would like to thank my friends, fellow students and family for uplifting words, coffee breaks and phone calls.

Glenn Hoel Kampesveen

Trondheim, June 2022

Contents

Glossary

This section summarises the different abbreviations and provides a list of symbols used in this document. Table 1 includes the abbreviations used to describe the different polyelectrolyte-nanoparticle systems.

Abbreviations

NP Nanoparticle

PE Polyelectrolyte

Table 1: Abbreviations for the different systems studied (*e.g.* read $4PE_q$ as "The system containing 4 quenched polyelectrolytes and 1 quenched nanoparticle").

System	N_{pol}	N_{np}	Annealed/Quenched
$1NP_a^{0pe}$	0	1	A
$1NP_q^{0pe}$	0	1	Q
$1PE_a^{0np}$	1	0	A
$1PE_q^{0np}$	1	0	Q
$1PE_a$	1	1	A
$2PE_a$	2	1	A
$4PE_a$	4	1	A
$6PE_a$	6	1	A
$1PE_q$	1	1	Q
$2PE_q$	2	1	Q
$4PE_q$	4	1	Q
$6PE_q$	6	1	Q

List of symbols

Latin

A^-	Conjugate base
$\langle \mathcal{A} \rangle$	Asphericity
C	Binding capacitance
d_{ads}	Adsorbing distance
d_{ss}	Surface-surface distance
e	Elementary charge
G	Ensemble property
H	Hamiltonian
H^+	Proton
HA	Weak acid
K	Kinetic energy
K_a	Acid dissociation constant
k_B	Boltzmann constant
k_{bond}	Harmonic constant
L	Polymer chain length
L_i	Length of axis i of the equivalent ellipsoid
ℓ_p	Persistence length
$N_{\text{ads}}^{\text{PE}}$	Number of adsorbed polyelectrolyte chains
N_{bond}	Number of bonds in the polyelectrolyte
N_C	Total number of particles in a polyelectrolyte-nanoparticle complex
N_{mon}	Number of monomers in a polyelectrolyte-chain
N_{part}	Number of monomers in the polyelectrolyte chain or the number of nanoparticle surface groups
N_{PE}	Number of polyelectrolytes in the system
N_r	Total number of particles within the threshold limit of a polyelectrolyte-nanoparticle complex
n	Number of configurations generated throughout the simulation

n_Y	Numbers of monomers by type Y
n_{rand}	Random generated number between 0 and 1
P	Pressure
$P(x)$	Probability as a function of x
$\vec{p}$	Momenta
pH	Logarithm of the concentration of H^+ ions in a solution
pK_a	Logarithm of acid dissociation constant
$\vec{R}$	Position of an atom
R_{cell}	Spherical cell radius
R_g	Radius of gyration
R_i	Radius of particle i
r_b	Bond length
$\vec{r}_{\text{cm}}$	Position of the polyelectrolyte's center of mass
r_{ci^-}	Counter ion radius
$\vec{r}_i$	Position vector for monomer i
$r_{i,\text{bond}}$	Bond distance for particle i
r_{ij}	Distance between particle i and j
r_{mon}	Monomer radius
r_{np}	Nanoparticle radius
r_0	Equilibrium bond separation distance
S	Number of annealed particles
s_i	Protonation state of particle i
T	Temperature
U	Potential energy
U_{bond}	Total bonding energy
$U_{\text{bond}}^{\text{PE}}$	Bonding energy between monomers in a polyelectrolyte
$\Delta U_{\text{charge change}}$	Change in potential for a charge chain move
$U_{\text{non-bond}}$	Total non-bonding energy
U_{prot}	Total protonation energy
V	Volume

$X(Y)$	Fraction of Y = loops, tails and trains in a polyelectrolyte
$\vec{x}$	Coordinate
Z_C	Total charge of a polyelectrolyte-nanoparticle complex
Z_r	Radial charge of a polyelectrolyte-nanoparticle complex
Z_i	Valency of particle i
z_i	Charge of particle i
z_{mon}	Monomer charge of quenched polyelectrolyte
z_{np}	Point charge of quenched nanoparticle

Greek

α	Average degree of ionisation
α^{PE}	Average degree of ionisation for polyelectrolytes
α^{ID}	Ideal degree of ionisation
α^{NP}	Average degree of ionisation for a nanoparticle
ϵ_0	Vacuum permittivity
ϵ_r	Relative permittivity
ζ-potential	Property that describes the electrostatic potential at a shear plane
μ	Chemical potential
μ_i	Reduced chemical potential
$\rho(x)$	Density distribution of a function $f(x)$
ρ_{NVT}	Canonical density distribution function

Chapter 1

Introduction

Polyelectrolytes and nanoparticles has been the interest of much research in the past decades, and are still an important topic. They are widely used in the industry, *e.g.* water treatment or food technology. Polyelectrolytes also have fundamental biological characteristics, since *e.g.* nucleic acids, proteins and polysaccharides are all polyelectrolytes. The understanding of the complexation between polyelectrolytes and nanoparticles could therefore lead to important knowledge when it comes to biological processes [1, 2, 3, 4].

In simulations, the presence of a nanoparticle together with weak polyelectrolytes has been showed to greatly influence the degree of ionization in both molecules. Both the attractive forces between polyelectrolyte and the oppositely charged nanoparticle and the repulsive forces between the polyelectrolyte chains affects the ionization and conformation of the polyelectrolytes [5], and the charge distribution along them [6].

In this work we studied how systems with one nanoparticle and 1 – 6 flexible polyelectrolytes are influenced by charge regulations. We studied the influence on complex properties like the number of adsorbed polyelectrolytes, various contact and charge profiles together with conformational properties like the radius of gyration, persistence length and asphericity.

The systems were calculated by Rita Dias, using Semi-Grand Canonical Monte Carlo simulations in a pH raging from 2 – 14. I have plotted and interpreted the data using Python (v3.8.2) based on a script from Morten Stornes. The figures are created in Inkscape, and snapshots are taken with VMD or view3dscene.

Chapter 2

Theoretical Background and Methodology

2.1 Monte Carlo Simulation

A statistical approach to study differential equations is by the use of Monte Carlo method. It is a numerical method based on successive random sampling to calculate statistical properties. It is thus a popular method for probing molecule systems in equilibrium.

2.1.1 The Metropolis Algorithm

The Monte Carlo simulation used to obtain the data presented in this thesis is based on the traditional Metropolis algorithm, first proposed in 1953 [7]. Its purpose was to find a method that could be used to calculate properties of systems that consist of an finite number of interacting, individual particles, with the use of less computer power and time than the standard Monte Carlo approach. The approach is as follows. If one knows the position of each particle in a system (configuration), the potential energy U can be easily calculated. Instead of generating a totally random new configuration and calculate the potential energy of that, a Monte Carlo move is applied to a single particle at a time. Which type of Monte Carlo move is tried out, depends on the constraints of the system itself. The change in potential energy ΔU is calculated between the first and the new attempted configuration. If $\Delta U < 0$, the move is accepted. Otherwise, a random number n_{rand} in an uniform distribution between 0 and 1 is chosen. If $n_{\text{rand}} < P(\text{accepted})$, the new configuration is accepted. The acceptance probability is given by

$$P(\text{accepted}) = \exp\left(-\beta \Delta U\right), \tag{2.1}$$

where $\beta = 1/k_B T$ with the Boltzmann constant k_B and temperature T. This procedure avoids that the system get "trapped" in local energy minimum. If $n_{\text{rand}} >$

P(accepted) the move is rejected, the original configuration is restored and another move is attempted. By using particle-wise moves to obtain a new state, one prevents using much computational power calculating high energy states of the system, and the system reach equilibrium (or a local minimum) more efficiently.

2.1.2 Canonical Ensemble Average

A biological system is always in motion. Particles fluctuates between positions spontaneously, and each snapshot of the system is called a configuration or state. An ensemble is the collection of such states together with the probability of that single state. In the canonical ensemble, the temperature T, the volume V and number of particles N are constant. This is sometimes referred to as the NVT-ensemble.

In such an ensemble, the states are specified by N momenta $\vec{p}$ and coordinates $\vec{x}$ compactly represented by $\left(\vec{p}^N, \vec{x}^N\right)$. The equilibrium average of some quantity G is calculated by

$$\langle G \rangle = \frac{\int G\left(\vec{p}^N, \vec{x}^N\right) \exp\left[-\beta H\left(\vec{p}^N, \vec{x}^N\right)\right] d\vec{p}^N d\vec{x}^N}{\int \exp\left[-\beta H\left(\vec{p}^N, \vec{x}^N\right)\right] d\vec{p}^N d\vec{x}^N}, \tag{2.2}$$

where $H\left(\vec{p}^N, \vec{x}^N\right)$ is the Hamiltonian of the system consisting of both the potential U (position dependent) and kinetic K (momenta dependent) energy. If G does not depend on the momenta, the kinetic energy cancels out and Equation (2.2) becomes

$$\langle G \rangle = \frac{\int G\left(\vec{x}^N\right) \exp\left[-\beta U\left(\vec{x}^N\right)\right] d\vec{x}^N}{\int \exp\left[-\beta U\left(\vec{x}^N\right)\right] d\vec{x}^N}, \tag{2.3}$$

which corresponds to a series of measurements of an ensemble of independent systems [8].

Now, let us consider a property G of the system as a function of the $3N$ coordinates of atoms $\vec{R}$. The average canonical property from Equation (2.3) can be rewritten as

$$\langle G \rangle = \frac{\int G\left(\vec{R}\right) \exp\left[-\beta U\left(\vec{R}\right)\right] d\vec{R}}{\int \exp\left[-\beta U\left(\vec{R}\right)\right] d\vec{R}}, \tag{2.4}$$

and by combining this with the canonical density distribution function $\rho_{\mathrm{NVT}}(\vec{R})$, we can rewrite $\langle G \rangle$ on the form $\int [\frac{f(x)}{\rho(x)}] \rho(x) dx$ by only take into account where the probability density function $\rho(x)$ of $f(x)$ can be large. This results in

$$\langle G \rangle = \int G\left(\vec{R}\right) \rho_{\mathrm{NVT}}\left(\vec{R}\right) d\vec{R}. \tag{2.5}$$

If it is possible to choose configurations for the system by $\rho_{\mathrm{NVT}}(\vec{R})$, $\langle G \rangle$ can be approximated by

$$\langle G \rangle \simeq \frac{1}{n} \sum_{i=1}^{n} G\left(\vec{R}_i\right) \tag{2.6}$$

where n is the number of configurations generated throughout the simulation and $\vec{R}_i$ a vector describing the positions of each atom in configuration i [9].

Grand Canonical

As canonical ensemble has constant N, V and T, the grand canonical ensemble has constant chemical potential μ, V and T. This allows for charge changes between the different states at fixed pH [10]. In Monte Carlo simulations the grand canonical average of a property $\langle G \rangle$ is approximated by, as in Equation (2.6), an average of G for a selected number of states during the equilibrium run.

2.2 Titrating Polyelectrolytes

Polymers or macromolecules are large molecules consisting of repeating units, also called monomers. Examples of monomers are sacharides and amino acids. These particular monomers form polysaccharides and proteins, respectively and have great importance in biological systems [11].

A polymer where the monomers are charged, is called a polyelectrolyte. A titrating polyelectrolyte is a polyelectrolyte where the charge of the monomers can change according to the pH in the system [12] *i.e.* the monomers consists of weak acidic or base functional groups. These are often referred to as annealed or weak polyelectrolytes in the literature [13, 14].

If the charge of the polyelectrolyte is independent of the pH in the system, the polyelectrolyte is called quenched. This can be obtained by constructing copolymers consisting of both charged and uncharged monomers and vary the charge fraction. Quenched polyelectrolytes are often referred to as strong polyelectrolytes [14].

2.2.1 Properties of an Acid, pH and p$K_{\mathbf{a}}$

Consider the reaction of a weak acid HA releasing a proton H^+ and forming the conjugate base A^-,

$$\mathrm{HA} \rightleftharpoons \mathrm{H}^+ + \mathrm{A}^-. \tag{2.7}$$

Here, HA could be a weak acid group in a polyelectrolyte or a small molecule, but important is the fact that the reaction is a true chemical reaction that involves the disruption/creation of chemical bonds [13].

To measure the acidity of a solution, pH is used and defined as

$$\mathrm{pH} = -\log[\mathrm{H}^+] \tag{2.8}$$

where $[H^+]$ is the concentration of H^+ ions in the solution. The acid dissociation constant K_a is defined as

$$K_a = \frac{[A^-][H^+]}{[HA]}, \tag{2.9}$$

with respective pK_a

$$pK_a = -\log \frac{[A^-][H^+]}{[HA]}. \tag{2.10}$$

2.2.2 Degree of Ionisation α

By using the mean field approximation, assuming that all titration sites have the same pK_a, we obtain the following relation from Equation (2.10) in a polyelectrolyte

$$pK_a = pH - \log \frac{\alpha}{1-\alpha} \tag{2.11}$$

where α is the degree of ionisation (often refereed to as the degree of dissociation, or the dissociation constant) of the monomers given by

$$\alpha = \frac{1}{N_{mon}} \sum_{i=1}^{N_{mon}} |z_i|, \tag{2.12}$$

where N_{mon} is the number of monomers in a polyelectrolyte-chain and z_i the charge of monomer i [12] .

The degree of dissociation α^{ID} of a single monomer in solution is given by the Henderson-Hasselbalch equation

$$\alpha^{ID} = \frac{1}{1 + 10^{\xi(pK_a - pH)}} \tag{2.13}$$

where ξ can either be $+1$ or -1 according to if the macromolecule is composed by acidic or basic groups, respectively [2].

Binding Capacitance C

The binding capacitance C of a macromolecule is calculated as the variance of the charges, given by

$$C = \frac{1}{N_{part}} \sum_{i}^{N_{part}} \left(\langle z_i^2 \rangle - \langle z_i \rangle^2 \right) = \frac{\partial \alpha}{\partial \mu} \tag{2.14}$$

and is a measure of how much charge that can be induced upon exposure with an electric potential [2, 15].

2.3 Potential Energy U

The potential energy of the system U consists of the bonding energy U_{bond} between the monomers in the polyelectrolyte, the non-bonding energy $U_{\text{non-bond}}$ between all particles and in the case of annealed particles, the protonation energy U_{prot},

$$U = U_{\text{bond}} + U_{\text{non-bond}} + U_{\text{prot}}. \tag{2.15}$$

The bonding energy between the monomers in a polyelectrolyte consisting of N_{bond} bonds has the same form as the sum of simple harmonic oscillators $U_{\text{harm}} = \frac{1}{2}kx^2$, giving

$$U_{\text{bond}}^{\text{PE}} = \sum_{i}^{N_{\text{bond}}} \frac{k_{\text{bond}}}{2}(r_{i,\text{bond}} - r_0)^2, \tag{2.16}$$

where k_{bond} is the harmonic constant, $r_{i,\text{bond}}$ the bond distance for particle i and r_0 the equilibrium separation distance. Since there could be more than one polyelectrolyte in a system, the total bonding energy becomes

$$U_{\text{bond}} = \sum_{j}^{N_{\text{PE}}} \sum_{i}^{N_{\text{bond}}} \frac{k_{\text{bond}}}{2}(r_{i,\text{bond}} - r_0)^2, \tag{2.17}$$

where N_{PE} is the number of polyelectrolytes j in the system. The non-bonding energy is given by

$$U_{\text{non-bond}} = \sum_{i<j} u_{ij}(r_{ij}), \tag{2.18}$$

where $u_{ij}(r_{ij})$ consists of the hard sphere potential and the electrostatic potential, defined by

$$u_{ij}(r_{ij}) = \begin{cases} \infty, & r_{ij} < R_i + R_j \\ \dfrac{Z_i Z_j e^2}{4\pi\epsilon_0\epsilon_r r_{ij}}, & r_{ij} \geq R_i + R_j, \end{cases} \tag{2.19}$$

where r_{ij} is the distance between particle i and j, R_i and Z_i are the radius and valency of particle i, respectively. e is the elementary charge and ϵ_0 and ϵ_r the vacuum and relative permittivity. For annealed systems with S annealed particles, the protonated potential is given by

$$\begin{aligned} U_{\text{prot}} &= \frac{\ln 10}{\beta} \sum_{i=1}^{S} \mu_i s_i \\ &= \frac{\ln 10}{\beta} \sum_{i=1}^{S} (\text{pH} - \text{p}K_{\text{a},i}) s_i, \end{aligned} \tag{2.20}$$

where μ_i the reduced chemical potential for particle i dependent of the proton activity $[\text{H}^+]$ and the intrinsic acidic constant K_a. s_i is the protonation state of particle i, which could have value 1 (protonated) or 0 (unprotonated). [2, 16]

Change in Potential Energy ΔU

Following the metropolis algorithm, upon a trial move, there is no need of calculating the total energies of the systems, but simply the change in potential energy ΔU between the two configurations. As an example, let us consider a charge change move. If one assumes that every monomer has a dissociation constant K_0, the change in potential for a charge change move becomes

$$\begin{aligned}\Delta U_{\text{charge change}} &= \Delta U_{\text{bond}} + \Delta U_{\text{non-bond}} + \Delta U_{\text{prot}} \\ &= \sum_{i<j} \Delta u_{ij}(r_{ij}) + \frac{\ln 10}{\beta} \sum_{i=1}^{S} (\text{pH} - \text{p}K_{\text{a},i}) \Delta z_i,\end{aligned} \tag{2.21}$$

as $\Delta U_{\text{bond}} = 0$ because there are no translation within the system. Since only particle i change charge, we can simplify the summations to take into account only the potential change in respect to particle i by

$$\Delta U_{\text{charge change}} = \sum_{j}^{i \neq j} \Delta u_{ij}(r_{ij}) + \frac{\ln 10}{\beta} (\text{pH} - \text{p}K_{\text{a},i}) \Delta z_i, \tag{2.22}$$

which needs less computer power to calculate than the potential energy U for the whole system.

Same simplifications can be done for the other Monte Carlo moves that will be presented in section 2.4, reducing the amount of time needed to reach equilibrium and to calculate the properties of interest.

2.4 Simulation Details

In previous studies, several models have been used to simulate polyelectrolytes. Both static and flexible chains, with static or titratable monomer charge groups [16, 17, 18]. In this thesis, a model of flexible chains has been studied together with a nanoparticle. A snapshot of 4PE$_a$ at equilibrium can be seen in Figure 2.1, as an example.

The studied systems consists of one nanoparticle and one to six flexible polyelectrolytes in solution together with their respective co-/counter-ions to preserve a neutral net charge. These are placed in a spherical box with radius R_{cell}. The solvent is considered to be an homeogenous medium with $\epsilon_r = 78.4$, corresponding to water at $T = 298\,\text{K}$. Two types of cases have been studied. One case where all macromolecules are annealed, and one case where all macromolecules are quenched.

The polyelectrolytes are modelled as hard spheres (monomer) with radius r_{mon} coupled together with flexible springs, each with a spring constant k_{bond}. The monomers in the annealed polyelectrolytes have a charge of either $z = 0$ (neutral) or $z = +1e$ (charged). The monomers can switch independently between being charged and neutral, according to a probability which depends on the pH in the solution and

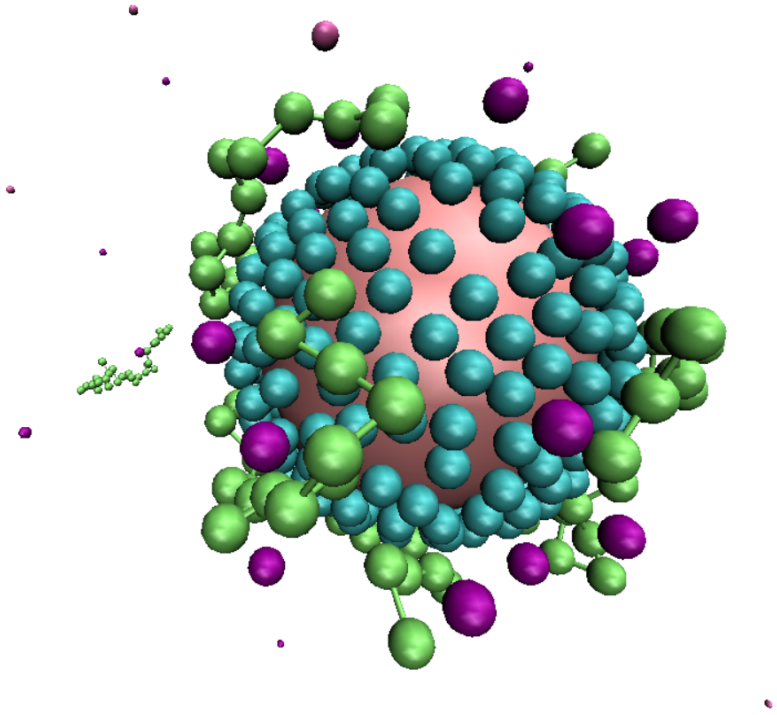

Figure 2.1: A snapshot of 4PE$_a$ at pH = 12.

their proximmity to other charged particles. The annealed nanoparticle is modelled as a hard sphere with radius r_{np} with 240 hard spheres with point charges at the surface of the nanoparticle to mimic acidic groups, which also can switch between neutral and charged ($z = -1e$) as described for the polyelectrolytes [2].

On the other hand, a quenched polyelectrolyte is a polymer consisting of monomers with a fixed charge z_{mon}, and the surface groups of the quenched nanoparticle is also given a fixed charge z_{np}. The charges for the quenched systems are chosen to be equal to the average degree of ionization from the results of the annealed systems.

Each polyelectrolyte consists of $N_{\text{mon}} = 30$ monomers with equilibrium bond separation r_0. The annealed nanoparticle has a p$K_{\text{a}} = 7$ and the annealed polyelectrolytes has a p$K_{\text{a}} = 9$.

The sizes and values of the input parameters in the Monte Carlo simulation presented in this section can be found in Table 2.1.

To run the Monte Carlo simulations, the MOLSIM (version 6.4.7) [19] software was used. During each step in the simulation, a Monte Carlo move is tried out. The Monte Carlo moves used in this work were: (a) Single particle move ($P(\text{move}) = 1/3$) applied to all particles except the nanoparticle and its surface groups; (b) chain move where the whole chain are translated ($P(\text{move}) = 1/6$); and (c) pivot move where the shorter subchain is rotated ($P(\text{move}) = 1/6$). For the annealed polyelectrolytes, there is an additional (d) charge chain move ($P(\text{move}) = 1/3$) where the charge

Table 2.1: Values of static input-parameters for the Monte Carlo simulations

Symbol	Description	Value	Unit
d_{ads}	Adsorbing distance	30	Å
T	Temperature	298	K
P	Pressure	101	kPa
R_{cell}	Spherical cell radius	600	Å
ϵ_r	Relative permittivity of solvent (water)	78.4	
r_{np}	Nanoparticle-radius	22	Å
r_{mon}	Monomer-radius	2	Å
r_{ci^-}	Counter ion-radius	2	Å
k_{bond}	Harmonic bonding constant	2.4088	N m^{-1}
r_0	Equilibrium bond separation	5	Å

of the titratable group (monomer and nanoparticle surface groups) switch between charged/uncharged, as illustrated in Figure 2.2.[1] $P(\text{move})$ is the probability of trying out the specific move *e.g.* a singe particle move ($P = 1/3$) is tried out twice as many times as the pivot move ($P = 1/6$).

Moves (b) and (c) are only applied to the polyelectrolyte.

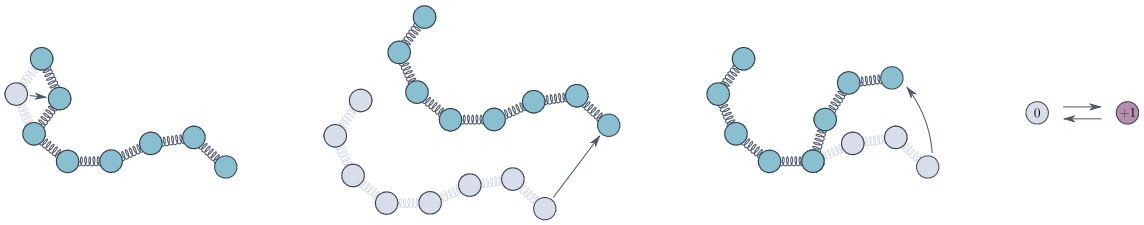

Figure 2.2: The allowed Monte Carlo moves are (a) translation of particle, (b) translation of chain, (c) rotation of subchain and (d) charge change.

2.5 Analysis

In addition to α and C, other properties were calculated such as the amount of loops, trains and tails, complex charge, radius of gyration, asphericity and persistence length.

2.5.1 Loops, Trains and Tails

The conformation properties of a polyelectrolyte-nanoparticle complex can be characterized by the distance between the nanoparticle and the monomer. If the distance

[1] The colours used in the figures (drawings and plots) are based on the colours from the Nord Palette [20].

between the nanoparticle and the monomer is less than a threshold of 8 Å (4 times the monomer radius), the monomer is characterized a belonging to trains. Monomers outside the threshold limit are characterized as a belonging to free polyelectrolytes, tails or loops depending if they are connected to 0, 1 or 2 trains, respectively. If the polyelectrolyte has at least one adsorbed monomer, it is characterized as a bound polyelectrolyte. Figure 2.3 illustrates the different characterizations. The fraction of monomers X belonging to loops, tails and trains are calculated by

$$X(Y) = \frac{\langle n_Y \rangle}{N_{\text{mon}}} \tag{2.23}$$

where $\langle n_Y \rangle$ is the number of monomers by type Y = trains, loops or tails. The total number of monomers in the polyelectrolyte is $N_{\text{mon}} = \sum_Y \langle n_Y \rangle$ [2].

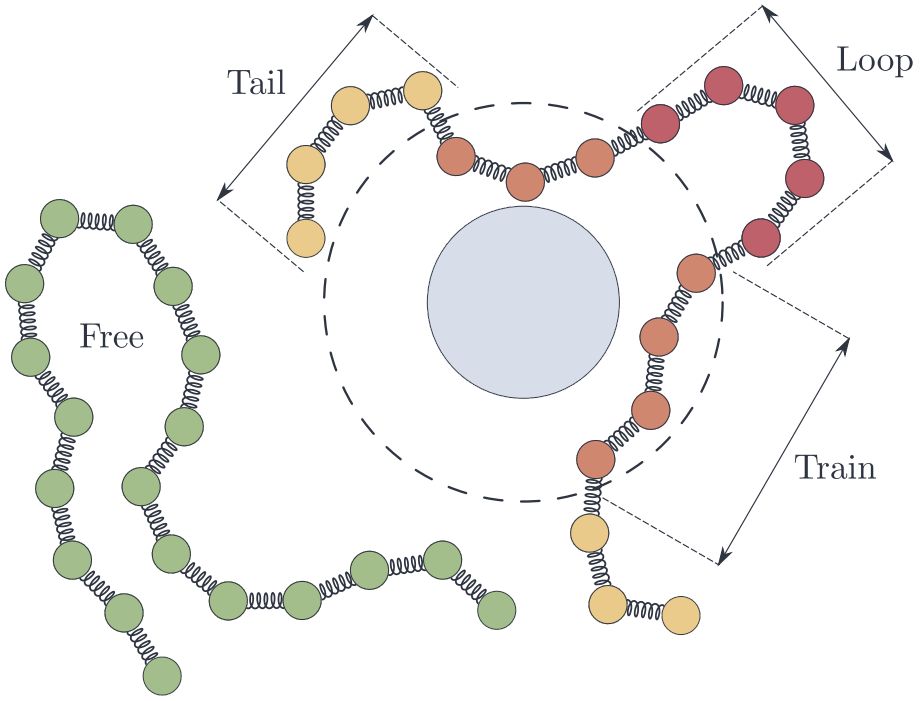

Figure 2.3: Scheme of a polyelectrolyte-nanoparticle complex. The polyelectrolyte is represented as monomers (circles) coupled together with springs. The nanoparticle is represented as the big, gray circle. The dotted circle is a representation of the adsorption threshold. Monomers on the inside of the threshold are characterised as trains (orange). A polyelectrolyte with one or more trains is a bound polyelectrolyte. Monomers on the outside of the threshold are characterised as tails (yellow) and loops (red), depending on if they are connected to one or two trains, respectively. If none of the monomers in the polyelectrolyte is inside the threshold limit, the polyelectrolyte is characterized as a free (green) polyelectrolyte. Figure 2 in [2] was used as an inspiration for this figure.

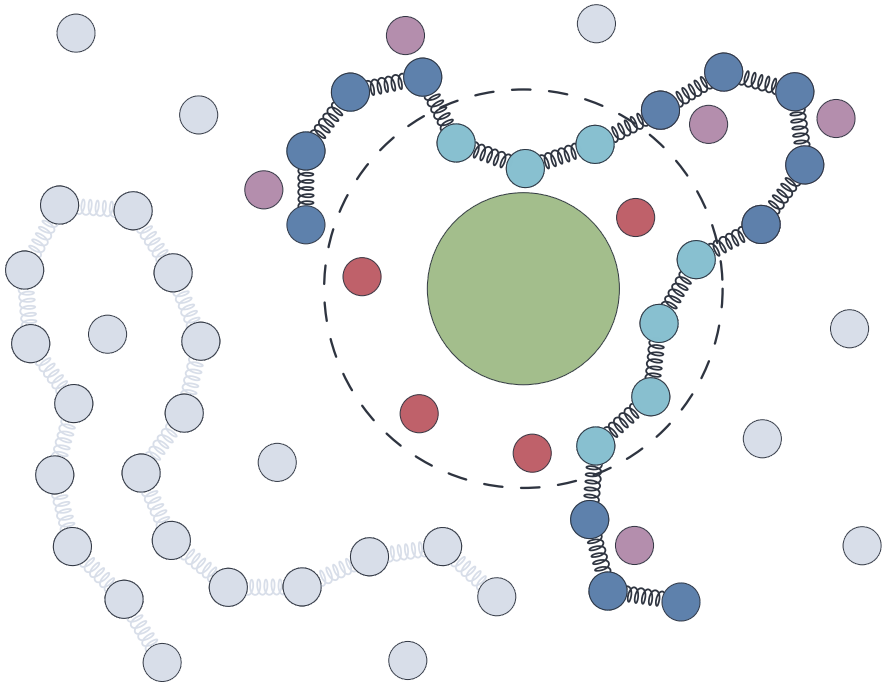

Figure 2.4: Scheme of a polyelectrolyte-nanoparticle complex. The particles in the complex that are used during calculation of the complex charge are colored (non-gray). These particles consists of all the particles inside the threshold limit (green, red and light blue) as well as the particles in loops and tails (dark blue) and the counter-/co-ions close to the monomers (purple). The polyelectrolyte is represented as monomers (circles) coupled together with springs. The nanoparticle is represented as the big, green circle. The dotted circle is a representation of the adsorption threshold. Free-floating small circles are counter-/co-ions in the system. Figure 2 in [2] was used as an inspiration for this figure.

2.5.2 Charge of a Polyelectrolyte-Nanoparticle Complex

The charge of the polyelectrolyte-nanoparticle complex Z_C is calculated as the sum of charges for all particles within the threshold limit, together with the charges of loops and tails for the polymers and the charges for the counter-/co-ions that are located close to the monomers in tails and loops (surface-surface distance $d_{\text{ss}} < 6\,\text{Å}$). These particles are represented with colour in Figure 2.4. The charge of the complexes can be calculated with

$$Z_C = \sum_{i=1}^{N_C} z_i \tag{2.24}$$

where N_C is the total number of particles in the complex, and z_i the charge for each particle [2].

Another way to present polyelectrolyte-nanoparticle charges is by only calculating the sum of charges for all particles within the threshold limit Z_r, represented by the

green, red and light blue particles in Figure 2.4. This radial charge can be calculated in the same way as Z_C, by

$$Z_r = \sum_{i=1}^{N_r} z_i \tag{2.25}$$

where N_r is the total number of particles within the threshold limit.

The radial and complex charge are theoretical models. They are used as an representation for the ζ-potential, a property that describes the electrostatic potential at a shear plane. Which plane of interest are dependent on the system itself [21]. Many properties of colloidal systems, like sedimentation and coagulation of particles in solutions, are determined by electrical charge, and therefore the ζ-potential becomes of importance [22].

2.5.3 Radius of Gyration R_g

The radius of gyration, a well used property in polymer science since it is possible to evaluate experimentally using scattering techniques [8], is given by

$$\langle R_g^2 \rangle = \frac{1}{N_{\text{mon}}} \left\langle \sum_{i=1}^{N_{\text{mon}}} (\vec{r}_i - \vec{r}_{\text{cm}})^2 \right\rangle \tag{2.26}$$

where $\vec{r}_i$ is the position vector for monomer i, $\vec{r}_{\text{cm}}$ the position of the polyelectrolyte's center of mass and N_{mon} the number of monomers in the polyelectrolyte. [23]

2.5.4 Persistence Length $\langle \ell_p \rangle$

The persistence length ℓ_p is a measure of the flexibility of a polymer chain. The polymer is considered to be flexible if $\ell_p \approx r_b$, and semi flexible if $\ell_p \gg r_b$ (worm-like) [24] where r_b is the length between two monomers, also known as bond length. The persistence lengths presented in this report are calculated by using the results for the radius of gyration, and calculated by

$$\langle \ell_p \rangle = \frac{3\langle R_g^2 \rangle}{L} \tag{2.27}$$

where L is the polymer chain length [25].

2.5.5 Asphericity $\langle \mathcal{A} \rangle$

A way of describing the asymmetry of a polymer is by the asphericity $\mathcal{A}$. It can be calculated by

$$\langle \mathcal{A} \rangle = \frac{\langle (L_1^2 - L_2^2)^2 + (L_2^2 - L_3^2)^2 + (L_3^2 - L_1^2)^2 \rangle}{2\langle (L_1^2 + L_2^2 + L_3^2)^2 \rangle} \tag{2.28}$$

where $L_1^2 \leq L_2^2 \leq L_3^2$ by definition are the square length of the axes of the equivalent ellipsoid. $\mathcal{A}$ is defined such that $\mathcal{A} = 1$ for a straight polymer, and $\mathcal{A} = 0$ for a spherical polymer. [26]

Chapter 3

Annealed Polyelectrolyte-Nanoparticle Systems

In this chapter, the annealed polyelectrolyte-nanoparticle systems will be studied. For the different system abbreviations, the reader is referred to Table 1 on page vi.

3.1 Titration Behavior

Snapshots of all the systems for selected pH values, are presented in Figure 3.1. The green chains are polyelectrolytes, the blue spheres are surface charges of the nanoparticle, the red sphere a representation of the nanoparticle with a reduced radius to enable wiving the surface charges. The purple spheres are counterions for the nanoparticle and the polyelectrolytes.

As can be observed visually, at low pH no polyelectrolytes are bound to the nanoparticle. By increasing the pH, adsorption of the polyelectrolytes increases leading to all polyelectrolytes adsorbed at pH = 10 which will be discussed more in detail in section 3.2.1. When the pH approaches 13, the polyelectrolytes desorbs and nanoparticle counterions adsorbs to the nanoparticle.

3.1.1 Average Degree of Ionisation α

The average degree of ionisation α, calculated using Equation (2.12), of the nanoparticles and polyelectrolytes are shown in Figure 3.2 as a function of pH. When the systems have a low pH, the polyelectrolytes are fully charged ($\alpha^{\mathrm{PE}} = 1$), and the nanoparticles are neutral ($\alpha^{\mathrm{NP}} = 0$). When the pH increases, the average polyelectrolyte-charge decreases, and the average nanoparticle-charge increases until the polyelectrolytes are neutral at high pH(= 14), and the nanoparticles are charged ($\alpha^{\mathrm{NP}} = 0.6$).

For the reference polyelectrolyte system in the absent of nanoparticle ($1\mathrm{PE}_a^{0\mathrm{np}}$, grey dashed curve), the curve has a similar shape to the ideal single monomer in solution,

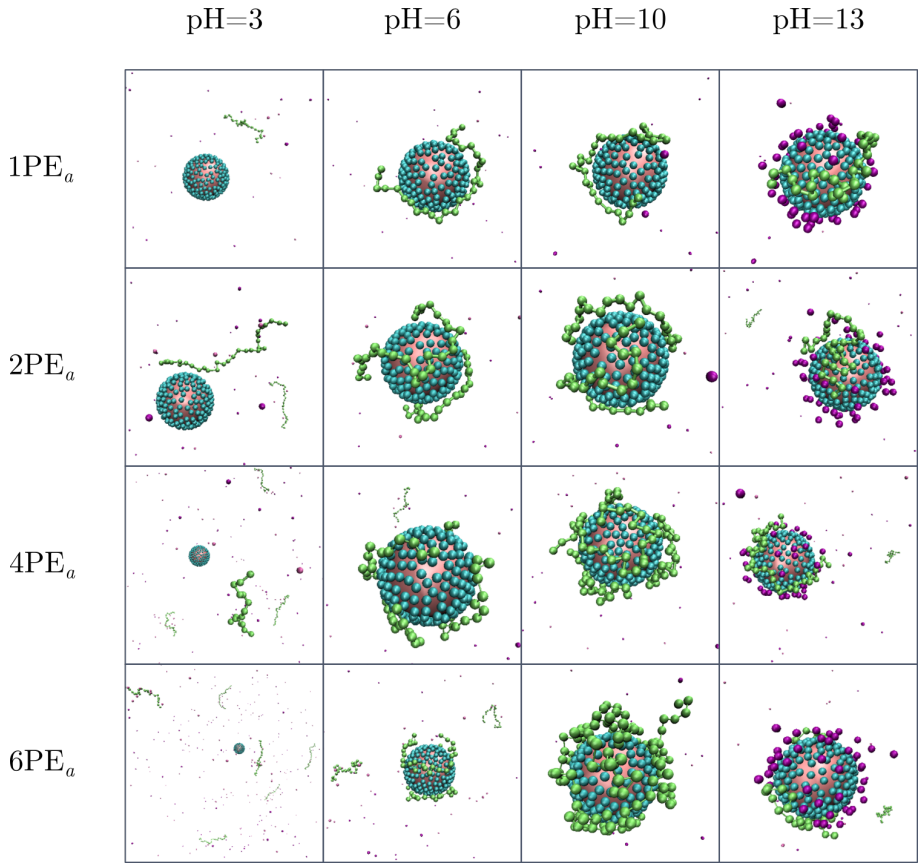

Figure 3.1: Snapshots of 1PE$_a$–6PE$_a$ for four different values of pH. The green chains are polyelectrolytes, the blue spheres are surface charges of the nanoparticle, the red sphere a representation of the nanoparticle with a reduced radius to enable wiving the surface charges. The purple spheres are counterions for the nanoparticle and the polyelectrolytes.

calculated according to Equation (2.13) with a constant degree of ionisation at extreme values of pH. The inflection point is shifted towards a lower pH value (pH = 7) for the reference system than for the ideal polyelectrolyte (pH = 9), and the change in α^{NP} is not as sensitive to change in pH, close to the inflection point, both consequences of the electrostatic repulsion within the polyelectrolyte chain [2, 13, 16].

A reference nanoparticle system in the absent of polyelectrolytes (1NP$_a^{0\mathrm{pe}}$, grey dotted curve) are included in the figure to compare the effects nanoparticles has on the nanoparticle charge. When pH increases, α^{NP} increases until reaching a maximum of $\alpha^{\mathrm{NP}} = 0.6$ when pH = 14. This is a consequence of a high density of surface charges. The effect is also described in [27], which studied charge behaviour of different surface concentrations on a nanoparticle.

Now, let us consider systems with a nanoparticle and polyelectrolytes. From Figure 3.2 it is clear that the presence of different macromolecules has an impact on the average degree of ionisation of both macromolecules, as the titration curves differ

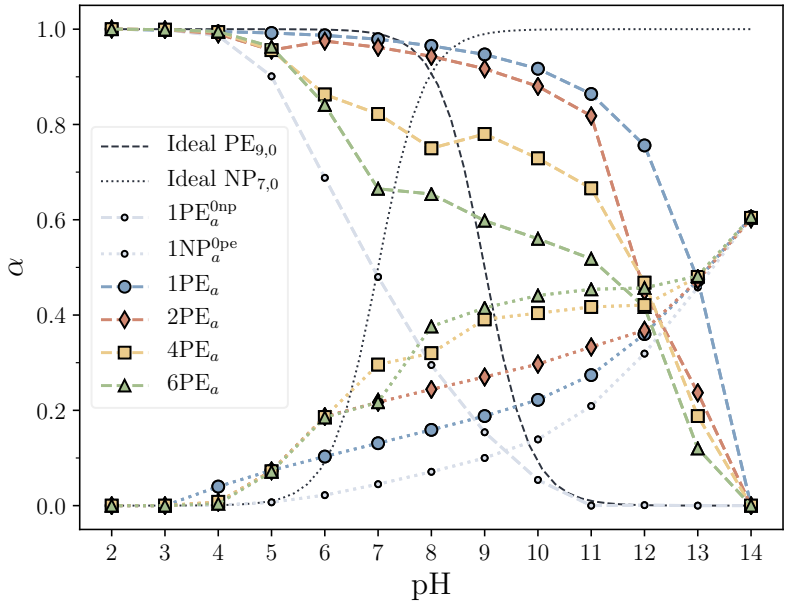

Figure 3.2: The average degree of ionisation α as a function of pH for 1-6 polyelectrolytes (PE, lines) and the corresponding nanoparticle (NP, dots) for the same system. The Ideal curve is calculated from Equation (2.13) with a pK_a of 9 for the polyelectrolytes and 7 for nanoparticle. Two reference systems consisting of i) one single polyelectrolyte (without nanoparticle) and ii) one single nanoparticle (without polyelectrolytes) are plotted in grey. The error bars are left out due to large fluctuations and to improve readability. The lines are guides to the eye

from 1PE$_a^{0np}$. The system 1PE$_a$ shows little change in α at low pH and a inflection point at pH $\approx$ 13. The behavior is discussed in [2], as the system is identical to the one used there (AP$_{9.0}$ + AN$_{7.0}$) except that Stornes and co-authors used a polyelectrolyte-chain with 90 monomers. In short, they found that the shift in the titrating curve is more pronounced with an increase in ΔpK_a between the nanoparticle and the polyelectrolyte because they will affect each others titration curves by enhancing the ionisation of each other. The system 2PE$_a$ follows approximately the same α-curve as for 1PE$_a$ up to pH = 11, but the polyelectrolytes are slightly less charged before the inflection point at pH $\approx$ 12. Worth notice, is the small dip in 2PE$_a$ at pH = 5. This happens when the system goes from one to two bound polyelectrolytes, as will be discussed in detail in section 3.2, Complex Properties.

For the systems 4PE$_a$ and 6PE$_a$, α^{PE} coincides with 1PE$_a$ at low pH followed by a rapid drop in pH $\in [5, 7]$, following approximately the same curve as the reference curve 1PE$_a^{0np}$ but with a higher α^{PE}. The curve then flattens at pH $\in [7, 11]$, as the curves did for 1PE$_a$ and 2PE$_a$ before the overall ionisation drops to zero at high pH. To summarize, adding several polyelectrolytes to a system with one nanoparticle, will make the overall ionisation of the polyelectrolytes lower in a behaviour that

seemingly combines features of bounded and non-bounded polyelectrolytes (to the nanoparticle).

Now, let us consider the nanoparticle. The average degree of ionisation for the nanoparticle α^{NP} in $1\mathrm{PE}_a$ increases when the pH increases. This is true for $2\mathrm{PE}_a$ as well, but it has a slightly higher increase for low values of pH. $4\mathrm{PE}_a$ and $6\mathrm{PE}_a$ increase even more at low pH, before reaching a saddle point when the pH approaches 11 before the ionisation continue to increase, reaching a maximum for higher studied pH. When adding more polyelectrolytes to the systems, the average degree of ionisation of the nanoparticle increases as a function of pH. The nanoparticles reaches a maximum α^{NP} below 1, as $1\mathrm{NP}_a^{0\mathrm{pe}}$.

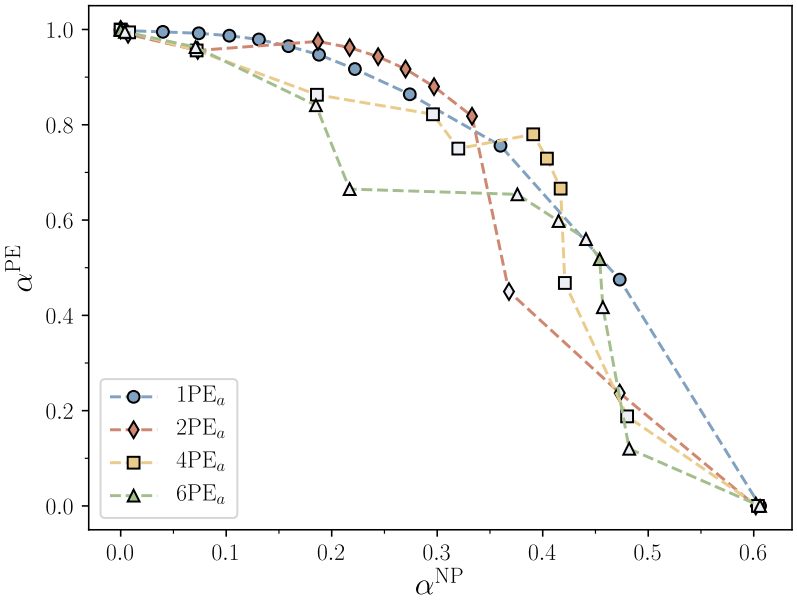

Figure 3.3: The average degree of ionisation α^{PE} for polyelectrolytes as a function of the average degree of ionisation α^{NP} of the nanoparticle. The grey markers on $1\mathrm{PE}_a$-$6\mathrm{PE}_a$ consists of at least one free polyelectrolyte, as will be presented in section 3.2.1. The lines are guides to the eye.

Adding polyelectrolytes to a system with one nanoparticle will affect the overall average degree of ionisation of the nanoparticle. To best appreciate this the ionisation of polyelectrolytes α^{PE} is plotted as a function of the ionisation of a nanoparticle α^{NP}, in Figure 3.3. In general, when α^{PE} decreases, α^{NP} increases. This results in a smooth curve for $1\mathrm{PE}_a$. For system $2\mathrm{PE}_a$, a small tendency of a step appears for α^{NP} between 0.2 and 0.4. By step, it means that α^{PE} can remain constant while α^{NP} changes before the α^{NP} remains constant while α^{PE} changes. The step behavior is more prominent the more polymers there are in the system. When the number of polyelectrolytes increases, the step appears for a lower α^{PE} (and higher α^{NP}). The step behavior is found for systems calculated with pH $\in [7, 12]$. One can clearly

see that the ionisation of a nanoparticle has great influence with the ionisation of polyelectrolytes.

3.1.2 Capacitance

The change of the average degree of ionisation with respect to pH, *i.e.* binding capacitance C calculated with equation (2.14), for both the polyelectrolytes (top) and the nanoparticles (bottom) are plotted as a function of pH in Figure 3.4. Firstly, we look at the polyelectrolytes. For the reference system $1\mathrm{PE}_a^{0\mathrm{np}}$ (dashed grey curve), it follows the same trend as previously reported by [2] that is increasing C as pH increases until pH = 6, before C decreases with further increase in pH for an annealed polyelectrolyte with $N_{\mathrm{mon}} = 90$.

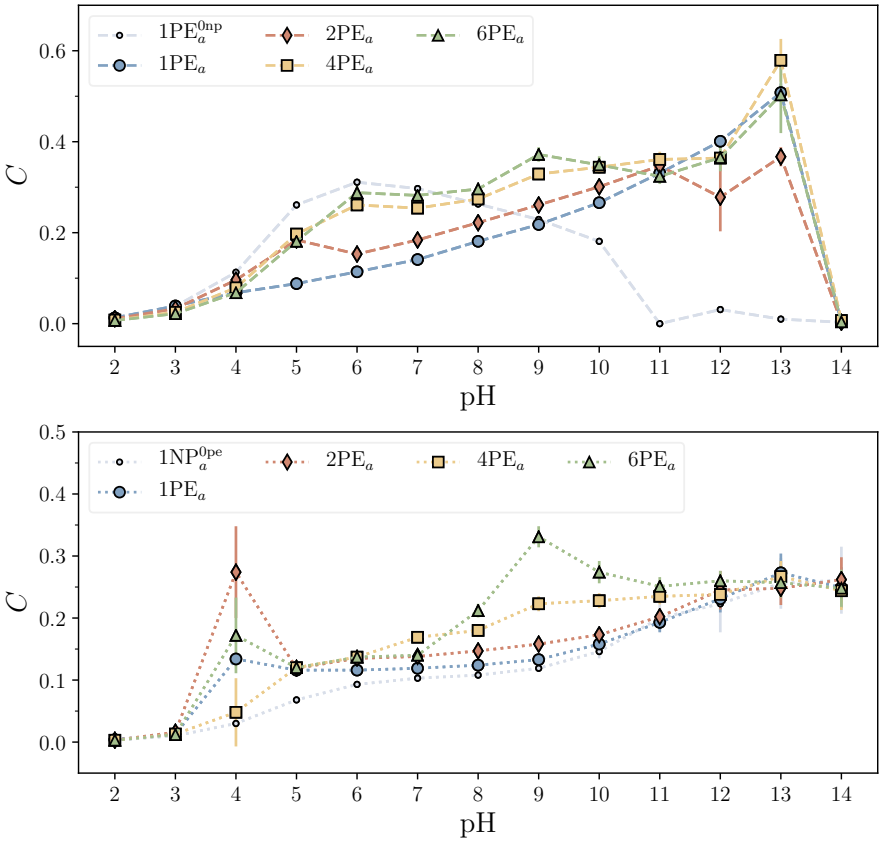

Figure 3.4: Binding capacitance C for polyelectrolytes (top) and nanoparticles (bottom) for systems consisting of one nanoparticle and $1-6$ polyelectrolytes (N_{pol}), as indicated. The lines are guides to the eye.

When a nanoparticle is present ($1\mathrm{PE}_a$, blue curve), the capacitance increases until pH is 13, then it drops to 0. Systems $2\mathrm{PE}_a$ to $6\mathrm{PE}_a$ behave approximately the same, but the more polyelectrolytes there are in the system, C has a higher value. Larger values of capacitance indicate that small variations in pH have a larger impact in ionization.

As for the capacitance of the nanoparticle, there are also significant differences between the control system $1NP_a^{0pe}$, and system with polyelectrolytes, especially for low values of pH.

An increase in polyelectrolytes also generally leads to an increase in C for both the polyelectrolytes and nanoparticle.

3.2 Complex Properties

3.2.1 Number of Adsorbed Polyelectrolytes

As the pH changes within the systems, the number of polyelectrolytes absorbed to the nanoparticle changes as well. Figure 3.5 shows how many chains are adsorbed during the titration. For extreme pH values, no polyelectrolytes are bound to the nanoparticle. This is because either the polyelectrolytes are neutral (high pH) or the nanoparticles are neutral (low pH). With no electrostatic forces present, there is no complexation.

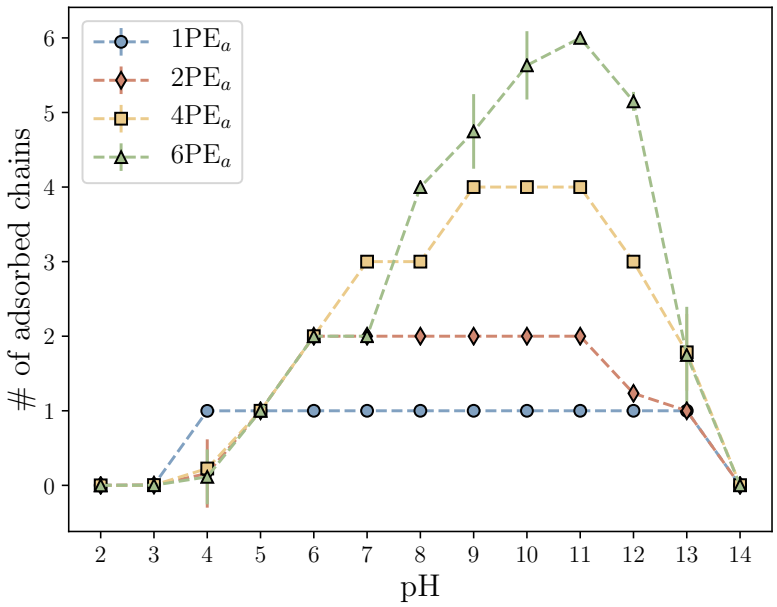

Figure 3.5: Annealed polyelectrolytes. Number of adsorbed chains as a function of pH. The lines are guides to the eye.

When both macromolecules are charged, the polyelectrolytes starts to associate to the nanoparticle. For $1PE_a$ the polyelectrolyte binds to the nanoparticle at pH = 4 and remains associated until pH = 13. For $2PE_a$, one polyelectrolyte binds at pH = 5, and the other one at pH = 6. Both polyelectrolytes remains bounded until they detach one by one, starting at pH = 11. $4PE_a$ shows the same behaviour as $2PE_a$ up to pH = 7 where the third chain adsorbs, and has all four polyelectrolytes

bounded when the pH reaches 9. $6PE_a$ also shows a step-by-step association of the polyelectrolytes and has all six bounded when pH = 10. All systems show full polyelectrolyte complexation when pH is 10 and 11.

The number of adsorbed chains are also plotted as a function of α^{PE} (left) and α^{NP} (right) in Figure 3.6 to best visualise the average charge dependence of the complexations. As α^{PE} increases, the number of adsorbed polyelectrolytes increases. The more diluted the system is (i.e the fewer polyelectrolytes in the system), the broader is the α^{PE}-range where all polyelectrolytes are bounded. Raging from a width of ≈ 0.5 for $1PE_a$ to ≈ 0.1 for $6PE_a$.

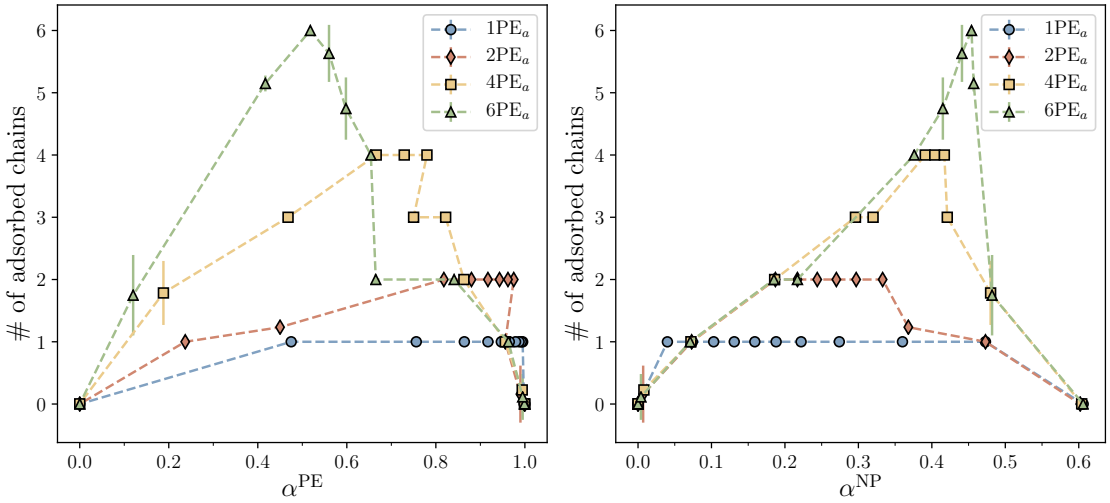

Figure 3.6: Annealed polyelectrolytes. Number of adsorbed chains as a function of α for polyelectrolytes (left) and nanoparticle (right). The lines are guides to the eye.

As expected, no chains are adsorbed when the nanoparticle or the polyelectrolyte are neutral. In $1PE_a$, one polyelectrolyte is adsorbed when α^{NP} is below 0.5. This is also true for $2PE_a$. In addition, the second polyelectrolyte is adsorbed between α^{NP} 0.15 and 0.35. For systems $4PE_a$ and $6PE_a$, all polyelectrolytes are adsorbed when $\alpha^{NP} \approx 0.4$ and $\alpha^{NP} \approx 0.45$, respectively.

If we compare thees results with Figure 3.3, one can see that when all the polyelectrolytes are bound to the nanoparticle (colored markers), $\alpha^{PE}(\alpha^{NP})$, the points of $2PE_a$-$6PE_a$ corresponds reasonably well with the simplest system, $1PE_a$. When there are free polyelectrolytes in the systems (grey markers), the ionisation shows the same plateau and drop behaviour as the reference systems. As a consequence, we see that the same degree of ionization of the polyelectrolyte, for example, is preserved, when the number of adsorbed chains varies from 2 to 4 in $4PE_a$ (Figure 3.6, α^{PE} =0.75) as highlighted in the plateau in figure 3.3. As an example, it is seen in Figure 3.3, for the pH : $6 \rightarrow 7$ ($\alpha^{NP} \approx 0.2$), that there are two bound and four free polyelectrolytes in $6PE_a$, and α^{PE} has a change of 0.2, which corresponds to the change in α^{PE} ($\alpha^{NP} \approx 0.03$) for the $1PE_a^{0np}$-$1NP_a^{0pe}$ system.

To summarise, the nanoparticle collects the most polyelectrolytes when $\alpha^{\mathrm{NP}} \in [0.35, 0.45]$. The ionisation of the polyelectrolytes are not that distinct, since every system has different ionisation degree when all the polyelectrolytes are adsorbed, at $\alpha^{\mathrm{PE}} \in [0.5, 1]$, $[0.8, 0.95]$, $[0.65, 0.8]$ and ~ 0.55 for $1\mathrm{PE}_a$, $2\mathrm{PE}_a$, $4\mathrm{PE}_a$ and $6\mathrm{PE}_a$ respectively.

3.2.2 Loops, Trains and Tails

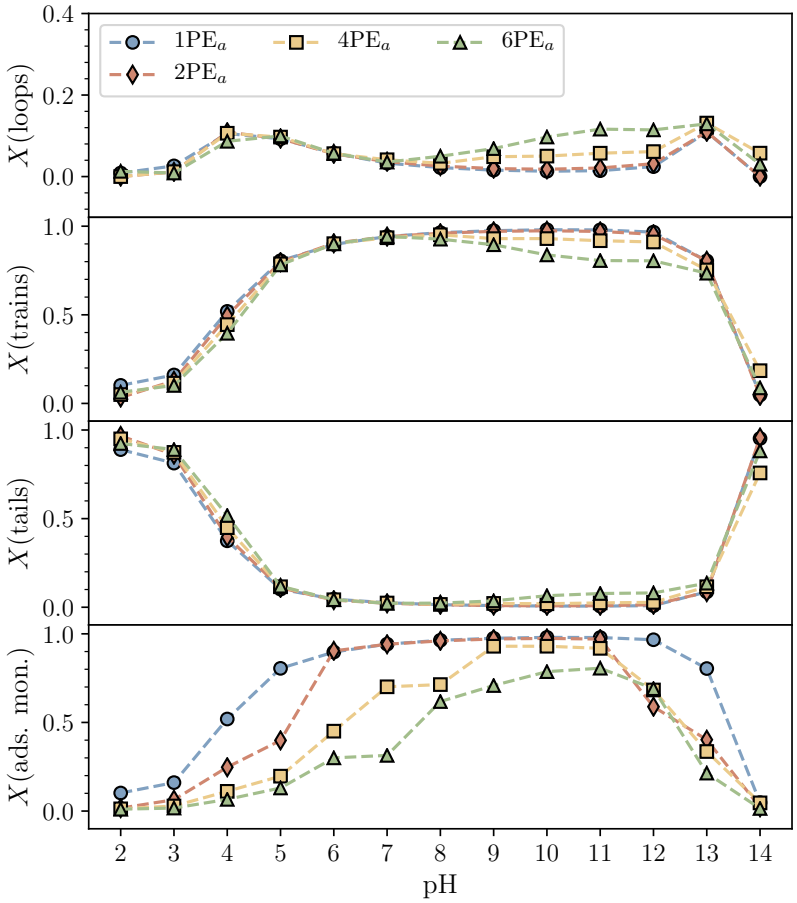

Figure 3.7: Fraction $X(Y)$ of monomers in Y = loops, trains and tails for the adsorbed polymers in each system (top three panels). Adsorbing distance is set to 30 Å from the center of the nanoparticle. The bottom panel shows the fraction of adsorbed monomers, also taking into account non-adsorbed chains. The lines are guides to the eye.

The fraction $X(Y)$ of monomers in loops, trains and tails in the polyelectrolyte-nanoparticle complexes are plotted in Figure 3.7 as a function of pH. For low pH, all systems consists of mostly tails. As the pH increases, the number of monomers

in trains and loops increases before the amount of trains becomes dominant around pH = 4. Consequently, the fraction of loops and tais decreases until pH = 7.

When pH increases further, there are differences in each system. First, the amount of monomers in tails, loops and trains for $1PE_a$ remains unchanged until pH = 12, where the amount of loops and tails increases, and the amount of trains decreases, consistent with a weaker adsorption and eventual desorption. $2PE_a$ shows about the same behavior as $1PE_a$. $4PE_a$ shows a larger fraction of of monomers in loops and tails for pH $\in [8, 12]$, and a decrease in X(trains) compared to $1PE_a$. $6PE_a$ behaves similar to $4PE_a$, but has even more increase/decrease compared to $1PE_a$. 95 % of the monomers in bounded polyelectrolytes are in trains at pH = 7.

The bottom panel in Figure 3.7 shows the fraction of adsorbed monomers, also taking into account non-adsorbed chains. For a pH $\in [6, 11]$, approximately all polyelectrolytes are connected to the nanoparticle in $1PE_a$ and $2PE_a$. This is partially the case for $4PE_a$ as well when the pH is between 9 and 11. For $6PE_a$, the number of adsorbed monomers increases for all pH, until a maximum is reached when pH = 10, with a total of 148 adsorbed monomers (of 180 available).

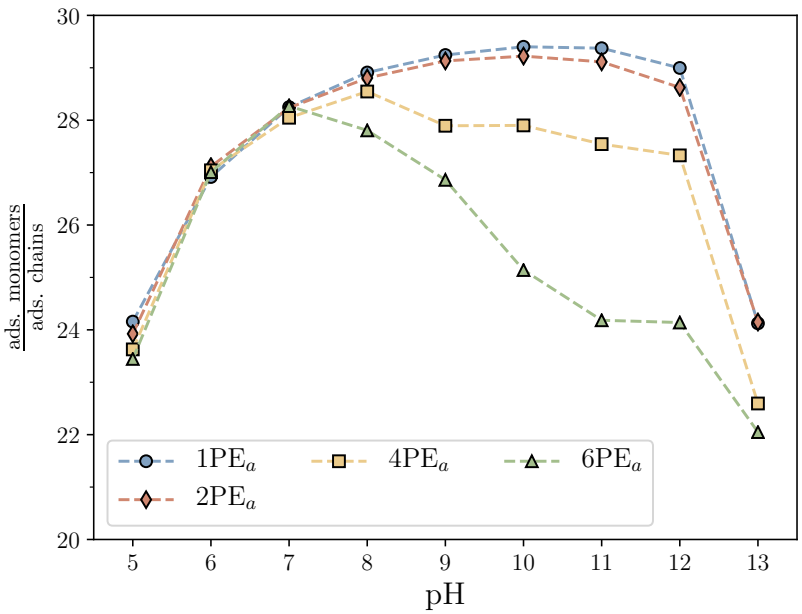

Figure 3.8: Ratio between the number of adsorbed monomers and the number of adsorbed chains as a function of selected pH-values. The lines are guides to the eye.

To compare the number of adsorbed monomers (Figure 3.7) with the number of bounded chains (Figure 3.5), one can look at their ratio in terms of pH. This is plotted in Figure 3.8. The plot is limited between pH = 5 and pH = 13 for readability, since for extreme values of pH both the number of adsorbed chains and monomers tend to 0.

In $1PE_a$, the amount of adsorbed monomers per chain increases as a function of pH, before it decreases after pH = 11. The polyelectrolytes are therefore close packed around the nanoparticle. The same is true for $2PE_a$. In $4PE_a$, the ratio increases up to pH $\approx$ 7 where three chains are adsorbed. About 28 monomers per chain are adsorbed until pH reaches 12, before the ratio drops.

For $6PE_a$, the ratio increases until pH $\approx$ 7 where two polyelectrolytes are bound. When the pH increases further, the ratio decreases and the number of adsorbed polyelectrolytes reaches 6 at pH = 11. One polyelectrolyte desorbs at pH = 12, but the ratio remains constant. At further increase in pH, the number of adsorbed monomers drops even more, leaving $^2/_3$ of the monomers bounded in the last 2 adsorbed polyelectrolytes.

3.2.3 Contact Profile

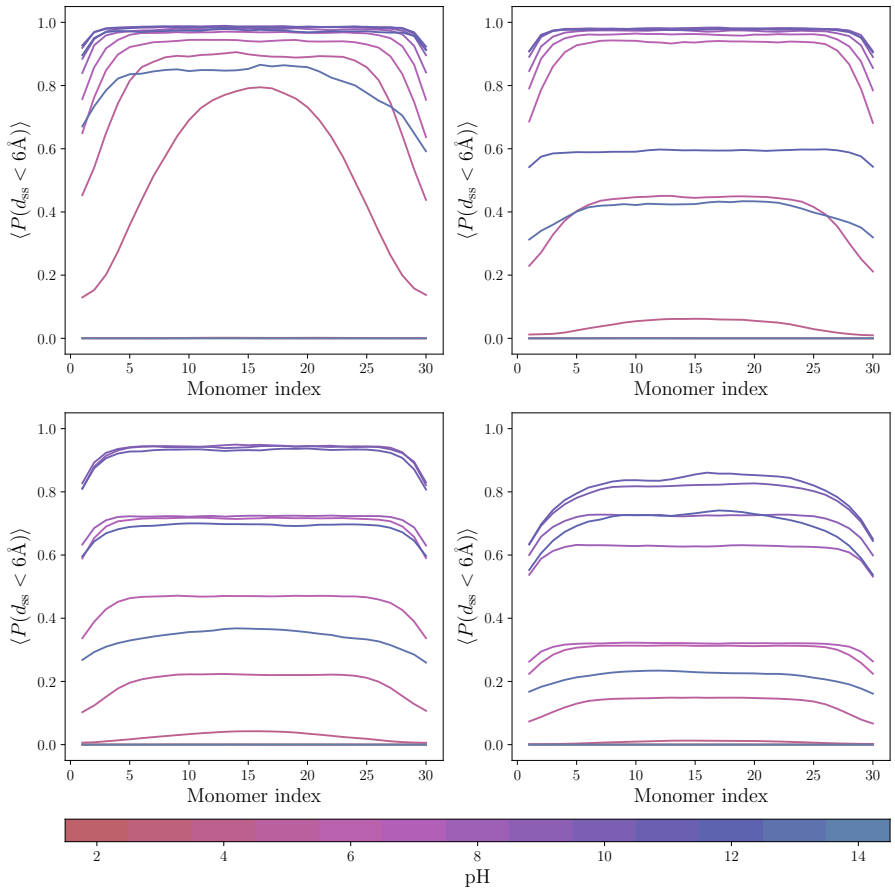

Figure 3.9: Averaged probability distribution of the contact profiles for $1PE_a$ (top left), $2PE_a$ (top right), $4PE_a$ (bottom left) and $6PE_a$ (bottom right). The pH in the system ranges from 2 (red) to 14 (blue).

The averaged probability distribution of the contact profile for polyelectrolytes adsorbed to the nanoparticle is presented in Figure 3.9 The contact profiles of the

individual polyelectrolytes can be viewed in Figure B.1, B.2, B.3 and B.4. The contact profiles show where along the polyelectrolyte chain the nanoparticle are most likely to be bounded to *i.e.* has a surface-surface distance d_{ss} of less than 6 Å between the monomers in the polyelectrolyte and the nanoparticle.

For all systems the probability of contact between the polyelectrolyte and nanoparticle increases with pH up to a certain values, after which there is a decrease towards zero for pH 14. Another general trend is that the middle of a polyelectrolyte is more likely to be in contact with the nanoparticle in comparison to the ends due to increased entropy in the ends and a weaker electrostatic attraction towards the nanoparticle. In 1PE_a and for pH = 4 the difference in probability-contact between the ends and the middle is ≈ 0.6, compared to a difference of 0.1 for larger pH ≈ 12. This behavior is in good agreement with the fraction of tails in Figure 3.7 where the system has the most monomers in the tail (low contact probability) at pH = 4, and a high probability of contact for the whole chain at pH = 12, corresponding to a low fraction of tails.

System 2PE_a has an almost identical contact profile as 1PE_a for pH $\in [6, 11]$. For pH values outside this interval the probability distribution is lower, approaching $1/2$ of the probability as for 1PE_a. This is a consequence of the data normalization. For values outside the interval there are one bound and one free polyelectrolyte. The free contributes with $P = 0$ for one whole chain, and the bound with $P > 0$ to the average.

The free polyelectrolytes contribution towards $P = 0$ (or the lack of contribution) is larger in 4PE_a than 2PE_a since for pH-values there are more free polyelectrolytes. Another distinction in 4PE_a compared to 1PE_a is that when all polyelectrolytes are bound at pH $\in [9, 11]$, the difference in P between the ends and the middle of the polyelectrolyte chain is larger, *i.e.* the tails are longer. In addition, the maximum probability value is lower. As a result, the polyelectrolyte consists of more loops which is confirmed by figure 3.7.

For 6PE_a, the identified characteristics of 4PE_a have an even larger weight, resulting in longer tails and loops for bound polyelectrolytes when all polyelectrolytes in the system are bounded, with the free polyelectrolytes contribution to the dampening factor. When all the polyelectrolytes are bound, the tails are longer for this system than 1PE_a.

In further studies, one could plot the average probability distribution for only the bound polyelectrolytes, to prevent the damping effect from the free polyelectrolytes. This could be done to compare the length of the tails, and the occurrences of loops in another way.

3.2.4 Charge profile

To appreciate the impact of monomer adsorption onto the monomer ionization, the charge profile of a polyelectrolyte in the absence ($1\text{PE}_a^{0\text{np}}$) and presence ($1\text{PE}_a$) of

the nanoparticle has been calculated and presented in Figure 3.10. For the reference system, there is a charge difference between the ends and the middle of the polyelectrolyte when pH $\in [5, 9]$. This is due to electrostatic repulsion within the chains as also discussed in [1] and [28]. Outside pH $\in [5, 9]$, the charges are distributed more evenly along the whole chain due to high/low ionisation degree.

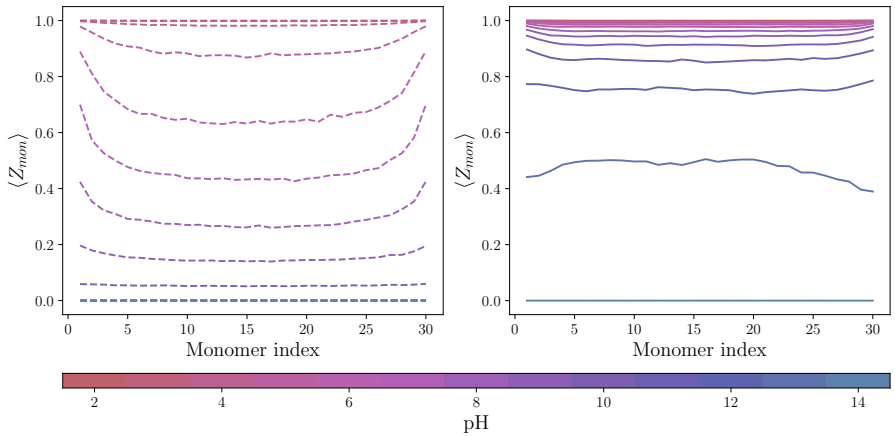

Figure 3.10: Average charge per monomer for $1PE_a^{0np}$ (left) and $1PE_a$ (right).

It can be observed that the polyelectrolyte charge profile is greatly affected by the addition of a nanoparticle. In system $1PE_a$, the polyelectrolyte is fully charged for low pH, and neutral when the pH = 14. At those pH, there is no charge difference between the ends and the middle of the polyelectrolyte. When pH = 13, the polyelectrolyte is charged, with a slightly higher charge for the monomers in the middle of the chain, than for the ends. When the pH decreases further, the charge of each monomer increases. For low pH-values, the ends of the polyelectrolyte are slightly more charged than the monomers in the center, but the charge difference between the middle and ends is lower than for $1PE_a^{0np}$. Since the contact profile in Figure 3.9 shows a higher contact probability towards the center of the polyelectrolyte, this results in a stronger ionisation of those monomers to minimise the energy of the system, leading to the more uniform charge distribution.

Figure 3.11 shows the average charge per monomer for each individual polyelectrolyte in $2PE_a$-$6PE_a$, and highlighted the different behaviour of the in the same system for some pH values. The figure is expanded in Figures B.5, B.6 and B.7 for readability.

In system $2PE_a$, and for extreme pH-values, both polyelectrolytes are either fully charged or neutral, but for pH = 5, $12 \wedge 13$, one polyelectrolyte is charged (with approximately the same charge as in $1PE_a$) and one polyelectrolyte is charged as $1PE_a^{0np}$. This corresponds to one bound and one free polyelectrolyte. When pH ≤ 11, *i.e.* both polyelectrolytes are adsorbed, the two polyelectrolytes have approximately equal charge. See figure B.5 for respective pH-values. Worth notice is that the average degree of ionisation α^{PE} increases, as also seen in figure 3.2, when the pH

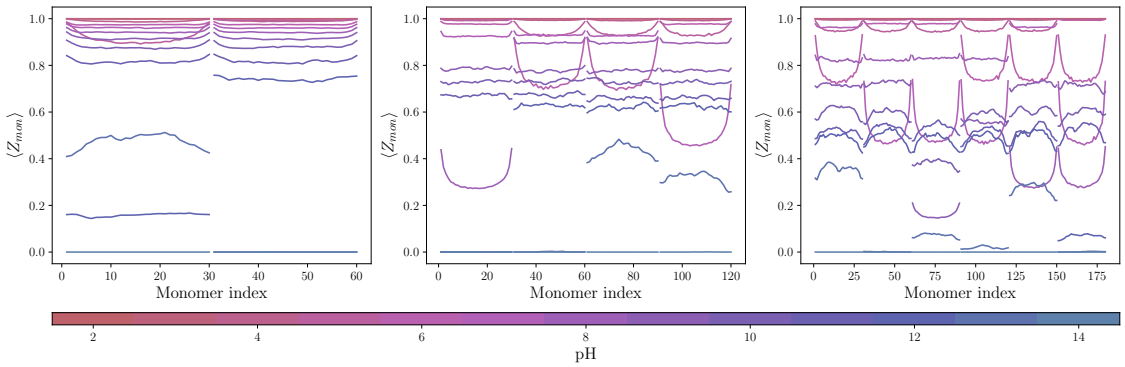

Figure 3.11: Average charge per monomer as a function of monomer index for $2PE_a$ (left), $4PE_a$ (middle) and $6PE_a$ (right). The pH in the system ranges from 2 (red) to 14 (blue).

goes from 5 to 6. This shows a further ionisation of the polyelectrolyte to minimise the energy of the system, as only described for $1PE_a$ in comparison to $1PE_a^{0np}$.

For systems $4PE_a$ and $6PE_a$, there are large variations between each polyelectrolyte for more pH values. This is a consequence of more free polyelectrolytes. The free polyelectrolytes possess a similar charge profiles as $1PE_a^{0np}$, and the bounded have approximately the same charge profiles as $1PE_a$, with two exceptions: i) the bounded polyelectrolytes have a higher charge in the middle of the chain than in the ends when pH = 13 ($2PE_a$, $4PE_a$) and pH $\in [9, 13]$ ($6PE_a$). This is because the tails in the polyelectrolytes tend to be more neutral/ have a charge distribution more equal the free polyelectrolyte in $1PE_a^{0np}$. ii) more than two distinct distribution profiles exists because of equilibrium behaviour of the systems *e.g.* at pH = 13, $4PE_a$ fluctuates between one and three bound polyelectrolytes and $6PE_a$ between three and four bound polyelectrolytes as been observed by video analysis of the systems. In future work, one can run the simulations for these fluctuating systems longer to see if they reach a stable equilibrium.

Figure 3.12 gathers the average of all polyelectrolytes in each system in figure 3.11, according to

$$\overline{\langle Z_i \rangle} = \frac{1}{N_{\text{pol}}} \sum_{j=1}^{N_{\text{pol}}} \langle z_{ij} \rangle, \tag{3.1}$$

where N_{pol} is the number of polyelectrolytes in the system, and $\langle z_{ij} \rangle$ the ensemble average over the charge of monomer index i of polyelectrolyte j.

Since $1PE_a$ in Figure 3.12 is exactly the same plot as $1PE_a$ in Figure 3.10 the following paragraphs compares to the previous description of $1PE_a$ in Figure 3.10.

System $2PE_a$ differs from $1PE_a$ in that the the averaged monomer charge is approximately half the value for pH $\in [12, 13]$ due to the presence of one free and one bound polyelectrolyte. When both polyelectrolytes are bound, the total average charge is slightly lower than for $1PE_a$.

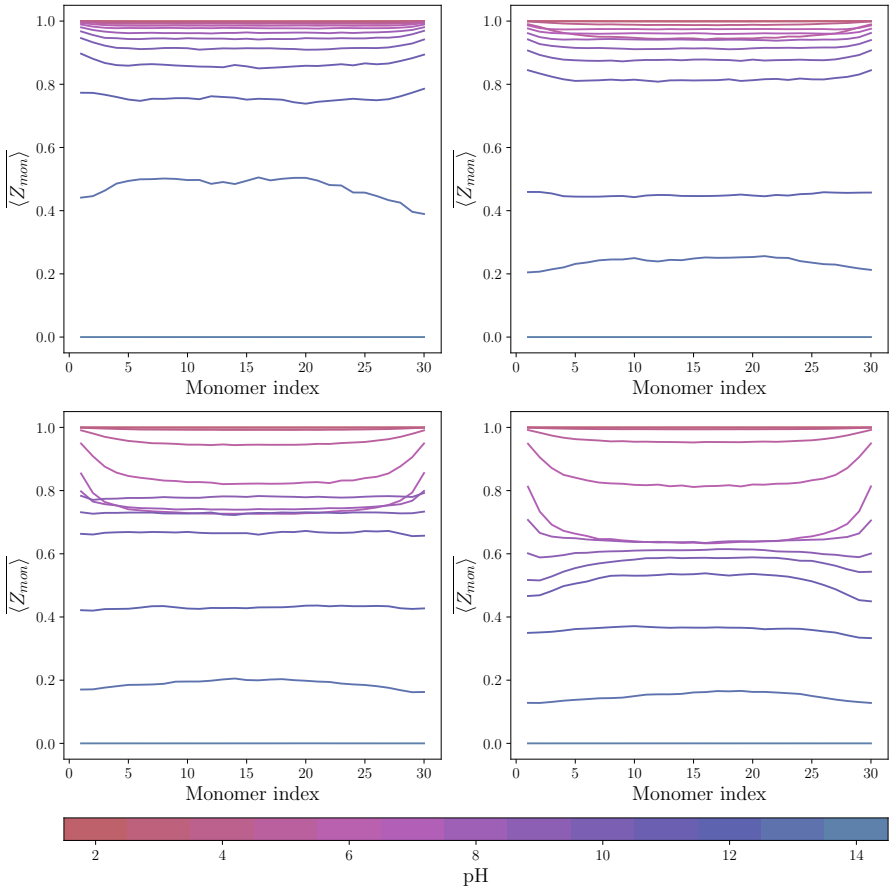

Figure 3.12: Average of the average charge per monomer for the system with 1 (top left), 2 (top right), 4 (bottom left) and 6 (bottom right) polyelectrolytes. The pH in the system ranges from 2 (red) to 14 (blue). The standard mean error is excluded due to readability.

In system 4PE_a, the charges are evenly distributed for extreme values of pH, but when the pH $\in [5, 8]$, the ends of the polyelectrolytes are more charged than the middle. This effect is even bigger in 6PE_a. In addition, 6PE_a has a local maxima in the middle and in the ends when pH $= [9]$. The double maxima has also been described in systems with annealed polyelectrolytes and a quenched nanoparticle [1], and is observed because 6PE_a consists of both bound (with a maxima in the middle and minima in the ends) and free (with a minima in the middle, and maxima in the ends) polyelectrolytes.

In further studies one could look at the charge difference between the ends and the middle, as Stornes and co-authors did [1]. They defined charge difference between the ends and the middle of the polyelectrolyte $\Delta Z = Z_{\text{end}} - Z_{\text{mid}}$ and plotted it as a function of α^{PE} for the adsorbed polyelectrolytes only. they found that a bounded polyelectrolyte has a lower ΔZ than a free polyelectrolyte, and a negative ΔZ for $\alpha^{\text{PE}} \in [0.2, 0, 3]$ which in our case is obtained for 1PE_a when $\alpha^{\text{PE}} \approx 0.45$ at pH $= 13$.

3.2.5 Charge Probability Distribution

Figure 3.13 shows the overall charge probability of the polyelectrolytes as a function of pH for different polyelectrolyte concentrations. For all systems, when the pH increases, α^{PE} decreases.

When all polyelectrolytes are in the same state (bound or free) they give rise to an unimodal probability distribution. This occurs at α^{PE} close to 0 or 1 (free), or at pH = 10 (bound). A bimodal distribution function occurs when both states are present in the system, which happens more frequently in $4\mathrm{PE}_a$ and $6\mathrm{PE}_a$ as a consequence of a higher concentration of polymers. The polyelectrolyte that are associated with the nanoparticle concentrate more charge than the free polyelectrolyte as also discussed in [1].

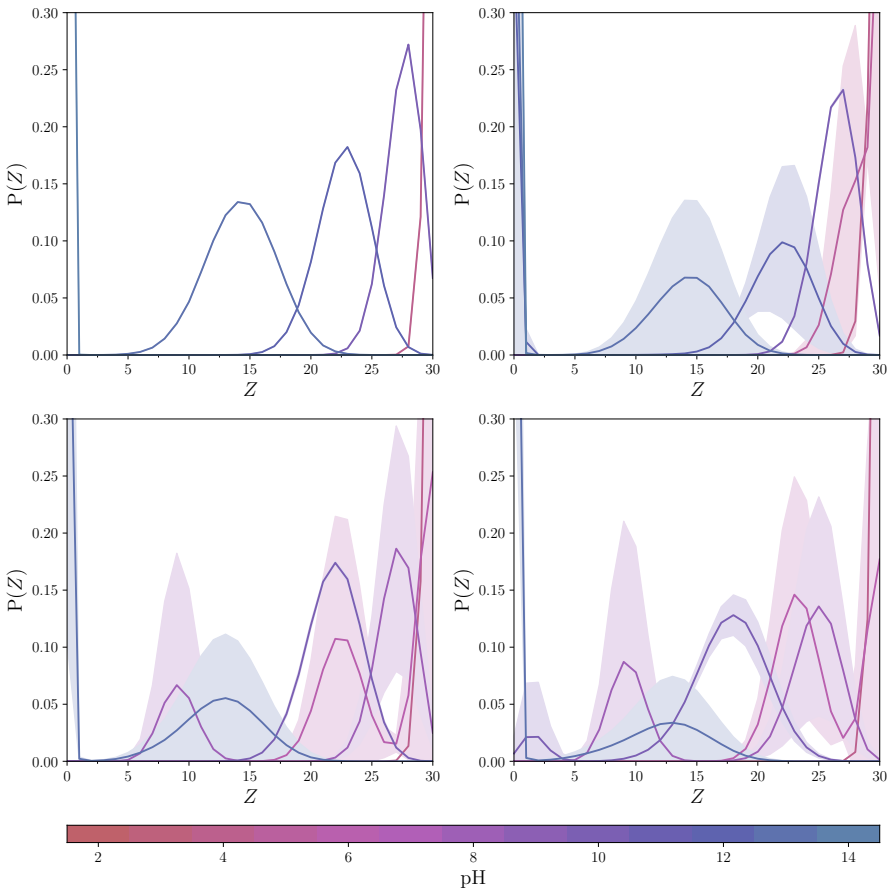

Figure 3.13: Charge probability distribution as a function of the polyelectrolyte charge for selected values of pH. The systems are $1\mathrm{PE}_a$ (top left), $2\mathrm{PE}_a$ (top right), $4\mathrm{PE}_a$ (bottom left) and $6\mathrm{PE}_a$ (bottom right).

3.2.6 Complex and Radial Charge

The complex Z_C and radial charge Z_r as a function of pH for 1PE$_a$–6PE$_a$ are shown in Figure 3.14. Recall that Z_r and Z_C are calculated based on the nanoparticle and ignore the free polyelectrolytes (see section 2.5.2 for details).

When pH = 2, the "complex" consists of only one neutral nanoparticle, which gives $Z_C = 0$. As the pH rises towards 4, one polyelectrolyte binds to the nanoparticle in 1PE$_a$, increasing Z_C. The complex charge decreases when the pH is further increased and the complex charge goes from overcharged to negatively charged at pH between 6 and 7 before reaching a minimum at pH = 14 where the complex consists of only the nanoparticle and counterions.

As the concentration of polyelectrolytes increases: i) the maximum value of Z_C shifts towards a higher pH (between 5 and 6); ii) 2PE$_a$–6PE$_a$ follows approximately the same curve until pH = 7 when new polyelectrolytes bind to the nanoparticle in 4PE$_a$ and 6PE$_a$ systems, resulting in a slower decrease/increase in Z_C; and iii) the point where the complex goes from being overcharged to negatively charged (isoelectric point) also shifts to higher pH values.

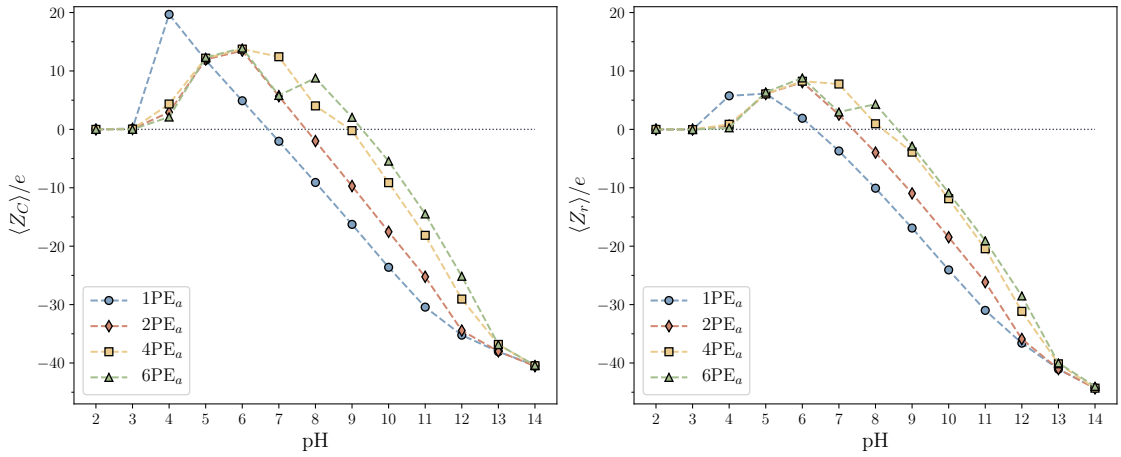

Figure 3.14: Annealed polyelectrolytes. Average complex Z_C (left) and radial Z_r (right) charge as a function of pH. The lines are guides to the eye.

The radial charge Z_r follows the same trends (i-iii) as the complex charge, but has a lower maximum value because Z_r does not take into account the positively charged loops and tails of the bound polyelectrolytes. As a consequence of this, the point where the system goes from being overcharged to negatively charged shifts towards a lower pH. Another distinction is that for pH $>$ 9 in 4PE$_a$ and 6PE$_a$, the Z_r are approximately the same. This can be an indication that the polyelectrolyte-nanoparticle complex has a maximum Z_r it can obtain for a certain pH, regardless of the increase in polyelectrolyte concentration over a certain value. Resulting in more tails and loops for 6PE$_a$, as discussed earlier.

The complex and radial charge as a function of pH is in good agreement with

experimental values of ζ-potential as the degree of shift in ζ potential increased with the concentration of branched polyethylenimine (polyelectrolytes) interacting with spherical particles of silica (nanoparticle) in water [29].

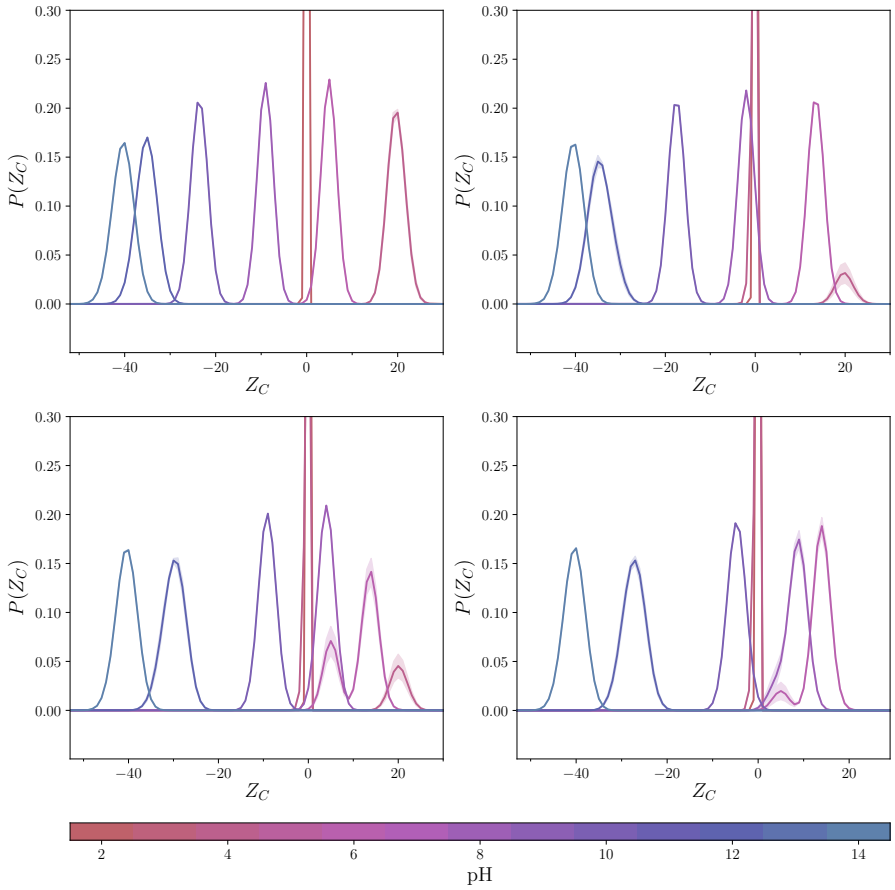

Figure 3.15: Probability distribution of the complex charge Z_C for 1PE$_a$ (top left), 2PE$_a$ (top right), 4PE$_a$ (bottom left) and 6PE$_a$ (bottom right). The pH in the system ranges from 2 (red) to 14 (blue). The shaded areas are the standard deviation error of the systems.

Figure 3.15 shows the probability distribution of the complex charge $P(Z_C)$ for systems with pH between 2 and 14. As expected, the complex charge probability varies with the pH. At low pH the complex charge value is positive due to adsorption of the polyelectrolyte chains, and at high pH the complex charge value is negative, reflecting the charge of the nanoparticle and associated counterions, as also seen in Figure 3.14 and discussed above. It is interesting to point out that the probability distributions are bimodal in nature in the systems with $N_{pol} > 1$ and certain pH conditions (*e.g.* for pH $= 6$ in the systems with $N_{pol} \in [4, 6]$ and for pH $= 4$ in the systems with $N_{pol} \in [2, 4]$).

Figure 3.16 shows the probability distribution of the radial charge $P(Z_r)$. The behaviour is very similar to what observed for $P(Z_C)$ but the distributions that were clearly bimodal in figure 3.15 is less evident in Figure 3.16. This indicates that

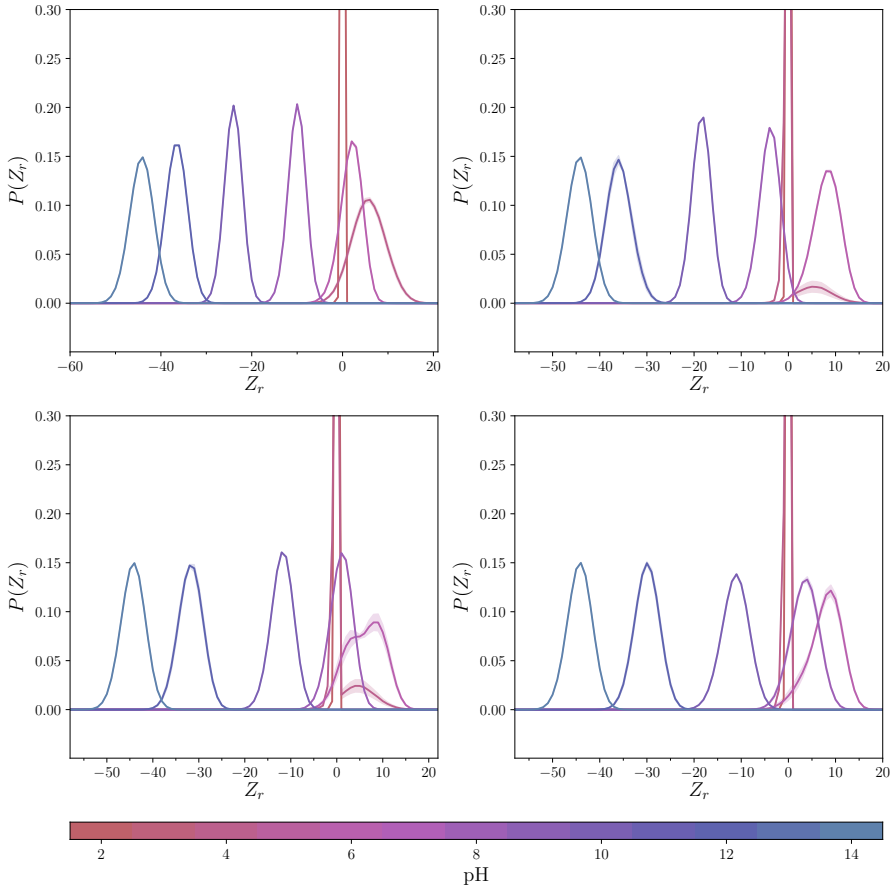

Figure 3.16: Probability distribution of the radial charge Z_r for 1PE_a (top left), 2PE_a (top right), 4PE_a (bottom left) and 6PE_a (bottom right). The pH in the system ranges from 2 (red) to 14 (blue). The shaded areas are the standard deviation error of the systems.

the charge of the tails and their associated counter ions has an impact on one of the normal distributions component in the bimodal distribution for the system's charge.

At pH close to 2, there is a quite distinct probability for both Z_C and Z_r, that the charge is 0 because the nanoparticle is neutral and does not attracting polyelectrolytes or counterions. For larger pH, distributions become broader indicating some charge variations within each system.

Since the Z_C and Z_r show approximately the same behaviour, only Z_C as a function of α^{PE} and α^{NP} is presented (Figure 3.17). As α^{PE} increases, Z_C increases. In 1PE_a and 2PE_a, the Z_C is quite stable for $\alpha^{\text{PE}} < 0.8$. When α^{PE} increases further, Z_C greatly increases. In 4PE_a, Z_C increases slowly until rapidly increasing at $\alpha^{\text{PE}} \approx 0.7$. 6PE_a shows the same behaviour as 4PE_a, but has the rapid increase occurs when $\alpha^{\text{PE}} \approx 0.6$.

The complex charge decreases when α^{NP} increases, except when $\alpha^{\text{NP}} < 0.05$ for 1PE_a and 2PE_a and $\alpha^{\text{NP}} < 0.2$ for 4PE_a and 6PE_a. As for the complex charge with

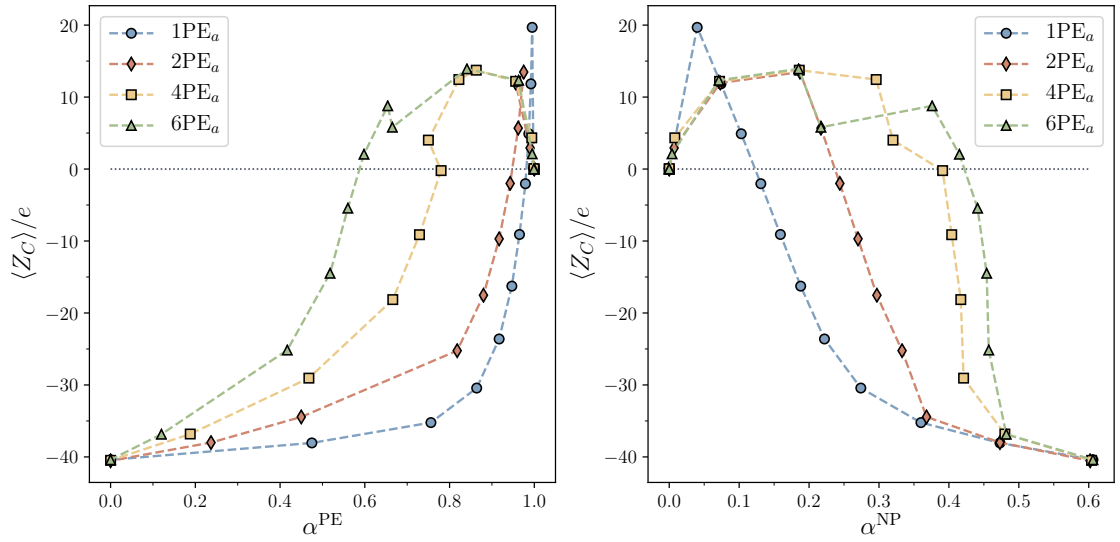

Figure 3.17: Annealed polyelectrolytes. Average complex charge Z_C as a function of α for a polyelectrolyte (left) and nanoparticle (right). The lines are guides to the eye.

respect to α^{PE}, the complex charge also shows a significant drop in $\langle Z_C \rangle$ for the systems with higher concentrations of polyelectrolytes occurring at $\alpha^{\mathrm{NP}} \approx 0.40$ for 4PE$_a$ and $\alpha^{\mathrm{NP}} \approx 0.40$ for 6PE$_a$. Such step functions indicate that in certain pH ranges the α^{PE} stays mostly constant with Z_C becoming more negative due to the deprotonation of the nanoparticle and vice-versa.

3.3 Conformational Properties

3.3.1 Radius of Gyration R_g

Figure 3.18 shows the probability distribution of the radius of gyration $P(R_g)$ for the four different polyelectrolyte-nanoparticle systems (1PE$_a$ to 6PE$_a$), and the control system 1PE$_a^{0\mathrm{np}}$ for selected values of pH. In 1PE$_a$, the maximum value of $P(R_g) \approx 0.15$ when pH $\in [2,4] \wedge [13,14]$, and increases to $P(R_g) \approx 0.35$ when pH $\in [5,12]$, *i.e.* and starting with a low pH value, the $P(R_g)$ shifts to lower R_g values and becomes shorter, and a further increase in pH shifts the $P(R_g)$further to the left and becomes again broader. The distributions for the extreme pH values correspond well both in position and shape of the free polyelectrolyte at the corresponding pH. The sharp $P(R_g)$ at around pH $\in [5,12]$ indicating that the polyelectrolyte is in close contact with the nanoparticle, matching the $R_g \approx 25\,\text{Å} \gtrsim r_{\mathrm{NP}}$. This is consistent with Figure 3.7, since the fraction of trains and adsorbed monomers is highest for these pH-values.

The system 2PE$_a$ follows the same main trends as 1PE$_a$, except for three distinctions: i) A bimodal distribution appears when pH $= 5$. This is an indication of one free and one bound polyelectrolyte in the system, which is confirmed by a visual

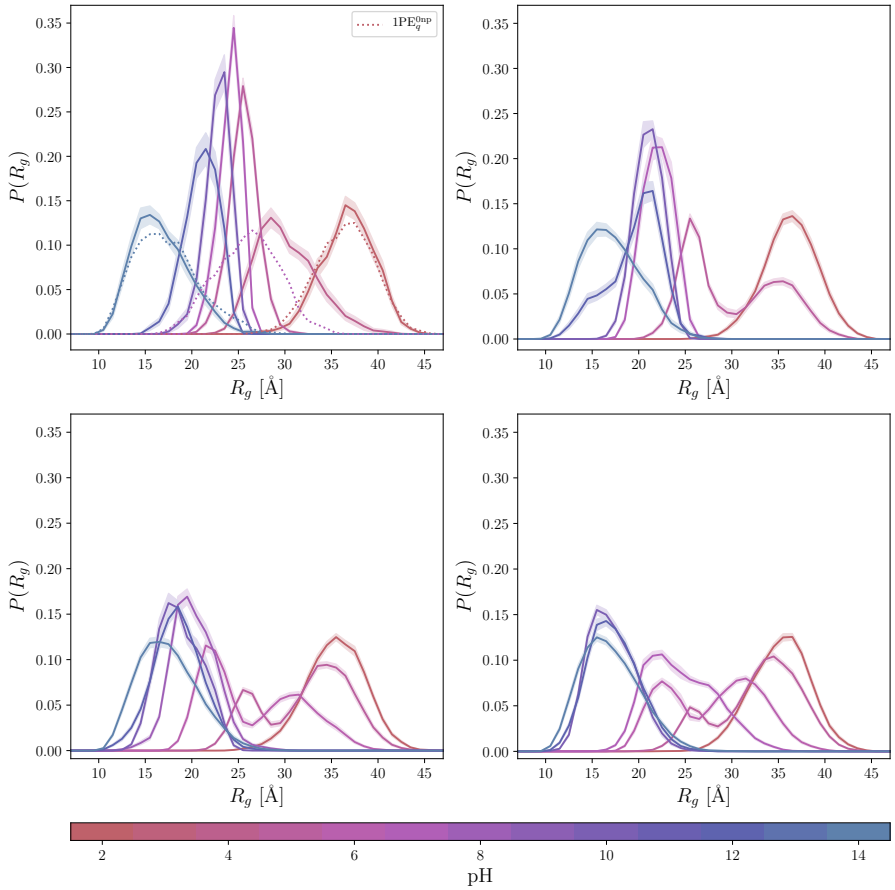

Figure 3.18: Probability distribution of the radius of gyration for the system with 1 (top left), 2 (top right), 4 (bottom left) and 6 (bottom right) annealed polyelectrolytes. The pH in the system ranges from 2 (red) to 14 (blue). The shaded areas are the mean square error of the systems. A free polyelectrolyte (top left, $1PE_a^{0np}$) is included as a reference system (dotted line) for pH $\in [2, 7, 14]$. Note the bimodal probability distribution function at pH = 5 for $2PE_a$-$6PE_a$, as a representation of both free and bound polyelectrolytes.

representation in Figure 3.19; ii) The distribution is narrower when pH $\in [5, 12]$ and the mean R_g is decreased, matching the $R_g \approx 22\,\text{Å} \approx r_{\text{NP}}$; and iii) A bimodal distribution appears when pH = 12, which indicates that the system again consists of both bound and free polyelectrolytes.

$4PE_a$ follows the same trends as $2PE_a$, but there are three additional distinctions: i) A bimodal distribution also appears when pH = 6; ii) The variance decreases when pH $\in [8, 10]$ with a global maxima for $P(R_g)$ when $R_g \approx 19\,\text{Å} \lesssim r_{\text{NP}}$; and iii) When pH $= 10 \rightarrow 12$, the maxima of $P(R_g)$ is shifted with approximately 1 Å to a larger R_g.

Lastly, the $6PE_a$ follows the same trends as $4PE_a$, with two additional distinctions: i) A bimodal distribution also appears when pH = 7; and ii) the maxima $P(R_g)$ for pH = 10 appears when $R_g \approx 17\,\text{Å} \lessapprox r_{\text{NP}}$, making $P(R_g)$ very similar to $1PE_a^{0np}$ at

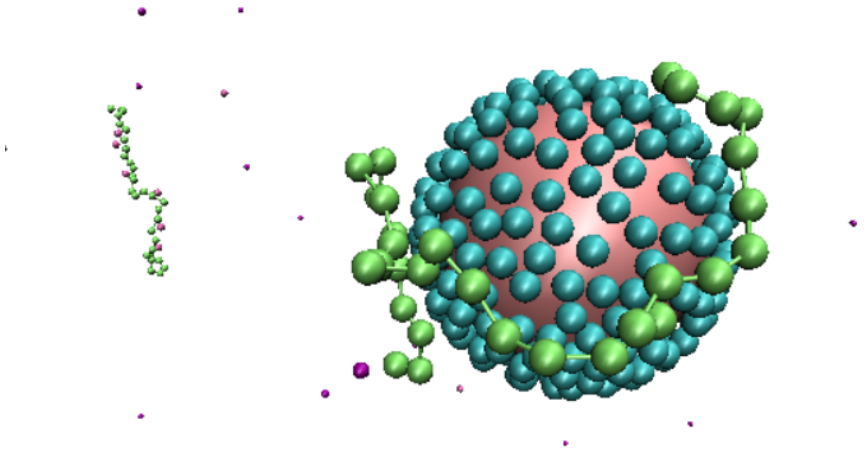

Figure 3.19: $2PE_a$ at pH = 5. The system consists of bound and one free polyelectrolyte.

pH = 14.

When the number of polyelectrolytes increases, the broadening of the $P(R_g)$ for systems with pH $\in [5, 12]$ increases. One to three bimodal distributions appear in $2PE_a$-$6PE_a$ for pH $\in [5, 7]$, indicating both free and bound polyelectrolytes in the system. The $\langle {R_g}^2 \rangle^{0.5}$ as a function of macrosteps for these pH-values are plotted in Figure B.8.

To summarize, at low pH, $R_g \approx 35\,\text{Å}$, which compares to a free fully ionized polyelectrolyte. When the pH increases and since the polyelectrolytes wraps around the nanoparticle, R_g approaches 20 Å, which is approximately the same as the radius of the nanoparticle $r_{np} = 22\,\text{Å}$.

When the pH goes above 10 for system $4PE_a$ and $6PE_a$, the R_g slightly increases before it starts to decrease at pH = 12 again. This is also indicated by the small drop in the amount of trains in Figure 3.7 for values of pH between 10 and 12. As the polyelectrolytes detaches from the nanoparticle, the number of tails and loops increases, leading to a smaller R_g before it eventually becomes free and reach R_g minima. The distribution at large pH values again resembles that of a free neutral polyelectrolyte.

3.3.2 Persistence length $\langle \ell_p \rangle$

Figure 3.20 shows $\langle \ell_p \rangle$ as a function of pH for a free polyelectrolyte ($1PE_a^{0np}$) as well as the results for $1PE_a$-$6PE_a$. The $\langle \ell_p \rangle$ of the polyelectrolyte in $1PE_a^{0np}$ increases slightly from pH = 2 to pH = 4 reaching a $\ell_p \approx 45\,\text{Å}$. With a greater increase in pH, the polyelectrolyte goes from being semi flexible to flexible when pH ≈ 8 ($\ell_p \to 10\,\text{Å}$). With further increase in pH, the persistence length remains quite stable at $\ell_p \approx 7\,\text{Å}$, a value close to the equilibrium bond separation $r_0 = 5\,\text{Å}$ or the bond length $\langle {r_b}^2 \rangle^{0.5} = 5.66\,\text{Å}$ obtained at pH = 14.

For the polyelectrolyte in $1PE_a$, $\langle \ell_p \rangle$ increases slightly from pH = 2 ($\ell_p \approx 44\,\text{Å}$)

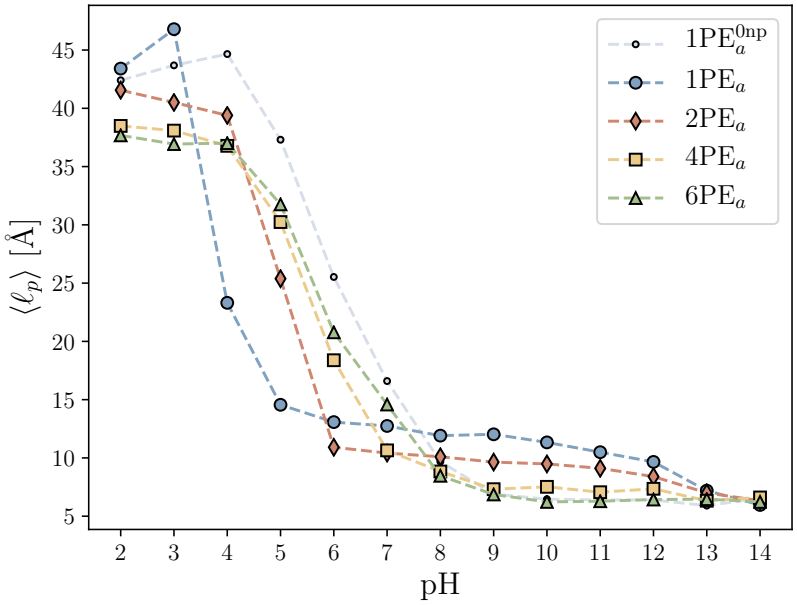

Figure 3.20: Annealed polyelectrolytes. Persistence length $\langle \ell_p \rangle$ for polyelectrolytes as a function of pH. The lines are guides to the eye.

to pH = 3 ($\ell_p \approx 47$ Å), before the polyelectrolyte goes from being semi flexible to flexible ($\ell_p \approx 15$ Å) at pH $\approx$ 5. In this pH range, the fraction of monomers in tails decreases from $\approx$ 80% to 10%. As the polyelectrolyte wraps itself around the nanoparticle, it gets more flexible. With further increase in pH, the persistence length decreases slowly until pH = 12 ($\ell_p \approx 10$). When the pH goes from 12 to 14, a drop in $\langle \ell_p \rangle$ is observed towards $\ell_p \approx 7$ Å as a consequence of the fraction of monomers in trains that goes from 95 % to 5 %, that the polyelectrolyte is again free and, at these pH values, mostly neutral.

In contrast to 1PE$_a$, 2PE$_a$'s persistence length decreases slightly from pH = 2 to pH = 4. At further increase in pH the persistence length goes from $\ell_p \approx 40$ Å to $\ell_p \approx 12$ Å when pH = 6. The polyelectrolytes then remains flexible when pH increases to 14.

The variation of $\langle \ell_p \rangle$ with pH is similar in systems 4PE$_a$ and 6PE$_a$, and will therefore be commented together. The persistence length decreases slightly from pH = 2 to pH = 4, then drops from $\ell_p \approx 37$ Å to $\ell_p \approx 10$ Å when pH = 8. With further increase in pH, $\ell_p \approx 7$ Å and remains stable at this value thereafter.

For low pH, as the concentration of polyelectrolytes increases, the starting $\langle \ell_p \rangle$ decreases. This could be a consequence of the polyelectrolytes interacting with each other or more likely, the increase in ionic strength. The $\langle \ell_p \rangle$ approaches 1PE$_a^{0np}$ as a consequence of many free polyelectrolytes contributing to the persistence length when the pH increases further.

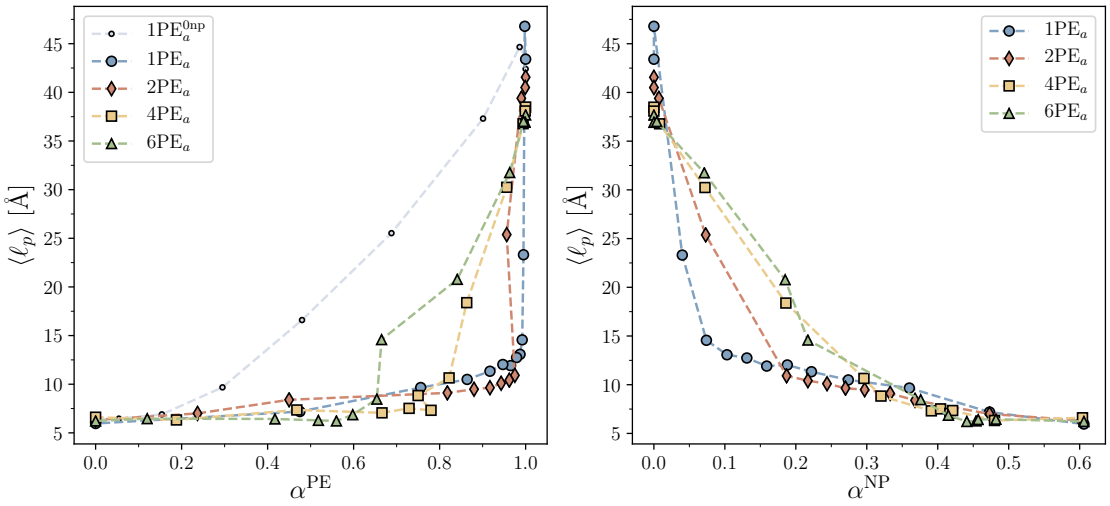

Figure 3.21: Annealed polyelectrolytes. Persistence length ℓ_p for polyelectrolytes as a function of α. The lines are guides to the eye.

Until now, the $\langle \ell_p \rangle$ has been plotted with respect to the pH. The polyelectrolytes charge will influence strongly the persistence length, and $\langle \ell_p \rangle$ is therefore plotted with respect to α^{PE} and α^{NP} in Figure 3.21.

It can be seen that as the α^{PE} of the polyelectrolyte (absence of nanoparticle, grey curve) increases so does the $\langle \ell_p \rangle$. The presence of the nanoparticle leads to a nearly constant $\langle \ell_p \rangle$ for α^{PE} up to nearly 1 after which there is a steep increase of $\langle \ell_p \rangle$. While the $2PE_a$ system shows the same behaviour, the $4PE_a$ and $6PE_a$ show a smoother transition as mixtures of free and complexes polyelectrolytes coexists in solution. This is also visible on the $\langle \ell_p \rangle$ dependency with α^{NP}.

3.3.3 Asphericity $\langle \mathcal{A} \rangle$

Asphericity is a measurement of the roundness of a polyelectrolyte. A value of $\langle \mathcal{A} \rangle$ close to 1 is cigar shaped while if $\langle \mathcal{A} \rangle \to 0$ the polyelectrolyte is near spherical. Figure 3.22 shows the asphericity as a function of pH.

$1PE_a^{0np}$ has an $\langle \mathcal{A} \rangle \approx 0.8$ until pH = 6 before it drops towards $\langle \mathcal{A} \rangle \approx 0.47$ at pH = 9. At further increase in pH, $\langle \mathcal{A} \rangle$ remains approximately constant. This highlights the transform from a charged (more extended) polyelectrolyte to a more neutral (more compact) polyelectrolyte.

Again, the presence of of a nanoparticle has a large impact on the conformation properties of the polyelectrolyte. For $1PE_a$, $\langle \mathcal{A} \rangle$ remains stable for very low pH until $\langle \mathcal{A} \rangle$ drops to $\langle \mathcal{A} \rangle \approx 0.3$ when pH = 5, as visualised in the $P(R_g)$, figure 3.18. The polyelectrolyte continues to have a spherical shape up to a pH of 11, above which it approach the same $\langle \mathcal{A} \rangle$ as for $1PE_a^{0np}$ that is, that of a neutral polymer in solution. The complexation of the polyelectrolyte to the nanoparticle in the pH

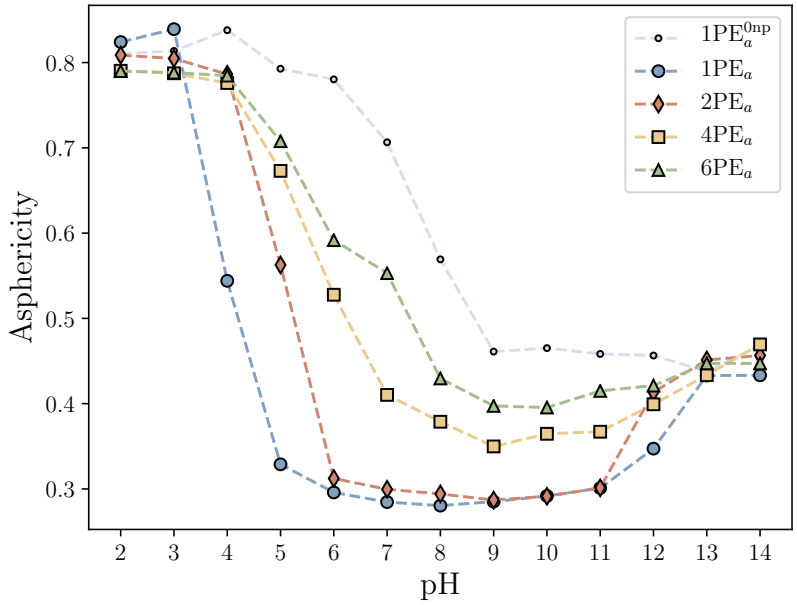

Figure 3.22: Annealed polyelectrolytes. Asphericity as a function of pH. 0 = spherical and 1 = cigar shaped (rod-like?) The lines are guides to the eye.

range $\sim 5 - 12$, and its tight packing around the nanoparticle. 2PE$_a$ has similar behaviour as 1PE$_a$, except that the complexation range is shorter (pH $\in [6, 11]$), as also observed in Figure 3.7 for the drop in asphericity at 1 value of pH larger than 1PE$_a$.

4PE$_a$ and 6PE$_a$ has approximately a constant $\langle \mathcal{A} \rangle$ for pH ≤ 4 due to few (almost 0) adsorbed polyelectrolytes. When the pH increases towards 9, $\langle \mathcal{A} \rangle$ decreases to 0.35 and 0.42, respectively. When the pH increases further, $\langle \mathcal{A} \rangle$ increases slowly towards 1PE$_a^{0np}$ at pH = 14.

Even though the radius of gyration decreases when pH increases (because the R_g of the neutral polyelectrolyte is lower than the radius of the nanoparticle), this is not the case for $\langle \mathcal{A} \rangle$. A reason for that could be that when the polyelectrolytes are complexed to the spherical nanoparticle, they acquire a spherical shape. When they are free, they tend to stretch out more due to a low ℓ_p.

To compare $\langle \mathcal{A} \rangle$ to the average degree of ionisation, $\langle \mathcal{A} \rangle$ is plotted as a function of α^{PE} and α^{NP} in Figure 3.23.

When α^{PE} increases, $\langle \mathcal{A} \rangle$ increases for the free polyelectrolyte in 1PE$_a^{0np}$. For 1PE$_a$ and 2PE$_a$, $\langle \mathcal{A} \rangle$ decreases when α^{PE} increases from 0 until $\alpha^{\mathrm{PE}} \approx 0.8$. 1PE$_a$ and 2PE$_a$ are most spherical when α^{PE} increases further from 0.8, before $\langle \mathcal{A} \rangle$ increases for values of α^{PE} close to 1. The same tendencies can be seen in 4PE$_a$ and 6PE$_a$, but with the increase in $\langle \mathcal{A} \rangle$ at $\alpha^{\mathrm{PE}} \approx 0.75$ and $\alpha^{\mathrm{PE}} \approx 0.65$ respectively.

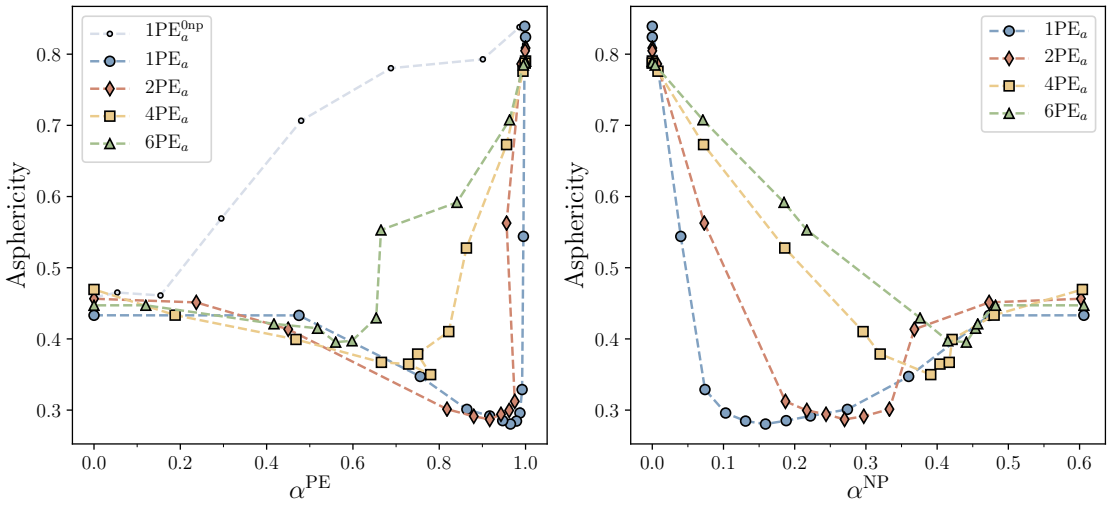

Figure 3.23: Annealed polyelectrolytes. Asphericity as a function of the average degree of ionisation α. $\langle \mathcal{A} \rangle = 0$: spherical and $\langle \mathcal{A} \rangle = 1$: cigar shaped (rod-like?) The lines are guides to the eye.

For $\langle \mathcal{A} \rangle$ as a function of α^{NP}, $\langle \mathcal{A} \rangle$ is highest when $\alpha^{NP} = 0$. In $1PE_a$, $\langle \mathcal{A} \rangle$ drops to 0.3 when $\alpha^{NP} \approx 0.1$. This state is where the polyelectrolyte is at its most spherical. When α^{NP} increases from here, $\langle \mathcal{A} \rangle$ also increases towards $\langle \mathcal{A} \rangle \approx 0.45$.

In $2PE_a$-$6PE_a$, the same tendencies as for $1PE_a$ are present except that the rapid decrease in $\langle \mathcal{A} \rangle$ are shifted towards a higher α^{NP} (0.2, 0.4 and 0.45 respectively).

3.4 Validity of simulations

As a consequence of the Monte Carlo method, and even using the Metropolis algorithm, calculated systems could get stuck in local energy minima. To evaluate this, one can calculate independent systems using different starting values (seeds). This has been done with $6PE_a$ using three seeds, referred to as system 1, 2 and 3.

In figure 3.24, the fraction of loops, tails, trains and adsorbed monomers are plotted as a function of pH for the thee different systems. As one can see, system 1 diverges significantly for pH 2 and 4. While a more careful evaluation is required, in this thesis it was dedicated to use the result of system 3 to compare with systems with a different number of polyelectrolytes.

This result differs from the other two systems, as these tends to behave like $1PE_a$–$4PE_a$ as presented previously in section 3.2.2. By this reason, system 3 was chosen as $6PE_a$.

For the interested readers other properties of the three different systems are presented in Appendix C. Those are the average degree of ionization as a function of pH (Figure C.1), the number of adsorbed chains as a function of α^{PE} and α^{NP} (Figure

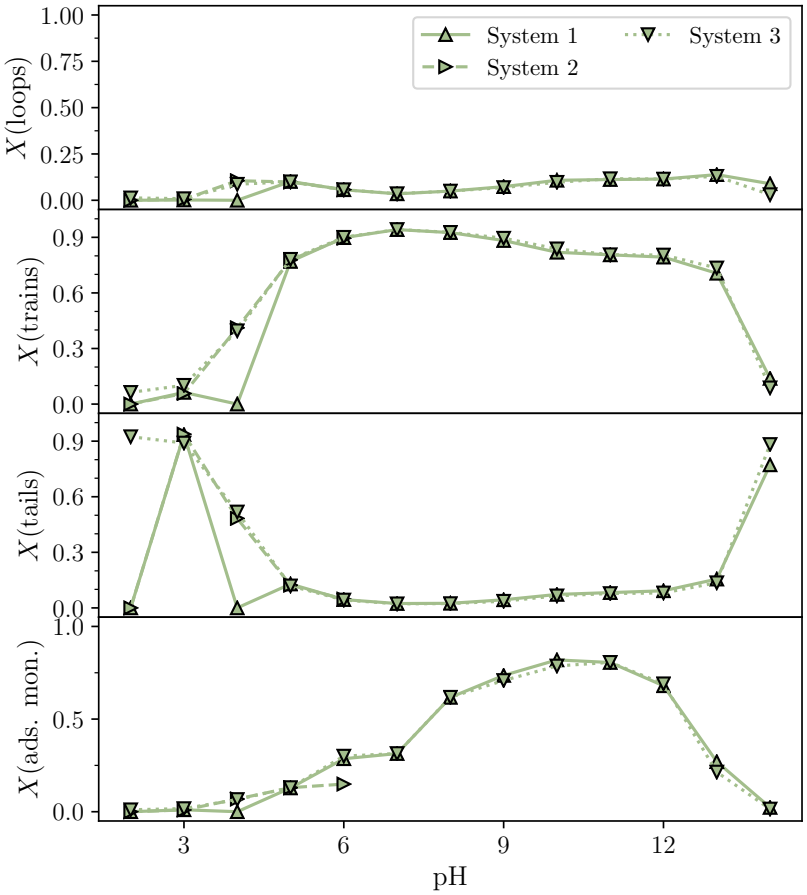

Figure 3.24: Fraction $X(Y)$ of monomers in Y = loops, trains and tails for the adsorbed polymers in each system (system 1, 2 and 3, all with $N_{\text{pol}} = 6$ and 1 nanoparticle) (top three panels). Adsorbing distance is set to 30 Å from the center of the nanoparticle. The bottom panel shows the fraction of adsorbed monomers, also taking into account non-adsorbed chains. The lines are guides to the eye.

C.2), the complex and radial charge as a function of pH (Figure C.3), the complex charge as a function of α^{PE} and α^{NP} (Figure C.4) and the probability distribution of the radius of gyration (Figure C.5).

In future research one should also calculate 1PE_a–4PE_a with different seeds to get values that describes the general system in a more precise way.

Chapter 4

Quenched Polyelectrolyte-Nanoparticle Systems

This chapter compares selected properties of quenched systems to annealed systems presented in the previous chapter.

Since quenched particles are independent of the systems pH, it makes no sense to plot ensemble properties as a function of pH. However, the properties are presented as a function of "pH". The quenched system with a specific "pH" $= i$ are calculated with monomers and nanoparticle surface groups with a fixed charge equivalent to the average degree of ionisation α obtained from the respectively annealed system with pH $= i$. The systems where either $\alpha^{\mathrm{PE}} = 0$ or $\alpha^{\mathrm{NP}} = 0$ in the annealed systems were not calculated.

Snapshots of all the systems for selected "pH"values, are presented in Figure 4.1. The cyan chains are polyelectrolytes, the blue spheres are co-ions for the nanoparticle, the red sphere a representation of the nanoparticle with a reduced radius to enable wiving the surface charges. The purple spheres are counterions for the polyelectrolytes.

4.1 Complex Properties

4.1.1 Number of Adsorbed Polyelectrolytes

The number of adsorbed polyelectrolyte-chains as a function of "pH"are shown in Figure 4.2. For all calculated values of "pH"in $1\mathrm{PE}_q$, one polyelectrolyte is bound to the nanoparticle. In $2\mathrm{PE}_q$, no polyelectrolytes are bound to the nanoparticle at "pH" = 4. One polyelectrolyte increased for each increase in "pH", until both polyelectrolytes are bound at "pH" = 6. Both polyelectrolytes remains adsorbed when the "pH"increases, even at "pH" = 13. For $4\mathrm{PE}_q$, all polyelectrolytes are free when "pH" = 4. Again, with each increase of "pH", one polyelectrolyte bounds to the nanoparticle, until every polyelectrolyte are adsorbed when "pH"reaches 8. All

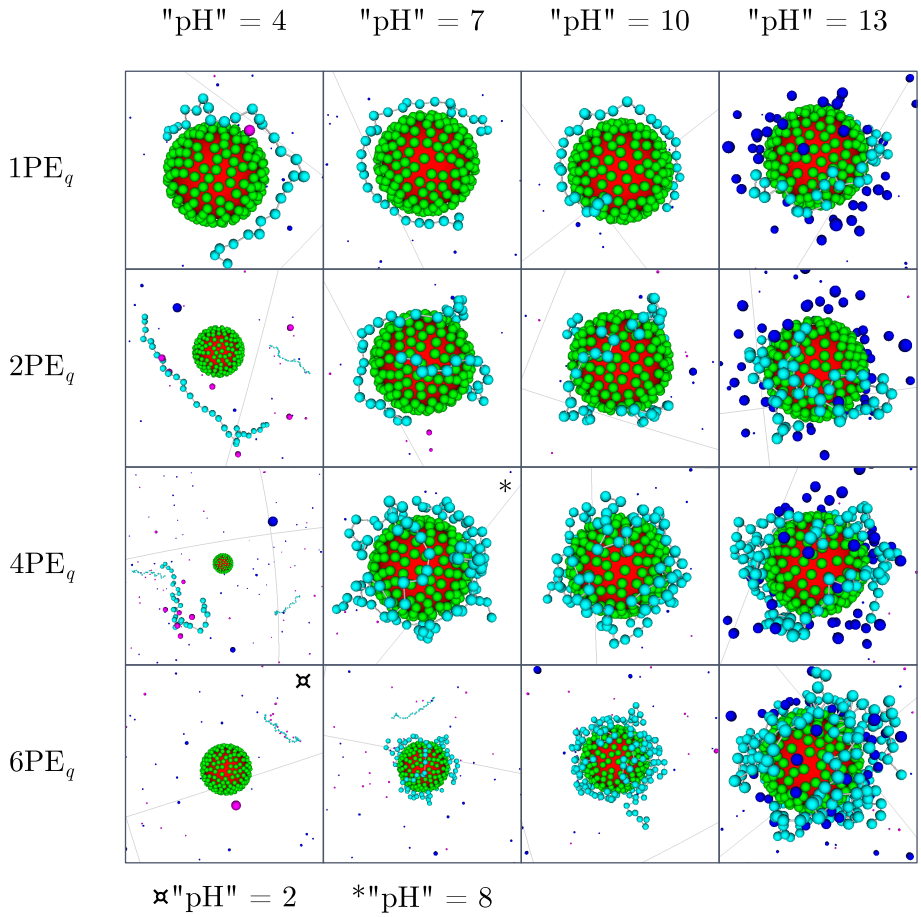

Figure 4.1: Snapshots of 1PE$_q$–6PE$_q$ for four different values of pH. The cyan chains are polyelectrolytes, the blue spheres are co-ions for the nanoparticle, the red sphere a representation of the nanoparticle with a reduced radius to enable wiving the surface charges. The purple spheres are counterions for the polyelectrolytes.

polyelectrolytes remains adsorbed through "pH" = 13. In 6PE$_q$, one polyelectrolyte is bond to the nanoparticle when "pH" = 4. When the "pH"increases, the polyelectrolytes adsorbs until all six are adsorbed when "pH" = 9 and remains adsorbed through "pH" = 13, as for the other quenched systems.

In comparison to the annealed systems in Figure 3.5, all the quenched systems behaves similar for pH = "pH" < 7. 4PE$_q$ and 6PE$_q$ are found to adsorb all polyelectrolytes at a lower "pH"than 4PE$_a$ and 6PE$_a$. All polyelectrolytes remains adsorbed for a wider range of pH for the quenched than the annealed systems, only desorbing when the polyelectrolyte charge is equal to zero, pH = 14.

The number of adsorbed chains as a function of α^{PE} (left) and α^{NP} (right) are presented in Figure 4.3. As for the annealed systems, the quenched systems show a constant number of adsorbed chains (equal to the maximum number of chains in the system) when $\alpha^{\mathrm{PE}} < 0.5$. For a further increase in α^{PE}, the number of adsorbed chains drops significantly due to the decrease in the nanoparticle charge It is inter-

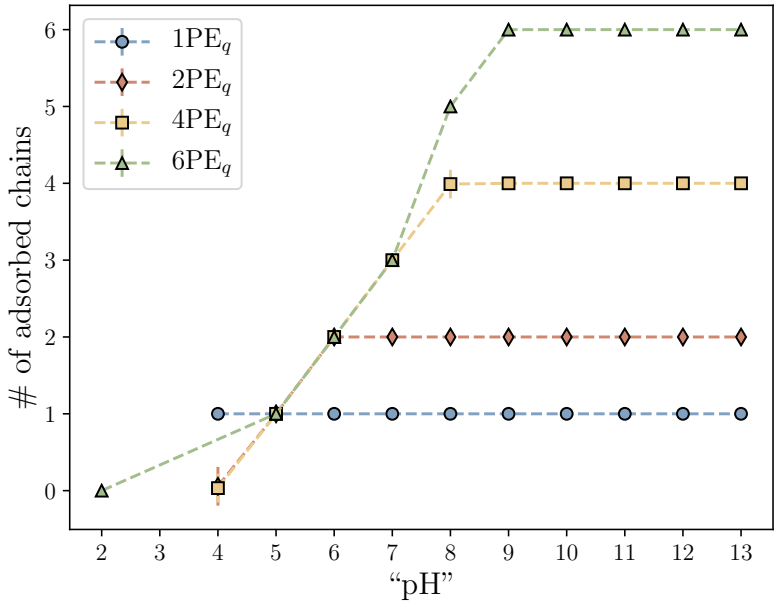

Figure 4.2: Number of adsorbed chains as a function of "pH". The lines are guides to the eye.

esting to note that the quenched polyelectrolytes are bound to the nanoparticle for a wider range of α^{PE} than the annealed.

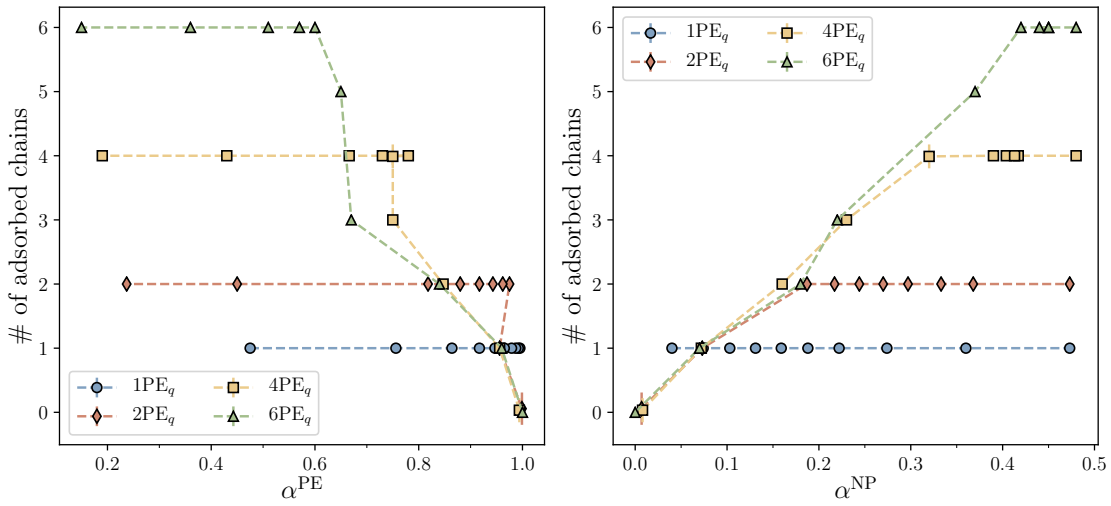

Figure 4.3: Number of adsorbed chains as a function of α for polyelectrolytes (left) and nanoparticle (right). The lines are guides to the eye.

The broadening of the quenched α^{PE}-range where all polyelectrolytes are adsorbed compared to the annealed system is also seen in the number of adsorbed chains as a function of α^{NP}. Worth notice is that the appearance of a different number

of adsorbed chains at the same α^{PE} as seen for the annealed system, can not be observed for the quenched systems e.g. at $\alpha^{\mathrm{NP}} = 0.4$ for $4\mathrm{PE}_a$ and $4\mathrm{PE}_q$. To find for which α^{NP} there exists (if there exists) several possibilities of number of adsorbed chains need further research.

4.1.2 Loops, Trains and Tails

To see how the polyelectrolytes are attached to the nanoparticle, the fraction of loops, tail, trains are shown in the top three panels in Figure 4.4 as a function of "pH". We recall from the annealed systems that; i) at pH $\in [5, 8]$ the fraction of loops, trains and tails is similar for all systems and ii) when pH $\in [9, 12]$ the fraction

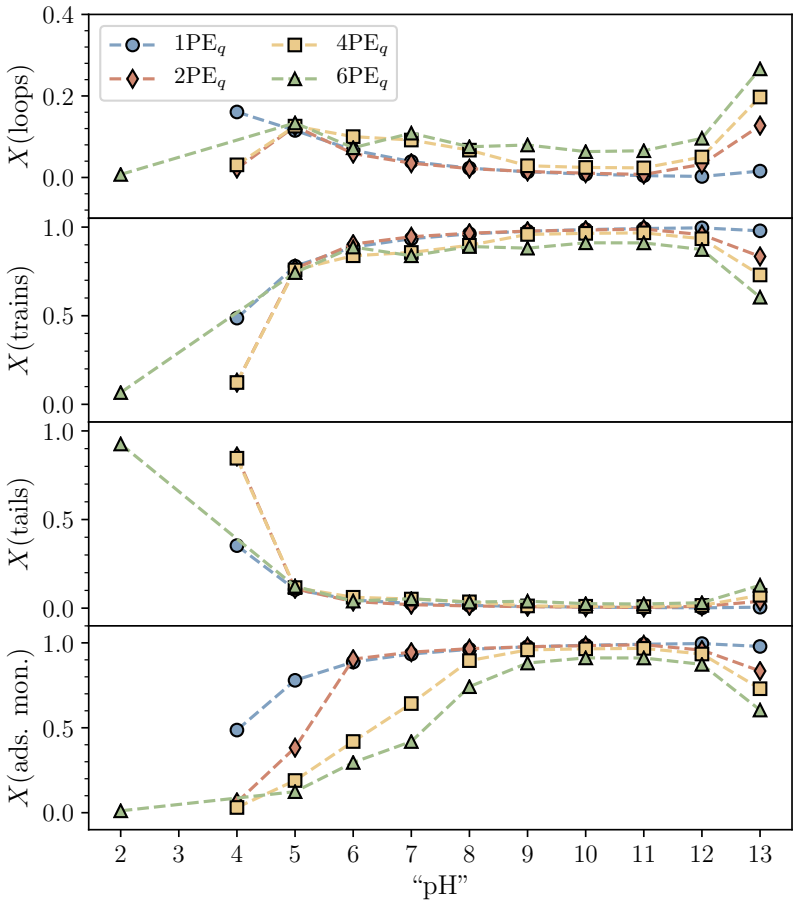

Figure 4.4: Fraction $X(Y)$ of monomers in Y = loops, trains and tails for the adsorbed polymers in each system (top three panels). Adsorbing distance is set to 30 Å from the center of the nanoparticle. The bottom panel shows the fraction of adsorbed monomers, also taking into account non-adsorbed chains. The lines are guides to the eye.

of loops increases as the number of polyelectrolytes in the system increases (Figure 3.7).

For the quenched systems, ii) appears at a wider range in pH $\in [7, 13]$, and as a consequence, i) is not prominent at pH $\in [7, 8]$. This can be partly explained by the monomer charge, with an example. In 6PE_a and 6PE_q at pH $= 7$, $\alpha^{\text{PE}} \approx 0.65$. But since the annealed systems are pH dependent, the bounded and free polyelectrolytes has a different α^{PE}, as seen in Figure B.7 with $\alpha^{\text{PE}} \approx 0.95$ and $\alpha^{\text{PE}} \approx 0.55$ respectively. The high α^{PE} of the bounded polyelectrolytes in 6PE_a results in few fraction of loops because of the increased electrostatic interactions between the nanoparticle and the polyelectrolytes. On the other hand, 6PE_q has equally charged polyelectrolytes with a lower α^{PE} resulting in a larger fraction of loops because of a decrease in electrostatic interactions with the nanoparticle and possibly also an increase in the repulsion (electrostatic and steric) between adsorbed polyelectrolyte chains.

4.1.3 Complex and Radial Charge

As a theoretical representation of the ζ-potential, the complex Z_C and radial Z_r charge of the quenched systems as a function of "pH", are presented in Figure 4.5. When the concentration of polyelectrolytes increases, the isoelectric point shifts towards higher pH values for both Z_C and Z_r, except for 6PE_a in Z_r.

In 1PE_q, the Z_C decreases as the pH increases.[1] In 2PE_q the complex charge increases when the pH increases and reaching a maxima at pH $= 6$. The complex charge then decreases for further increase in pH, as for 1PE_q. For 4PE_q and 6PE_q, Z_C increases at low pH until pH $= 5$. The Z_C remains approximatly constant for

[1] An increase from pH $= 2$ is expected. This is because systems with a neutral nanoparticle were not calculated (resulting in $Z_C = 0$).

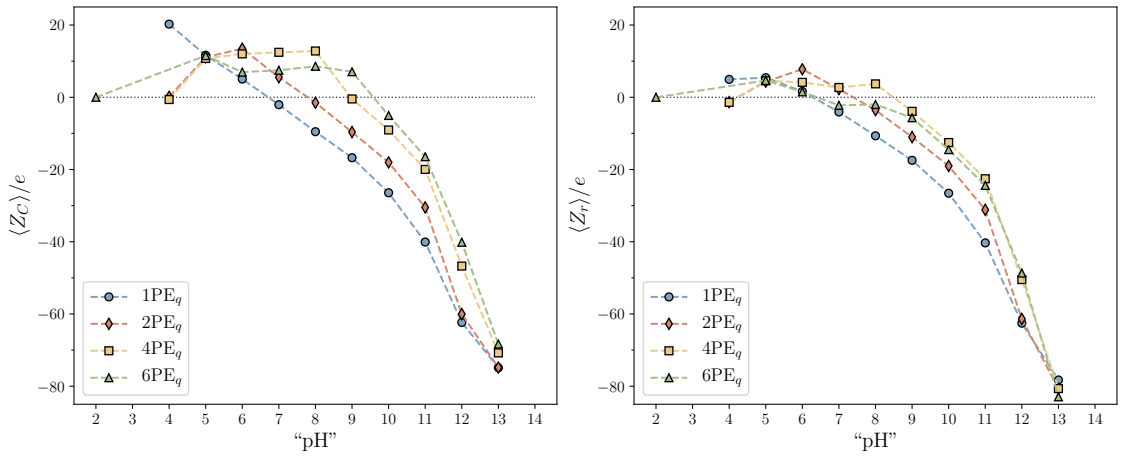

Figure 4.5: Average complex charge Z_C (left) and radial charge Z_r (right) as a function of "pH". The lines are guides to the eye.

an increase in pH until Z_C decreases when pH reaches 8 and 9 for $4PE_q$ and $6PE_q$ respectively. The plateau observed for Z_C for the quenched systems is more obvious than for the annealed systems.

At high pH the values of Z_C and Z_r reaches -70 and -80, which is lower than for the annealed systems (-40 and -45 respectively). The nanoparticle has a large density of surface particles. In the annealed particles the electrostatic repulsion between particles, and counterion condensation, dictates a maximum positive charge. For the quenched nanoparticle the average ionization of the annealed nanoparticle, α^{NP}, for the corresponding pH is used, and α^{NP} is also used for the nanoparticle's counterions. So even if the average charge of nanoparticles is, in average, similar the counterion condensation will be weaker due to the lower charge of the counterions.

4.2 Conformational Properties

4.2.1 Radius of Gyration R_g

The probability distributions of the radius of gyration are presented as a function of "pH"in figure 4.6.

The quenched systems show similar behaviour to the annealed systems. This includes: i) bimodal distributions when more than one polyelectrolyte are present; ii) the radius of gyration decreases as the "pH"increases; and iii) when the polyelectrolytes are bound to the nanoparticle, the $P(R_g)$ is sharper.

For the quenched systems, the peak in $P(R_g)$ at "pH" $\in [7, 12]$ is higher (*i.e.* the distribution is narrower) than for the annealed systems. This is more prominent in the diluted systems ($1PE_a$ and $2PE_a$).

4.2.2 Persistence length $\langle \ell_p \rangle$

Figure 4.7 shows the persistence length $\langle \ell_p \rangle$ as a function of "pH". The general trend for the quenched systems is similar to the annealed systems with: i) a sharp drop in $\langle \ell_p \rangle$ when the "pH"increases for the low "pH"range; and ii) a near constant $\langle \ell_p \rangle$ for the higher values of "pH", when the polyelectrolytes are adsorbed to the nanoparticle.

The more diluted the system is, the stiffer is the polyelectrolyte when it is bound to the nanoparticle. In comparison to the annealed systems, the quenched systems show a higher constant $\langle \ell_p \rangle$ for high "pH"values. The difference is larger ($2 - 3$ Å) for the diluted systems than for $4PE_q$ and $6PE_q$.

4.2.3 Asphericity $\langle \mathcal{A} \rangle$

Lastly, the asphericity is plotted as a function of "pH"in Figure 4.8. The general shape of the quenched systems shows the same behavior as the annealed systems

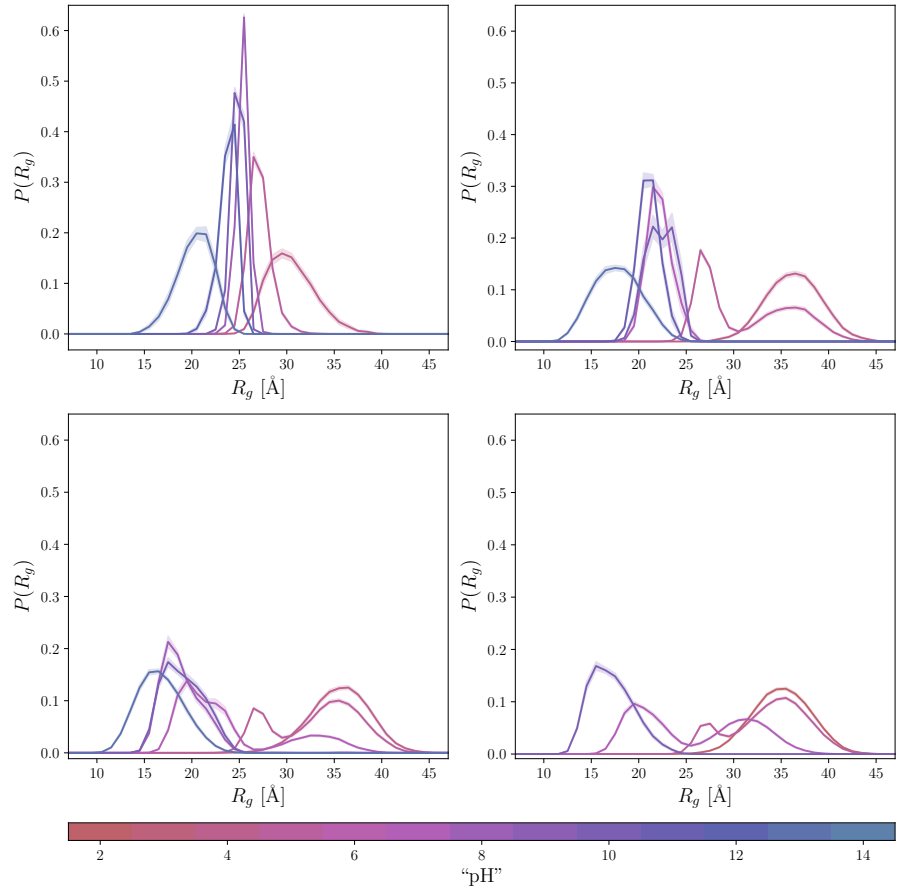

Figure 4.6: Probability distribution of the radius of gyration for $1PE_q$ (top left), $2PE_q$ (top right), $4PE_q$ (bottom left) and $6PE_q$ (bottom right). The pH in the system ranges from 2 (red) to 14 (blue). The shaded areas are the mean square error of the systems.

with: i) a drop in $\langle \mathcal{A} \rangle$ when "pH"increases at low "pH"values; ii) the α^{PE} remains constant when all polyelectrolytes are bound to the nanoparticle; and iii) when the polyelectrolytes desorbs from the nanoparticle, the $\langle \mathcal{A} \rangle$ increases at high "pH".

The main difference between the annealed systems and the quenched systems is that for $1PE_q$ and $2PE_q$, $\langle \mathcal{A} \rangle$ is lower when the polyelectrolytes are adsorbed to the nanoparticle *i.e.* the polyelectrolytes seem to be more spherical in the quenched system. This behaviour can also be observed for $4PE_q$ and $6PE_q$, but are less prominent.

This is likely due to the fact that in the quenched systems the charge is equally distributed along the polyelectrolyte chains, while in the annealed systems the polyelectrolyte is able to concentrate charge in center of the chain, more likely to be in contact with the nanoparticle, creating neutral-like tails. This is however not very obvious in the conformational indicators, trains, tails and loops.

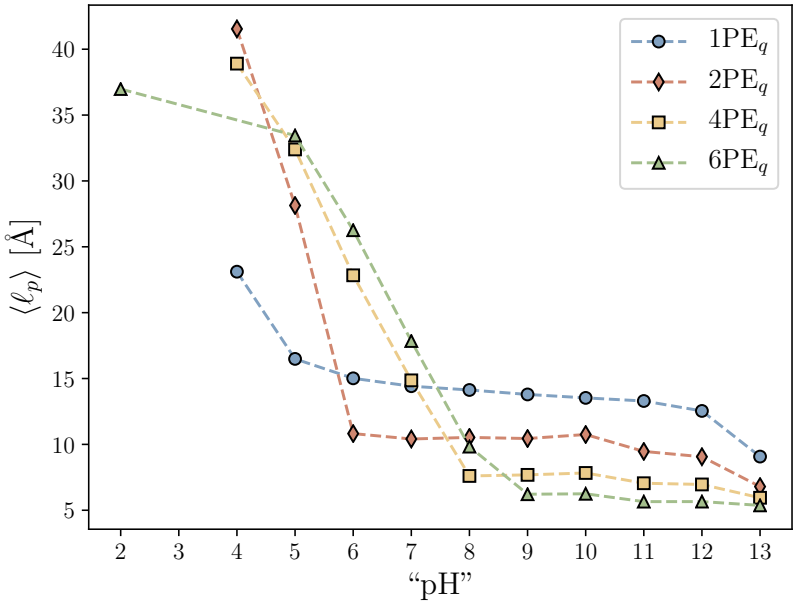

Figure 4.7: Persistence length $\langle \ell_p \rangle$ for polyelectrolytes as a function of "pH". The lines are guides to the eye.

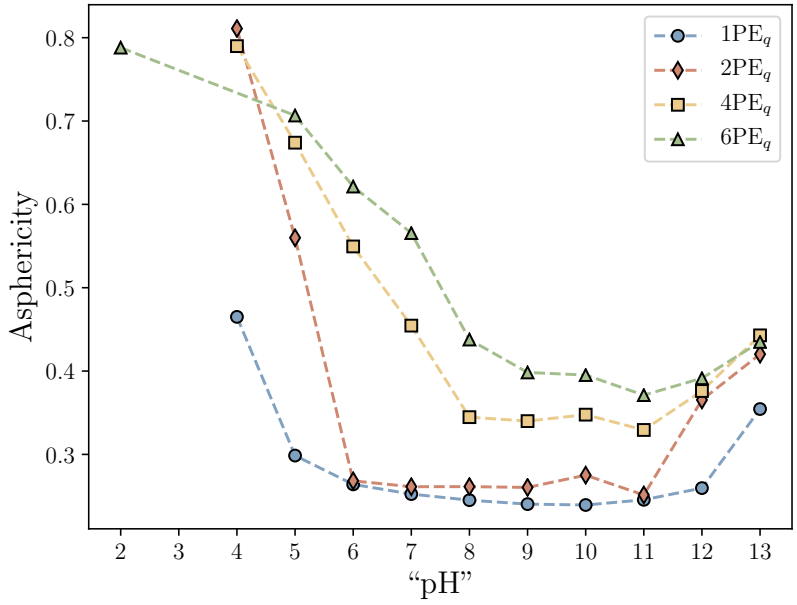

Figure 4.8: Asphericity as a function of "pH". 0 = spherical and 1 = cigar shaped. The lines are guides to the eye.

Chapter 5

Conclusion

In this work fully annealed and fully quenched systems consisting of one nanoparticle and different concentrations of polyelectrolytes were studied by Monte Carlo simulations. We have looked at the titration behavior, complex properties and conformational properties of the systems. The different properties have been presented in sequential fashion, first discussing the annealed systems and then comparing them to selected properties obtained from the quenched systems.

By adding polyelectrolytes to a system with one nanoparticle, the overall degree of ionisation of both macromolecules will be affected. Generally, α^{NP} increases and α^{PE} decreases as a function of pH when the number of polyelectrolytes in the system increases if we compare it to systems with one nanoparticle and one polyelectrolyte.

When the concentration of polyelectrolytes increases, all polyelectrolytes are adsorbed by the nanoparticle for a shorter pH range. When the number of adsorbed polyelectrolytes increases it leads to more monomers in tails and loops as a consequence of repulsing forces between the polyelectrolytes adsorbed by the nanoparticle.

As expected, when the concentration of polyelectrolytes increases, the pH of the isoelectric point for the complex and radial charge increased.

The presence of a nanoparticle greatly influences the radius of gyration, persistence length and the asphericity of the polyelectrolytes in respect to pH and "pH".

Annealed systems allows for concentration of charge in polyelectrolytes that are in contact with the nanoparticle, leading to the coexistence of polyelectrolytes that are complexed and free by changing the pH.

5.1 Further Research

In the future one should study the quenched systems in more detail. Systems with quenched polyelectrolytes and an annealed nanoparticle can also be studied, to compare the influence the polyelectrolytes has on the nanoparticle charge.

One should also study the annealed systems more closely to see how inhomogeneities in the charge on the nanoparticle surface affects the charge and physical confirmations of a polyelectrolyte, and the influence the counterions has on the different charge distributions.

The simulations should also be compared with experiments, to see if the models could be a good tool to describe real system behaviour.

5.2 Professional Relevance

The new curriculum in physics in upper secondary school (from 2021) implements digital skills in the following way (in norwegian):

> "Digitale ferdigheter i fysikk innebærer å bruke digitale ressurser til å [...] analysere, modellere og presentere data. [...] Videre innebærer det å bruke programmering [...] til å utforske fysiske problemstillinger." [30]

which, could be translated to (my translation),

> "Digital skills in physics is to use digital resources to analyse, model and present data. Further, to use programming as a tool to explore physical problems."

This project has provided me with insight in computer simulations and visual presentations of scientific data to explore physical systems and draw conclutions from data obtained by simulations. It has also provided me with some knowledge in biology and chemistry. This experience could help me when I, in the future, will educate children, young adults and future scientist, the joy of physics. And provide them with some of the tools needed to become better citizens.

Bibliography

[1] M. Stornes, P. Linse, and R. S. Dias. "Monte Carlo Simulations of Complexation between Weak Polyelectrolytes and a Charged Nanoparticle. Influence of Polyelectrolyte Chain Length and Concentration". In: *Macromolecules* (2017). DOI: 10.1021/acs.macromol.7b00844.

[2] M. Stornes, P. M. Blanco, and R. S. Dias. "Polyelectrolyte-nanoparticle mutual charge regulation and its influence on their complexation". In: *Colloids and Surfaces A: Physicochemical and Engineering Aspects* (2021). DOI: 10.1016/j.colsurfa.2021.127258.

[3] M. Stornes, B. Shrestha, and R. S. Dias. "pH-Dependent Polyelectrolyte Bridging of Charged Nanoparticles". In: *Journal of Physical Chemistry B* (2018). DOI: 10.1021/acs.jpcb.8b06971.

[4] S. Ulrich, M. Seijo, and S. Stoll. "The many facets of polyelectrolytes and oppositely charged macroions complex formation". In: *Current Opinion in Colloid & Interface Science* (2006). DOI: 10.1016/j.cocis.2006.08.002.

[5] S. Ulrich, A. Laguecir, and S. Stoll. "Complex formation between a nanoparticle and a weak polyelectrolyte chain: Monte Carlo simulations". In: *Journal of Nanoparticle Research* (2004). DOI: 10.1007/s11051-004-3548-4.

[6] F. Carnal and S. Stoll. "Adsorption of Weak Polyelectrolytes on Charged Nanoparticles. Impact of Salt Valency, pH, and Nanoparticle Charge Density. Monte Carlo Simulations". In: *Journal of Physical Chemistry B* (2011). DOI: 10.1021/jp205616e.

[7] N. Metropolis et al. "Equation of state calculations by fast computing machines". In: *Journal of Chemical Physics* (1953).

[8] D. C. Rapaport. *The art of Molecular Dynamics Simulation*. Cambridge University Press, 2004.

[9] M. J. Field. *A Practical Introduction to the Simulation of Molecular Systems*. Cambridge University Press, 2007.

[10] A. P. Sassi et al. "Monte Carlo simulations of hydrophobic weak polyelectrolytes: Titration properties and pH-induced structural transitions for polymers containing weak electrolytes". In: *The Journal of Chemical Physics* (1992). DOI: 10.1063/1.463346.

[11] J. Hardin. *Becker's world of the cell*. Pearson, 2017.

[12] S. K. Tripathy, J. Kumar, and H. S. Nalwa. *Handbook of polyelectrolytes and their applications: Vol. 3: Applications of polyelectrolytes and theoretical models*. Ed. by H. S. Nalwa. Vol. 3. American Scientific Publishers, 2002.

[13] J. Landsgesell et al. "Simulations of ionization equilibria in weak polyelectrolyte solutions and gels". In: *Soft Matter* (2019). DOI: 10.1039/c8sm02085j.

[14] E. Raphael and J.-F. Joanny. "Annealed and Quenched Polyelectrolytes". In: *Europhysics Letters* (1990).

[15] M. Lund and B. Jönsson. "Charge regulation in biomolecular solution". In: *Quarterly Reviews of Biophysics* (2013). DOI: 10.1017/S003358351300005X.

[16] C. E. Reed and W. F. Reed. "Monte Carlo study of titration of linear polyelectrolytes". In: *The Journal of Chemical Physics* (1992). DOI: 10.1063/1.462145.

[17] M. Ullner et al. "A Monte Carlo study of titrating polyelectrolytes". In: *Journal of Chemical Physics* (1996). DOI: 10.1063/1.471071.

[18] T. Akesson, C. Woodward, and B. Jonsson. "Electric double layer forces in the presence of polyelectrolytes". In: *Journal of Chemical Physics* (1989). DOI: 10.1063/1.457006.

[19] J. Reščič and P. Linse. "MOLSIM: A modular molecular simulation software". In: *Journal of Computational Chemistry* (2015).

[20] Arctic Ice Studio. *Nord*. Mar. 7, 2022. URL: https://www.nordtheme.com/docs/colors-and-palettes (visited on 03/07/2022).

[21] I. Vibhu et al. "Zeta potential of colloidal particle in solvent primitive model electrolyte solution: A density functional theory study". In: *Molecular Physics* (2013). DOI: 10.1080/00268976.2012.728637.

[22] R. J. Hunter. *Zeta potential in colloid science: principles and applications*. Academic Press, 1981.

[23] Y. Hirose et al. "Monte Carlo Simulation Studies of Conformational Properties of Polyelectrolytes with Maleic Acid Units". In: *Polymer Journal* (1995). DOI: 10.1295/polymj.27.519.

[24] H.-P. Hsu, W. Paul, and K. Binder. "Standard Definitions of Persistence Length Do Not Describe the Local "Intrinsic" Stiffness of Real Polymer Chains". In: *Macromolecules* (2010). DOI: 10.1021/ma902715e.

[25] R. S. Dias et al. "Modeling of DNA compaction by polycations". In: *The Journal of Chemical Physics* (2003). DOI: 10.1063/1.1609985.

[26] G. Zifferer and O. F. Olaj. "Shape asymmetry of random walks and nonreversal random walks". In: *The Journal of Chemical Physics* (1994). DOI: 10.1063/1.466926.

[27] A. Clavier et al. "Surface charging behavior of nanoparticles by considering site distribution and density, dielectric constant and pH changes - a Monte Carlo approach". In: *Physical Chemistry Chemical Physics* (2015). DOI: 10.1039/c4cp04733h.

[28] M. Ullner and B. Jonsson. "A Monte Carlo study of titrating polyelectrolytes in the presence of salt". In: *Macromolecules* (1996). DOI: 10.1021/ma960309w.

[29] B. C. Ong, Y. K. Leong, and S. B. Chen. "Interparticle forces in spherical monodispersed silica dispersions: Effects of branched polyethylenimine and molecular weight". In: *Journal of Colloid and Interface Science* (2009). DOI: 10.1016/j.jcis.2009.05.018.

[30] Utdanningsdirektoratet (2021). *Læreplan i Fysikk (FYS01-02)*. Fastsatt som forskrift. Læreplanverket for Kunnskapsløftet 2020.

Appendix A

Poster from the Biophysics Conference

This page is intentionally left blank. The poster is in the next page.

MC Simulations of Complexation between Annealed/Quenched Polyelectrolytes and an Annealed/Quenched Nanoparticle

Glenn Hoel Kampesveen[a] and Rita de Sousa Dias[a]

[a]Dept. Physics, NTNU–Norwegian Univ. of Science and Technology, Trondheim, Norway

Contact: glennhk@stud.ntnu.no

INTRODUCTION

Polyelectrolytes (PEs) and nanoparticles (NPs) has been the interest of much research in the past decades, and are still an important topic. PEs and NPs are widely used in the industry, e.g. water treatment or food technology. PEs also have fundamental biological characteristics, since e.g. nucleic acids, proteins and polysaccharides are all PEs. The understanding of the complexation between PEs and NPs could therefore lead to important knowledge when it comes to biological processes. [1-4]

SYSTEMS

Annealed particles are titratable, i.e. dependent on the systems pH. Quenched particles has a fixed charge no matter the pH. If PEs and NPs are oppositely charged, they will attract each other and form complexes, as in Figure 1.

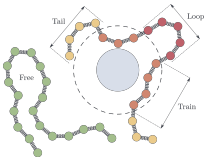

Figure 1: *One free (green) and one bond (yellow, orange, red) polyelectrolyte. The monomers in the bond polyelectrolyte are categorised as trains, loops and tails, depending on their distance to the nanoparticle (grey).*

METHODS

Metropolis Monte Carlo simulations are used to simulate the interaction of one nanoparticle and 1-6 polyelectrolytes for different values of pH. To find equilibrium states for the different systems, different moves are tried and the potential energy of the new system are calculated. If the new configuration has a lower potential energy, the move is likely accepted.

The used Monte Carlo moves are single particle move, pivot move where the shorter sub chain is rotated and chain move where the whole chain is moved. For the annealed polyelectrolytes, there is an additional charge chain move.

The potential energy of the system U are calculated by the sum of the bonding energy, non bonding energy and the protonation energy (charge change eneregy), by

$$U = U_{\text{bond}} + U_{\text{non-bond}} + U_{\text{prot}}$$

The average deegree of ionisation α is a value that describes the amount of charge in the system. It is calculated by summizing the absolute charges z_i and divide by the number of particles N

$$\alpha = \frac{1}{N}\sum_{i=1}^{N} |z_i|$$

RESULTS

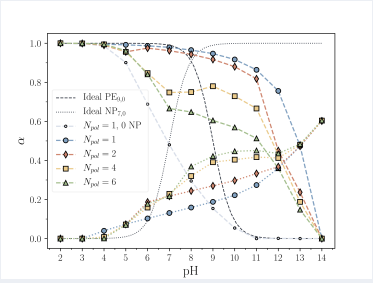

Figure 2: *Average degree of ionisation α as a funcrion of pH for systems with 1-6 polyelectrolytes (lines) and corresponding nanoparticle (dots).*

When the pH is low, PEs are fully charged and the NP is neutral. Opposite for high pH, as seen in Figure 2.

PE-NP-complexation occurs at intermediate pH-values, as seen in figure 3. This behavior is also seen in probability distribution of the radius of gyration in Figure 4.

When the number of PEs increases, some are free and some bond to the NP at intermediate pH-values. This leads to an decrese in the average ionisation of the PEs (Figure 2).

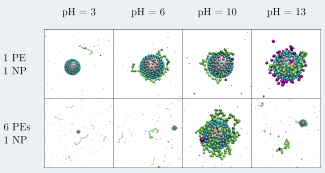

Figure 3: *Snapshots of different PE-NP systems at chosen values of pH.*

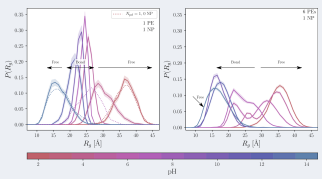

Figure 4: *Probability distribution of the radius of gyration.*

ANNEALED / QUENCHED

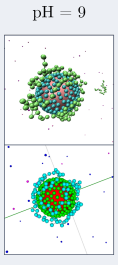

Figure 5: *Two representations of the same system. Left: PEs (green) NP surface charge (blue). Right: PEs (blue), NP surface charge (green).*

For 6PE systems typically the number of adsorbed chains is lower for the annealed systems (Figure 5).

This arises from the abillity to concentrate the charge in the PEs that are associated to the NP (Figure 7).

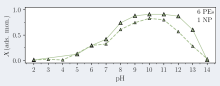

Figure 6: *Number of adsorbed monomers for annealed (dots) and quenched (line) complexes*

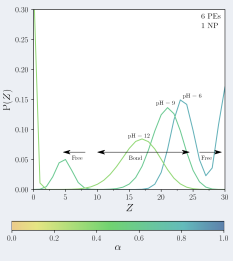

Figure 7: *Probability distribution of the polymer charge for an annealed system*

CONCLUSIONS

Changing the pH in the systems shows a rich behavior.

For extreme pH-values the PEs are free and either fully charged or neutral.

When the number of chains increases (the concentration), the systems consists of more free chains for lower pH-values.

Anneaeled systems allows for concentration of charge in the PEs that are in contact with the NP, leading to the coexistence of PEs with differnt charge.

By using annealed micromolecules, one can control the formation of complexes by changes in the pH.

References:

[1]Morten Stornes, Per Linse, and Rita S. Dias. In: MACROMOLECULES 50.15 (Aug. 2017), pp. 5978–5988. issn: 0024-9297.

[2]Morten. Stornes, Pablo M. Blanco, and Rita S. Dias. In: COLLOIDS AND SURFACES A-PHYSICOCHEMICAL AND ENGINEERING ASPECTS 628 (Nov. 2021). issn: 0927-7757.

[3]Morten Stornes, Binaanta Shrestha, and Rita S. Dias. In: JOURNAL OF PHYSICAL CHEMISTRY B 122.44 (Nov. 2018), pp. 10237–10246. issn: 1520-6106.

[4]Serge Ulrich, Marianne Seijo, and Serge Stoll. In: Current Opinion in Colloid Interface Science 11.5 (2006), pp. 268–272. issn: 1359-0294.

Figure A.1: The poster presented at the Biophysics Conference.

Appendix B

Supplementary plots

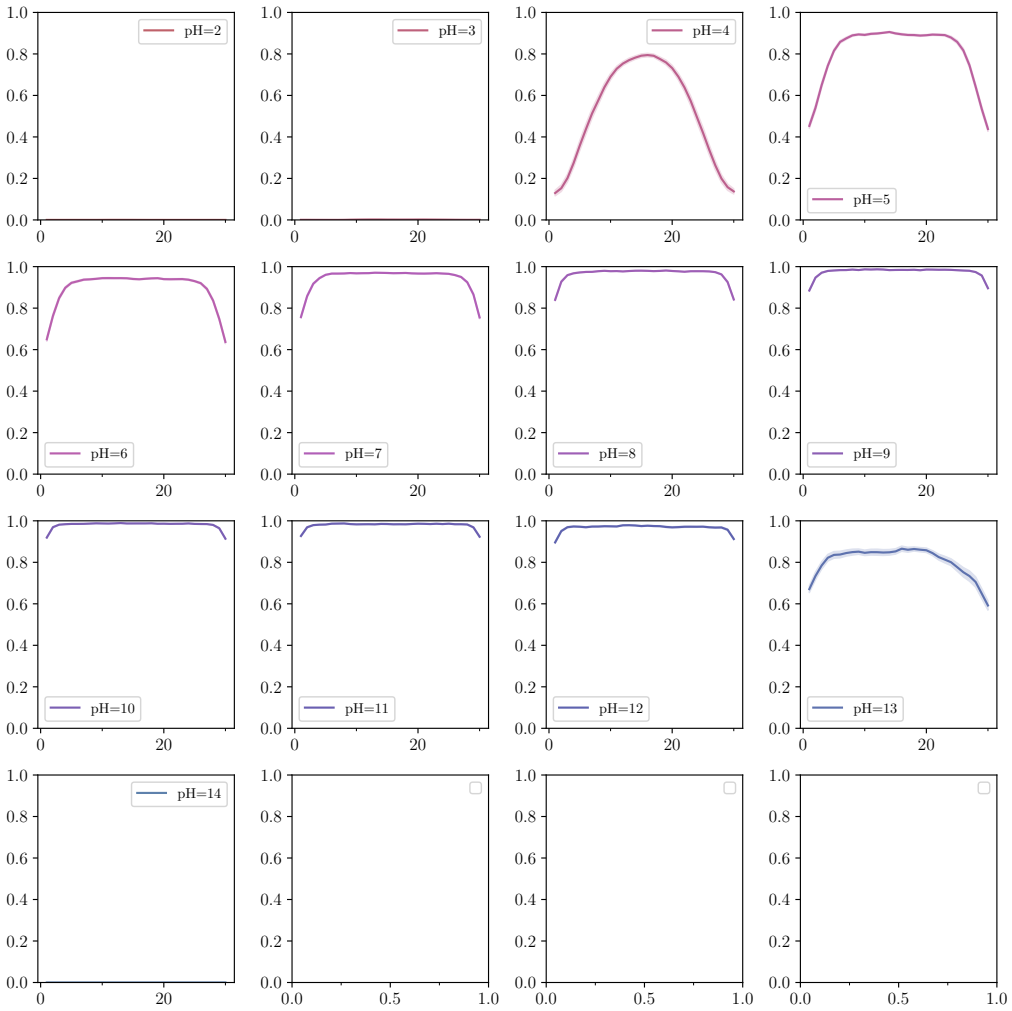

Figure B.1: The probability distribution of the contact profiles for each polyelectrolyte for system $1PE_a$. The pH in the system ranges from 2 (red) to 14 (blue).

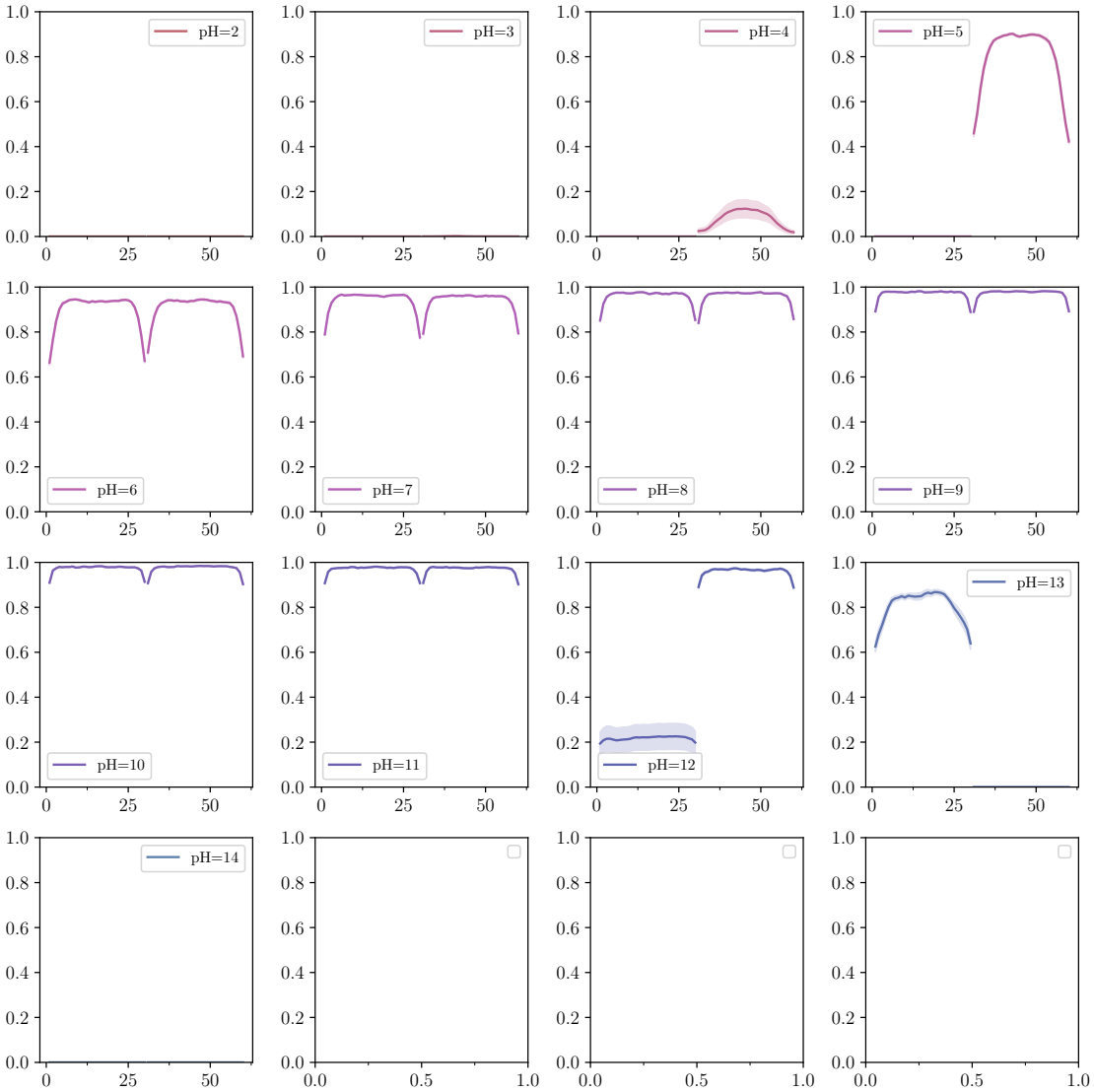

Figure B.2: The probability distribution of the contact profiles for each polyelectrolyte for system $2PE_a$. The pH in the system ranges from 2 (red) to 14 (blue).

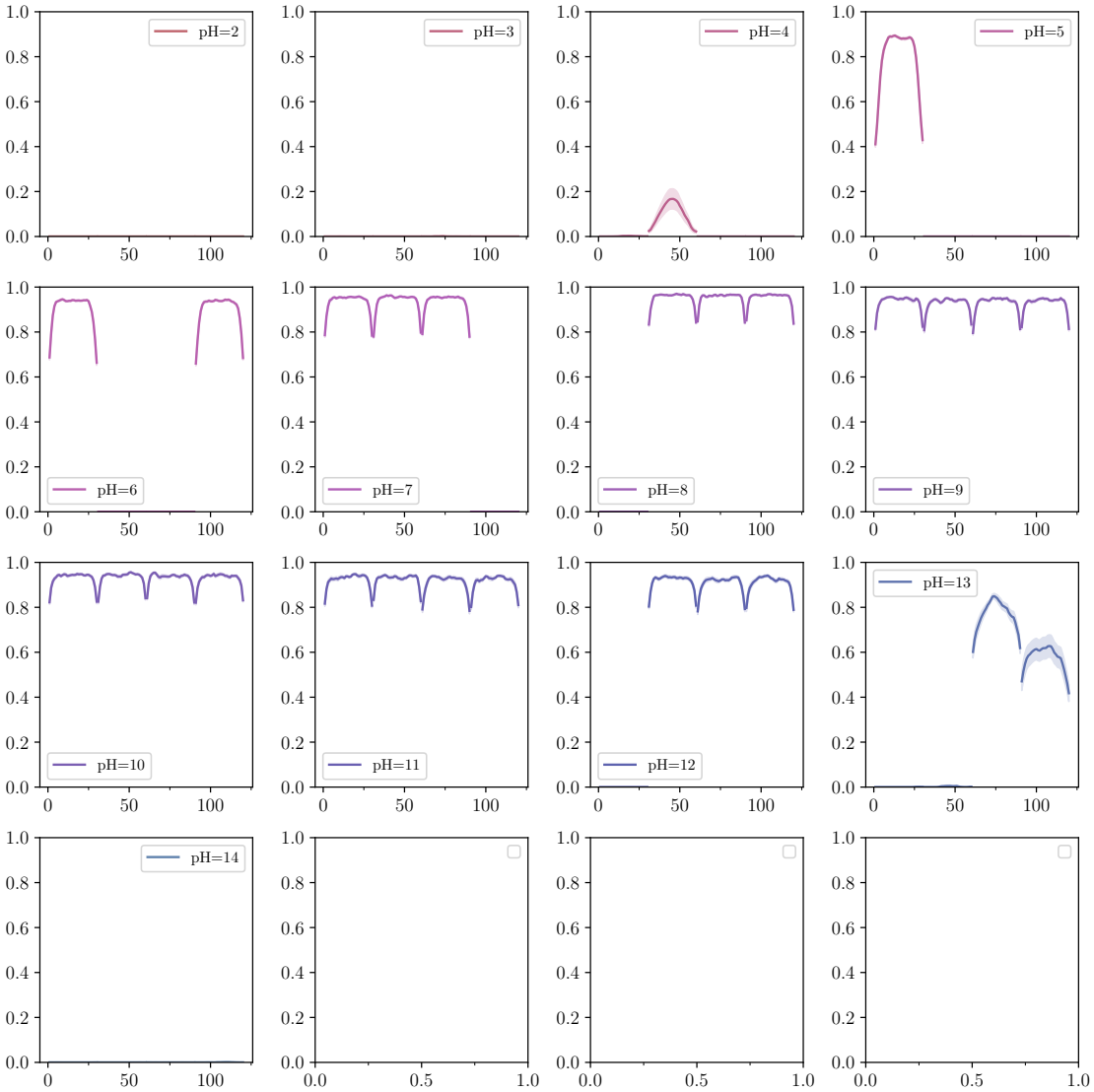

Figure B.3: The probability distribution of the contact profiles for each polyelectrolyte for system 4PE$_a$. The pH in the system ranges from 2 (red) to 14 (blue).

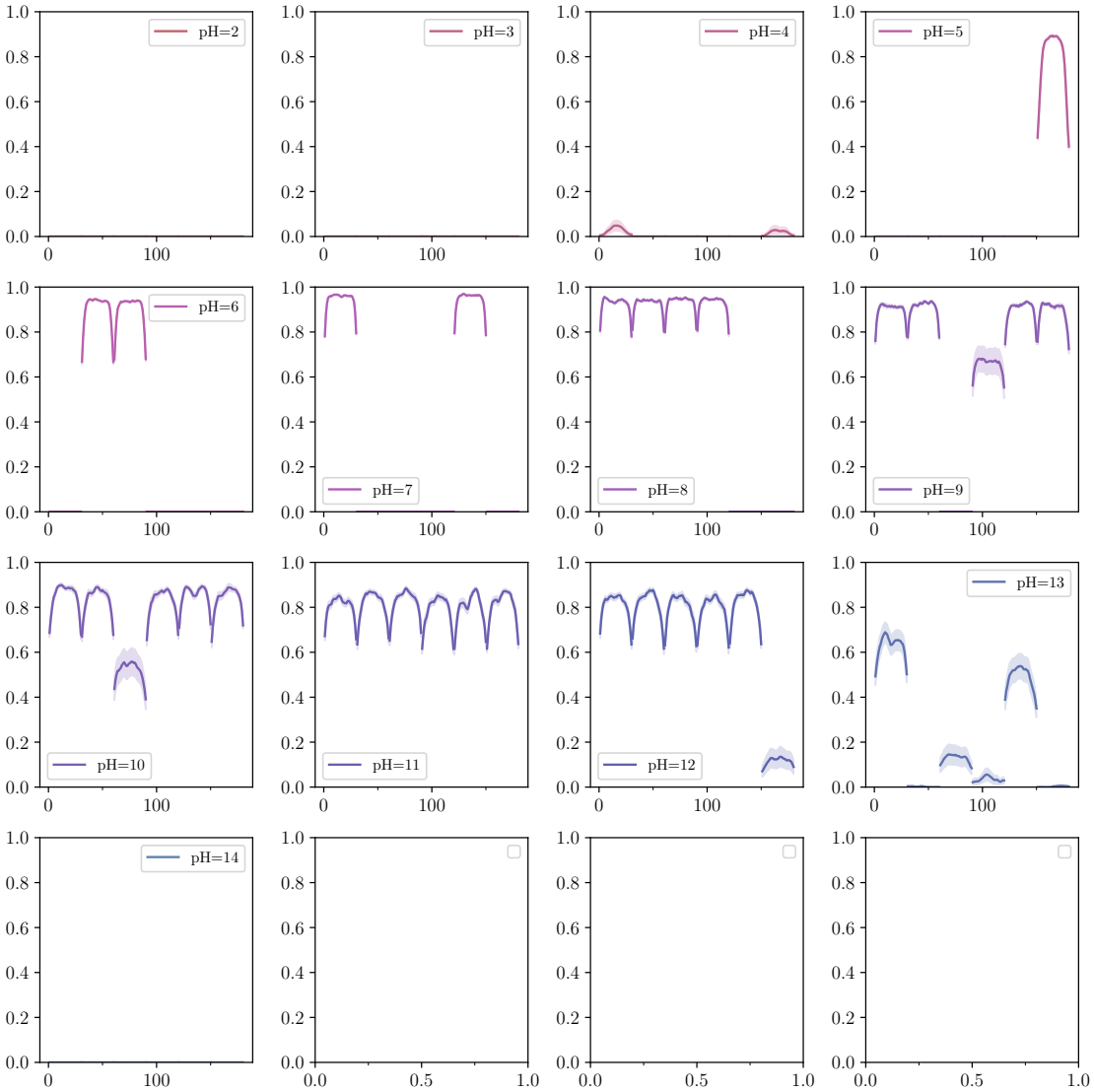

Figure B.4: The probability distribution of the contact profiles for each polyelectrolyte for system 6PE$_a$. The pH in the system ranges from 2 (red) to 14 (blue).

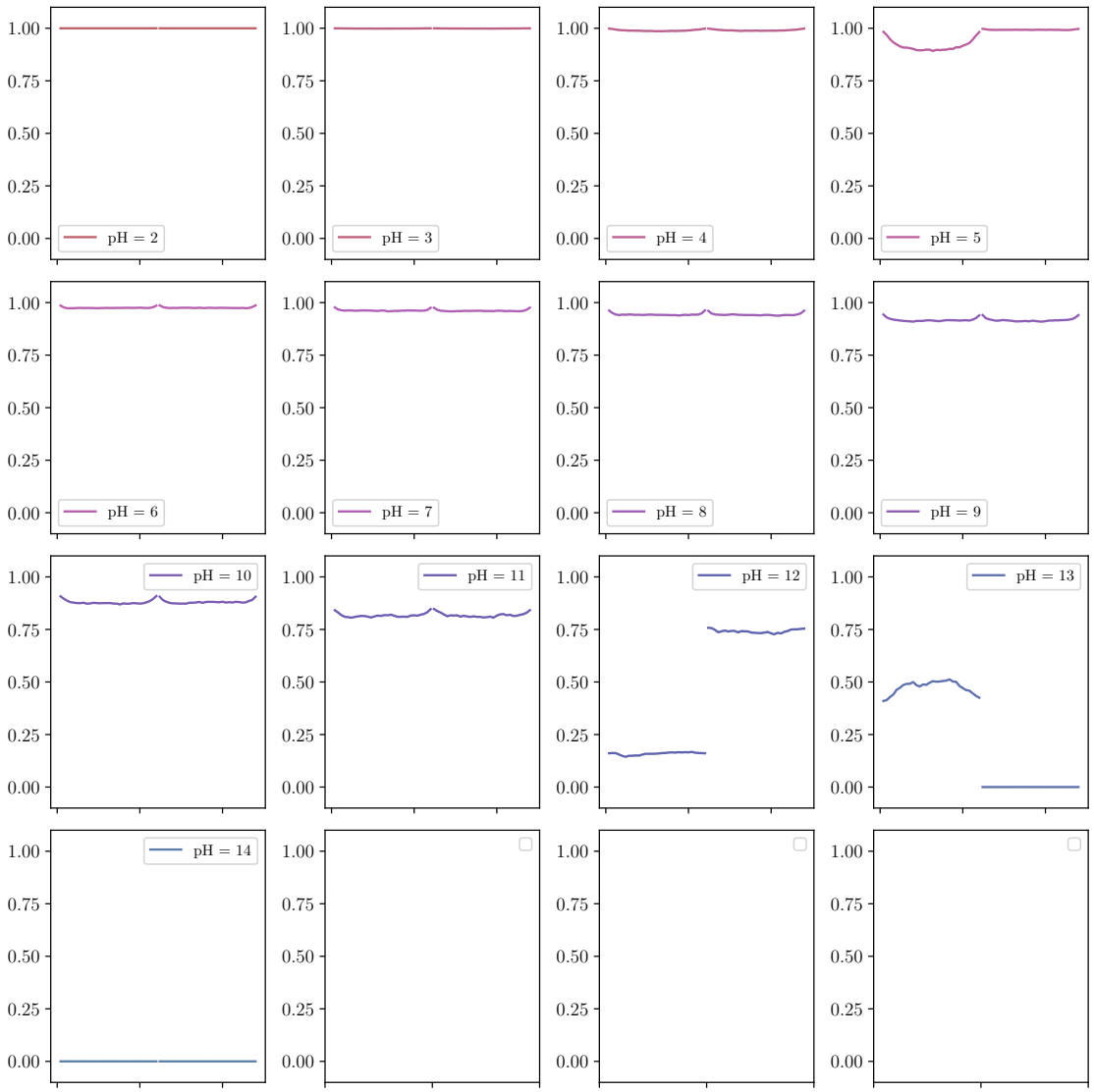

Figure B.5: Average charge per monomer for 2PE$_a$. Same as Figure 3.11, left, but plotted in different windows for comparison.

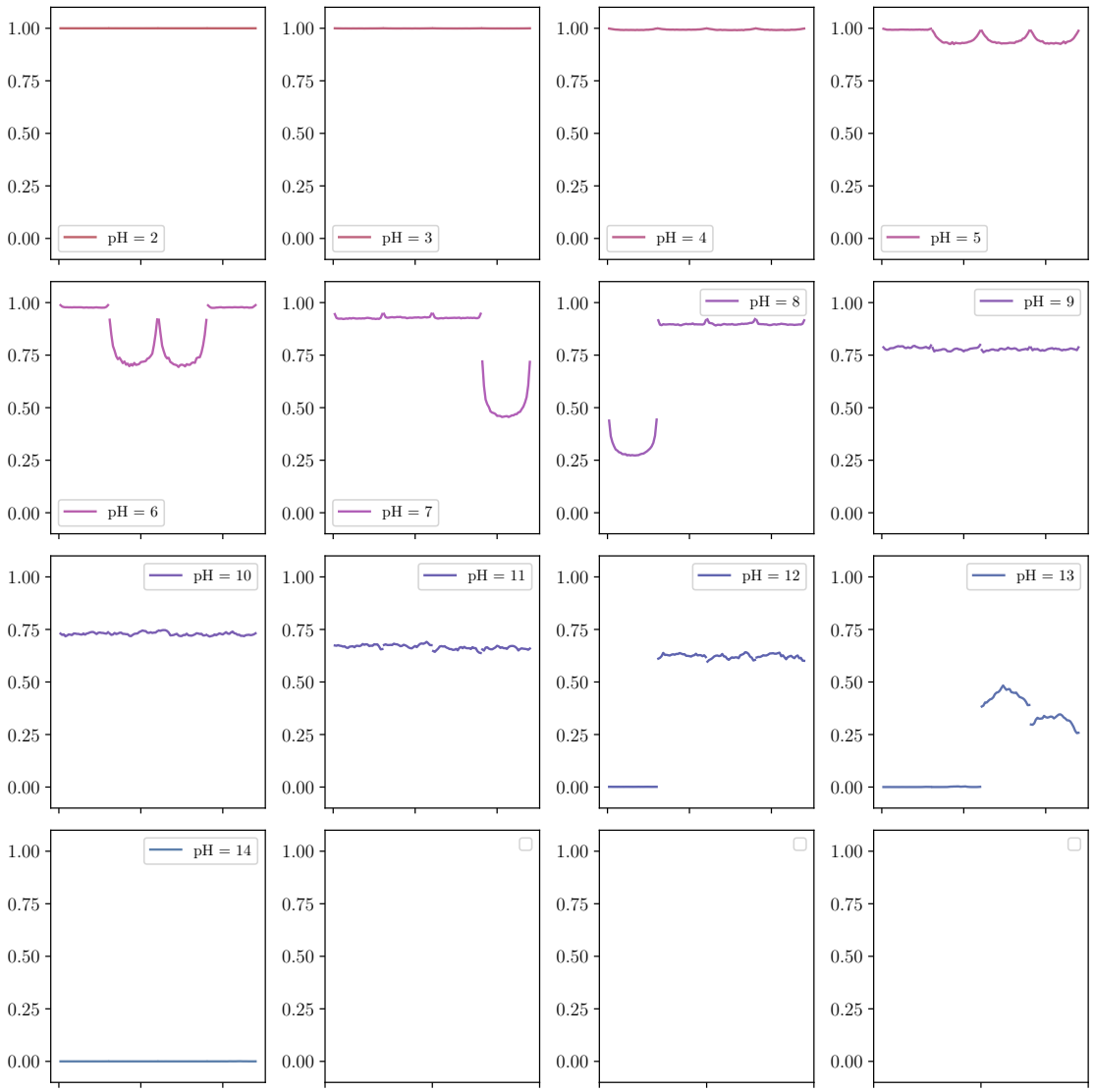

Figure B.6: Average charge per monomer for 4PE$_a$. Same as Figure 3.11, center, but plotted in different windows for comparison.

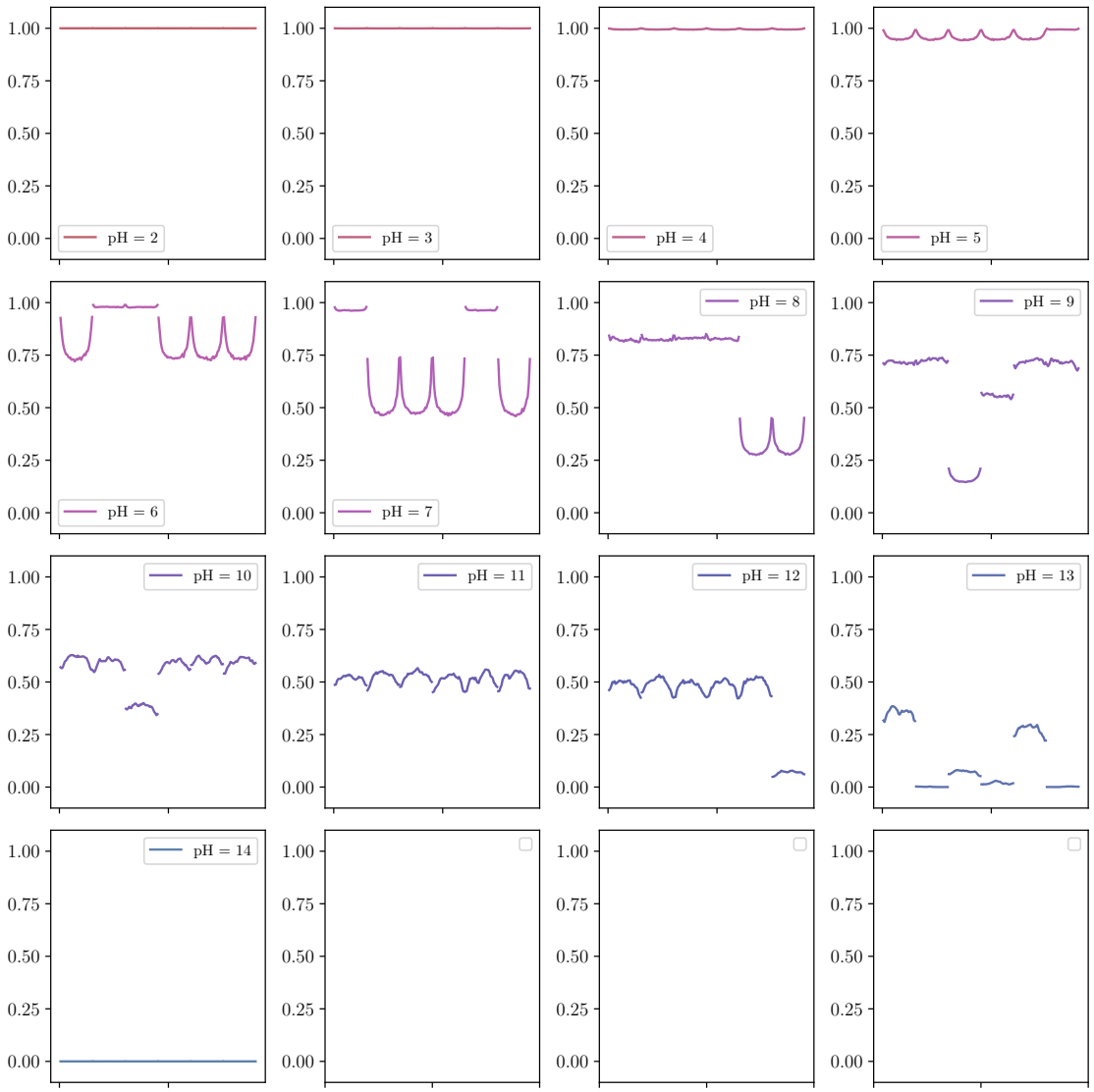

Figure B.7: Average charge per monomer for 6PE$_a$. Same as Figure 3.11, right, but plotted in different windows for comparison.

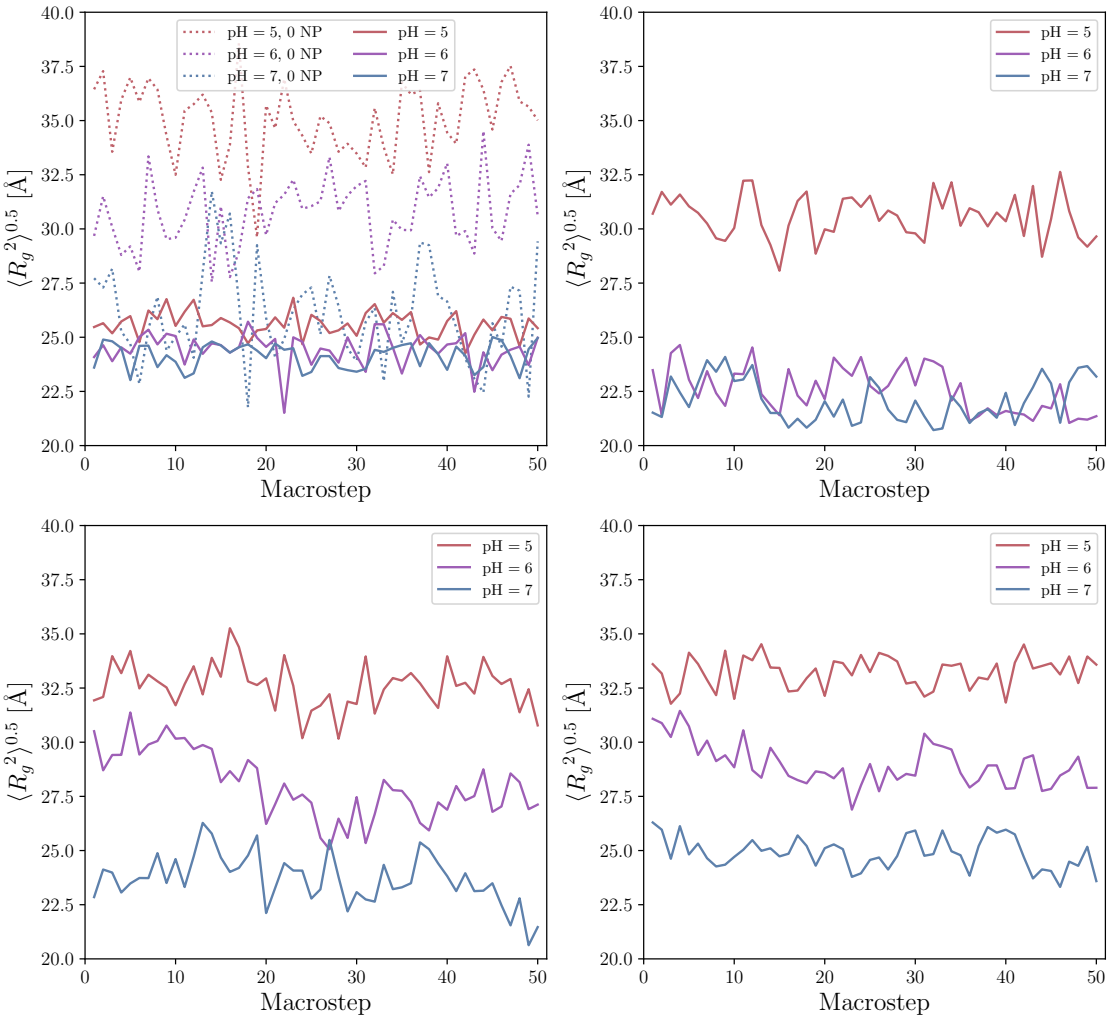

Figure B.8: Radius of gyration as a function of macrosteps for the system with 1 (top left), 2 (top right), 4 (bottom left) and 6 (bottom right) annealed polyelectrolytes. The dotted system (top left) is a reference system, with 1 polyelectrolyte and 0 nanoparticles.

Appendix C

Validity of simulations 6PE$_a$

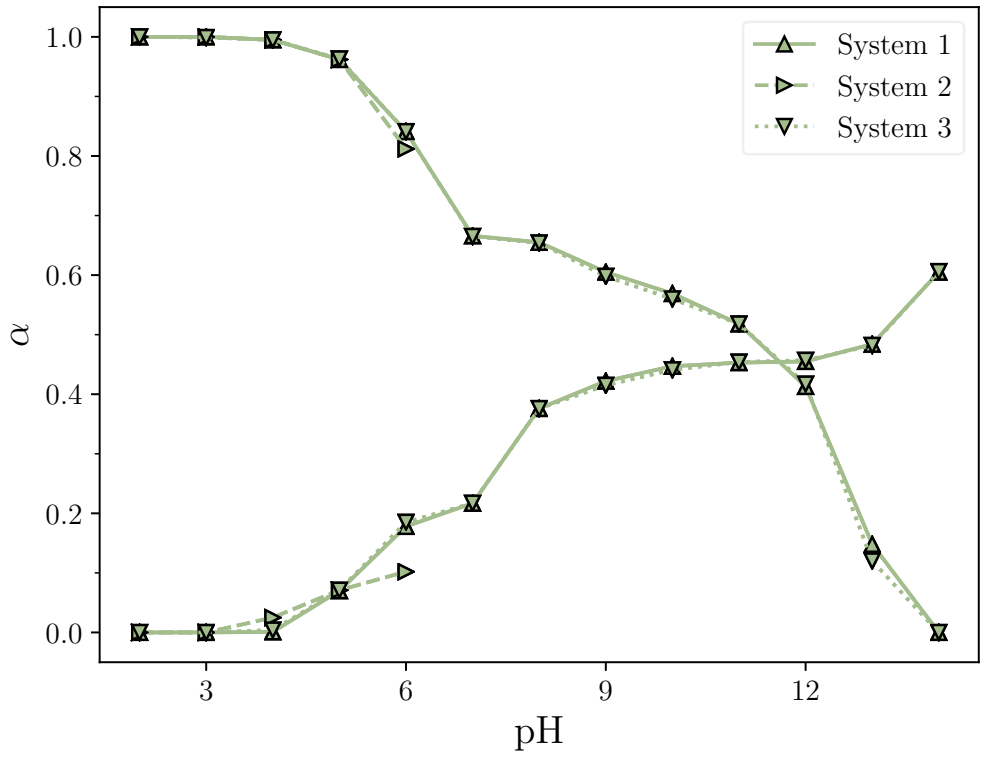

Figure C.1: Average degree of ionisation of the three simulations

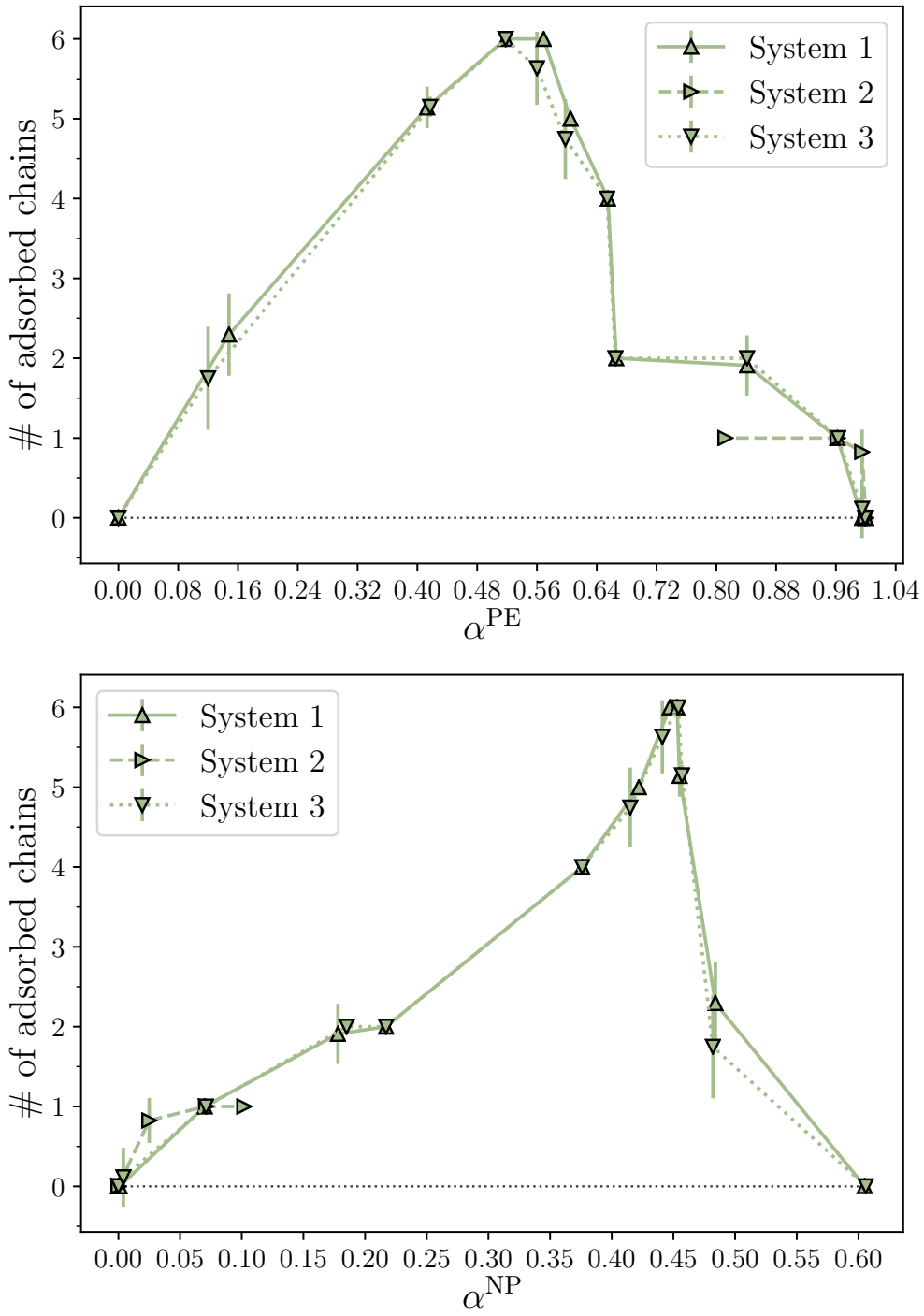

Figure C.2: Adsorbed chains for the three simulations

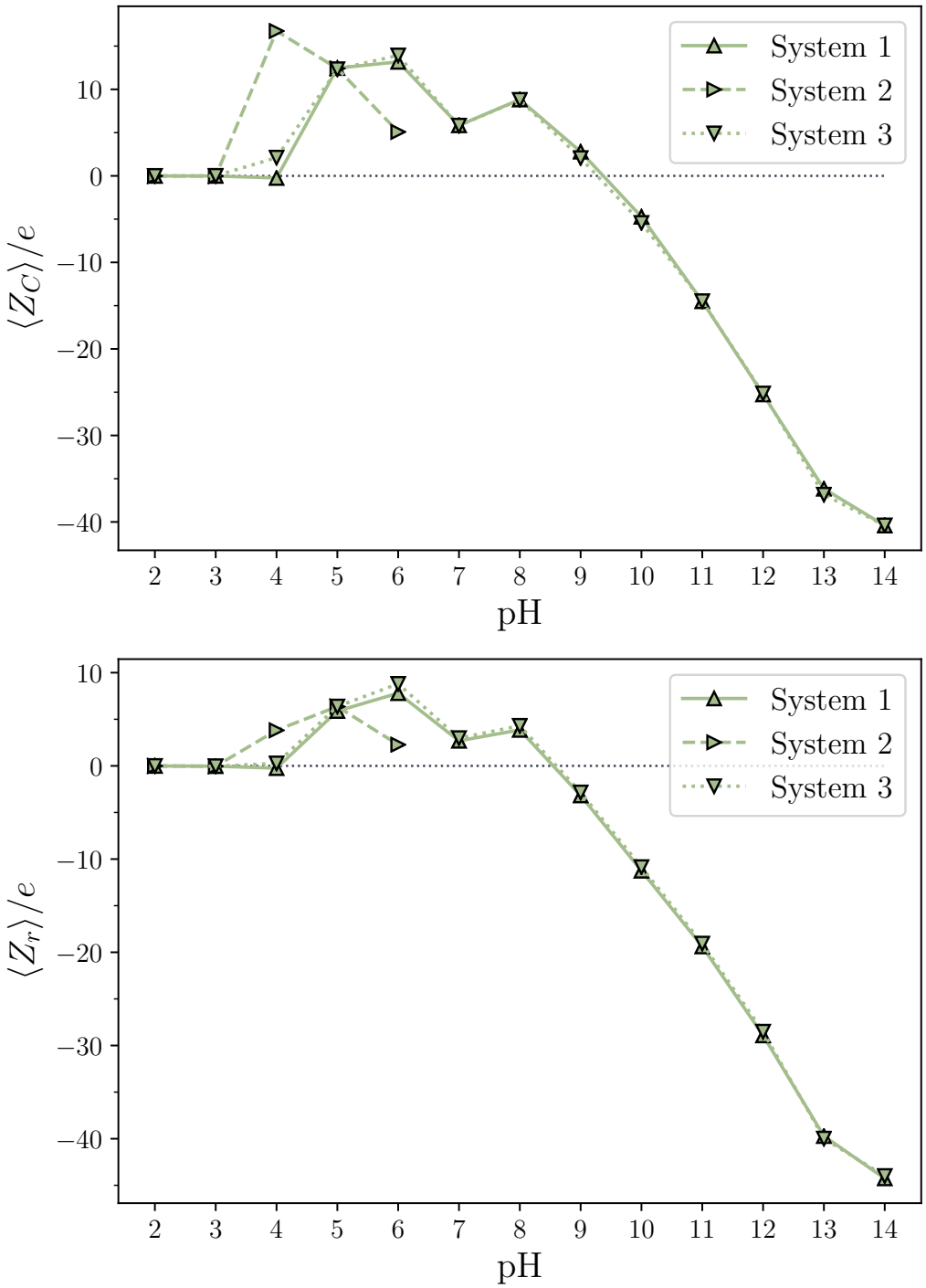

Figure C.3: Complex charge as a function of pH for the three simulations.

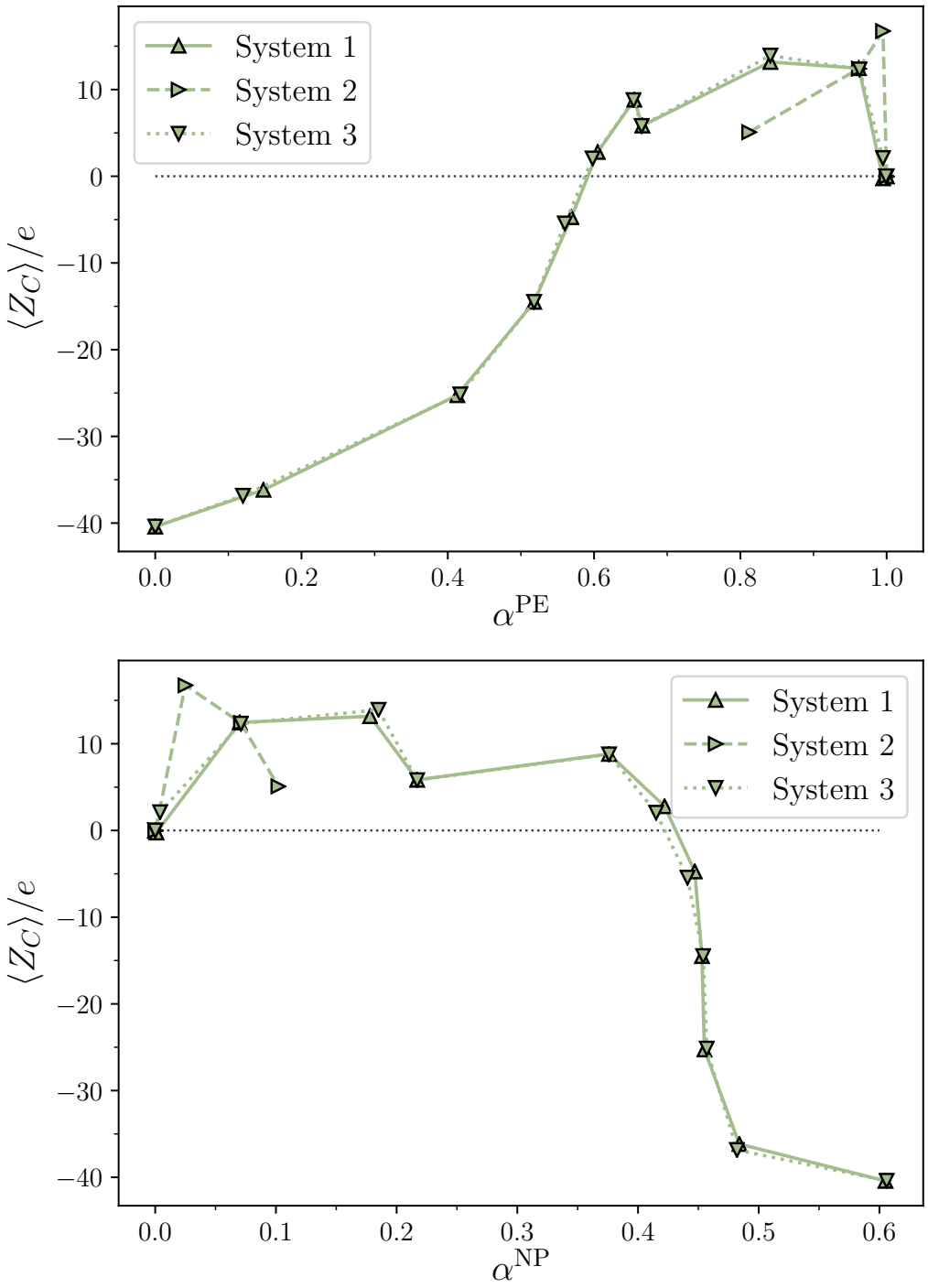

Figure C.4: Complex charge as a function of α for the three simulations.

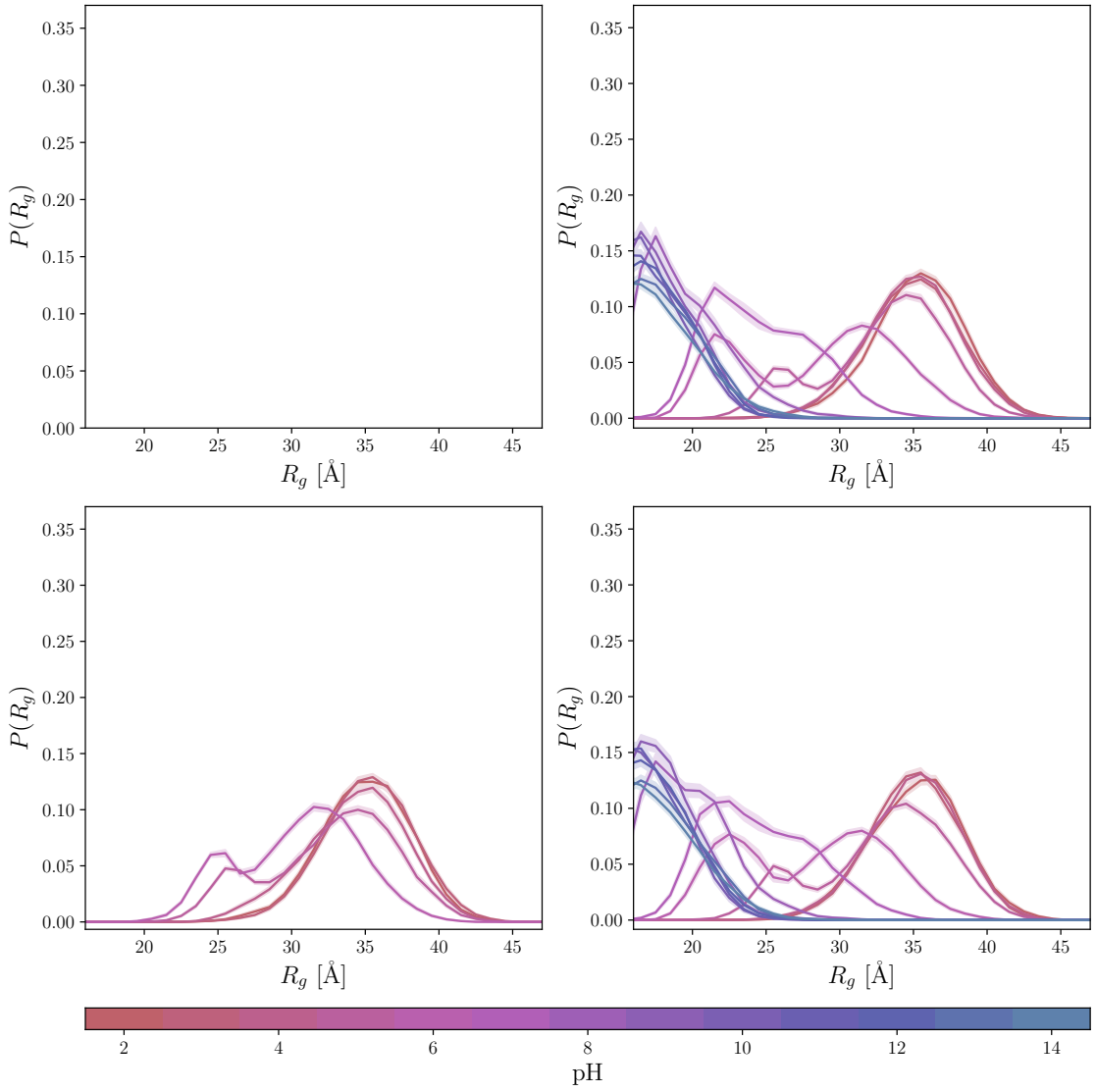

Figure C.5: Probability of the radius of gyration for the three simulations

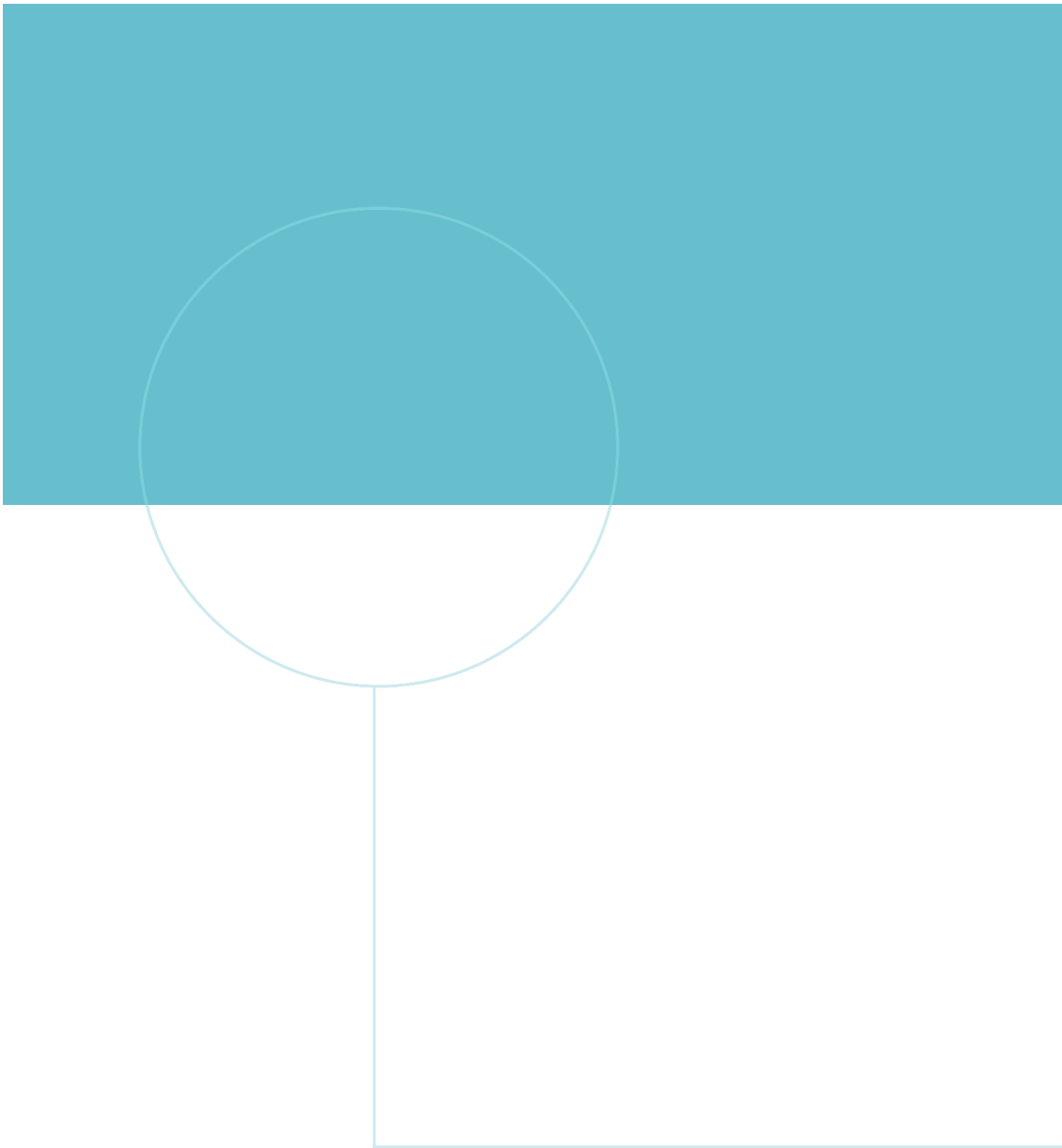

NTNU

Norwegian University of
Science and Technology